

Functionally distinct *Botrytis cinerea* Argonaute proteins in plant-microbe interaction

Dissertation der Fakultät für Biologie
der Ludwig-Maximilians-Universität München



vorgelegt von

Lihong Huang

aus

Liuzhou

Jahr

München, Oktober, 2021

Mit Genehmigung der Fakultät für Biologie
der Universität München

Ersgutachter/in:	<u>PD. Dr. Arne Weiberg</u>
Zweitgutachter/in:	<u>Prof. Dr. Wolfgang Frank</u>
Tag der Abgabe:	<u>14-07-2021</u>
Tag der mündlichen Prüfung:	<u>20-10-2021</u>

Eidesstattliche Versicherung

Ich versichere hiermit an Eides statt, dass die vorgelegte Dissertation von mir selbstständig und ohne unerlaubte Hilfe angefertigt ist.

München, den

Lihong Huang

22.10.2021

Erklärung

Hiermit erkläre ich, dass die Dissertation nicht ganz oder in wesentlichen Teilen einer anderen Prüfungskommission vorgelegt worden ist. Ich habe nicht versucht, anderweitig eine Dissertation einzureichen oder mich einer Doktorprüfung zu unterziehen.

München, den

Lihong Huang

22.10.2021

Table of content

Table of content	4
Zusammenfassung (Deutsch):	7
Abstract (English):	9
List of figures	11
Supplemental figures	12
List of tables	12
List of abbreviations	13
1. Introduction	16
1.1 Life cycle and virulent factors of <i>Botrytis cinerea</i>	16
1.2 RNA interference in plant-pathogen interaction	18
1.2.1 The discovery of RNA interference	18
1.2.2 RNAi mechanism	19
1.2.2.1 RNA-dependent RNA polymerases	20
1.2.2.2 Dicer/Dicer-like proteins	21
1.2.3 RNAi in plant, plant development and immunity	22
1.2.4 RNAi in fungi and fungal pathogenesis	24
1.2.4.1 Genes involving in Quelling	24
1.2.4.2 Genes involving in MSUD.....	25
1.2.5 Cross-kingdom RNAi	28
1.3 Argonaute proteins	29
1.3.1 Crystal structure and mechanism.....	29
1.3.2 Subcellular localization	32
1.3.3 Agos in fungi	33
1.3.4 Agos in <i>A.thaliana</i>	34
1.3.4.1 Agos categories	34
1.3.4.2 Agos and associated sRNAs.....	34
Aims of the thesis	36
2. Material and Methods	37
2.1 Plant materials	37
2.2 <i>Botrytis cinerea</i> growth	37
2.2.1 <i>Botrytis cinerea</i> strains and maintenance	37
2.2.2 Mycelial growth	37
2.2.3 Conidium morphology	38
2.2.4 Sporulation	38
2.3 Generation of transgenic <i>Botrytis cinerea</i>	38
2.3.1 Identification and phylogeny of Argonaute proteins.....	38
2.3.2 Vector construction	38
2.3.3 Protoplast transformation and homokaryotic purification	39

Functionally distinct *Botrytis cinerea* Argonaute proteins in plant-microbe interaction

2.3.4	Genomic DNA extraction and genotyping	40
2.3.5	Integration verification by southern blotting.....	40
2.3.6	Western blot.....	41
2.4	Gene expression	42
2.4.1	Total RNA extraction.....	42
2.4.2	Quantitative RT-PCR (qRT-PCR).....	42
2.4.3	Stem-loop RT PCR.....	43
2.5	Inoculation test	43
2.5.1	Infection assay with conidial suspension or mycelial plugs.....	43
2.6	Transcriptomics analysis.....	44
2.6.1	Small RNA library cloning, sequencing and profiling analysis	44
2.6.2	RNA library cloning, sequencing and preprocessing	44
2.6.3	DistHeatMap and Principal component analysis (PCA) plot visualization and clustering 45	
2.6.4	Differentially expressed genes (DEGs) identification, GO term (incompletion) and KEGG analysis	45
2.7	Fluorescence microscopy.....	45
2.8	RNA-immunoprecipitation.....	45
3.	Results	47
3.1	Identification of Argonaute proteins in <i>B. cinerea</i>	47
3.2	<i>Ago</i> expression levels in <i>B. cinerea</i> and from infected tomato and <i>Arabidopsis</i>	49
3.3	<i>Ago</i> proteins-mediated regulation on virulence in <i>B. cinerea</i>	50
3.3.1	Generation of <i>Ago</i> loss-of-function mutants by homologous recombination.....	50
3.3.2	Loss of <i>Ago</i> unalter vegetative morphology in <i>B. cinerea</i>	53
3.3.3	<i>Ago2</i> loss-of-function mutants impair pathogenicity in <i>B. cinerea</i>	54
3.4	Heterokaryon complementation	56
3.4.1	Introduction a complemented fragment in $\Delta ago2$ unalter vegetative morphology	56
3.4.2	Gain of <i>Ago2</i> complemented reduced virulence in <i>B. cinerea</i>	57
3.5	<i>Ago1</i> and <i>Ago2</i> localize in the cytoplasm and cytoplasmic granules in <i>B. cinerea</i>	58
3.6	Mechanism of <i>Ago</i>-mediated regulation on pathogenicity in <i>B. cinerea</i>	59
3.6.1	22-nt sRNAs are not the cause of reduced virulence in <i>Botrytis</i> $\Delta ago2$	59
3.6.2	<i>Ago2</i> regulates genes involving in cellulose-binding domain synthesis, arginine biosynthesis, galactose metabolism and lipid metabolism	63
4.	Discussion	68
4.1	<i>Ago2</i> positively regulate virulence in <i>B. cinerea</i>	68
4.2	24-28-nt sRNAs are likely the intermediary associated with <i>Ago2</i> regulating pathogenicity in <i>B. cinerea</i>	68
4.3	5' nucleotide of mRNA-derived sRNAs is not the sole selection of Agos in <i>B. cinerea</i> ..	69
4.4	<i>Ago</i> proteins are functionally distinct in <i>B. cinerea</i>	69

Supplemental figures and tables	72
References	85
Acknowledgements	106

Zusammenfassung (Deutsch):

Der nekrotrophe, filamentöse und phytopathogene Pilz *Botrytis cinerea* (*B. cinerea*) verursacht weltweit an mindestens 200 Eudikotyledonen und Monokotyledonen eine schwere Grauschimmelkrankheit. Neben verschiedenen Enzymen sezerniert *Botrytis* auch sRNAs als virulente Faktoren in Wirte, welche die Pflanzenphysiologie und Pflanzenimmunität über Cross-Kingdom-RNA-Interferenz (ckRNAi) manipulieren. Dabei erfolgt die Translokation der sRNA-Effektoren bidirektional zwischen Pathogen und Wirt. Die Rolle der Ago-vermittelten Regulation auf die Pathogenität durch RNA-Interferenz (RNAi) in *B. cinerea* ist jedoch noch unklar.

In dieser Doktorarbeit wurden vier Gene, *Ago1*, *Ago2*, *Ago3* und *Ago4* in *B. cinerea* identifiziert, die für Ago-Proteine kodieren. Die phylogenetische Analyse zeigte, dass *Ago1*, *Ago3* und *Ago4* zur Klade der Quelling gehören und *Ago2* in die Gruppe der MSUD in *Botrytis cinerea* fällt. Das Expressionsmuster zeigte, dass *Botrytis* die endogene *Ago2*-Expression als Reaktion auf eine Infektion von Tomaten im Früh- und Spätstadium unterdrückt, was auf eine mögliche Funktion von *Ago2* im Cross-Talk der Pilz-Wirt-Interaktion hinweist. Bei der Phänotypisierung homokaryotischer Mangel-Mutanten von *Botrytis*, denen *Ago1*, *Ago2*, *Ago3* bzw. *Ago4* fehlten, konnte ich beobachten, dass der Verlust der *Ago*-Gene keinen Einfluss auf die Myzelmorphologie, Konidiengröße und Konidienbildung hatte, was darauf hindeutet, dass *Ago*-Gene für die Entwicklung und das Wachstum von *Botrytis* in der vegetativen Phase nicht erforderlich sind. Darüber hinaus zeigten *Ago2*-Loss-of-Function-Mutanten eine verminderte Virulenz im Vergleich zu WT und die Komplementierung von *Ago2* stellte die verminderte Pathogenität wieder her, was zeigt, dass *Ago2* zur Pathogenität von *Botrytis* während der Infektion auf Tomate beiträgt. Die Abundanz von sRNAs war in den *Ago2*- und *Ago3*-Mutationstämmen erhöht, was die Rolle der mRNA-Degradation für *Ago2* und *Ago3* anstelle der Stabilisierung im post-transcriptional silencing (PTGS) impliziert. In der Zwischenzeit waren die Transkripte des Retroelements LTR2 in der *Ago1*- oder *Ago2*-Loss-of-Function-Mutante signifikant erhöht und LTR1 wurde in der *Ago3*-Loss-of-Function-Mutante herunterreguliert, was darauf hindeutet, dass *Ago2* ein dominanter Slicer in *B. cinerea* sein könnte, während *Ago3* wahrscheinlich ein untergeordneter Slicer ist, der mit *Ago2* konkurriert, indem er sRNAs und interferierende RNAi bindet, und *Ago4* möglicherweise nicht an PTGS beteiligt ist. Bemerkenswert ist, dass aus mRNA-seq von *Ago2* Loss-of-Function-Mutanten acht differentiell exprimierte Gene (DEGs), die in zellulären Komponenten angereichert sind, und drei DEGs (*BCIN_16g04050*, die eine Glutamat-Dehydrogenase kodieren, *BCIN_09g04410* kodiert eine Galaktose-Oxidase und *BCIN_03g04090* kodiert eine Glycerin-Kinase), die im KEGG-Pfad angereichert sind, identifiziert wurden, die eine

Rolle in der Arginin-Biosynthese, dem Galaktose-Stoffwechsel bzw. dem Lipid-Stoffwechsel spielen. Ein sRNA-Profilung aus diesen identifizierten Genen deckte auf, dass 24-28-nt sRNAs, wahrscheinlich microRNA-like RNAs, in *Ago2*-Mutationsstämmen dramatisch verloren gingen. Zusammengenommen reguliert *Ago2* die Pathogenität positiv, möglicherweise über die Regulierung dieser Gene, die in GO- oder KEGG-Pfaden angereichert sind und die die Ziele der 24-28-nt miRNAs sein könnten, die eine positive Rückkopplungsschleife in *B. cinerea* bilden.

Abstract (English):

A necrotrophic filamentous phytopathogenic fungus *Botrytis cinerea* causes severe grey mould disease on at least 200 eudicots and monocots worldwide. In addition to various enzymes, *Botrytis* also secretes sRNAs as virulent factors into hosts manipulating plant physiology and immunity via cross-kingdom RNA interference (ckRNAi) and the translocation of sRNA effectors is bidirectional between pathogen and hosts. However, the function of Ago-mediated regulation on pathogenicity by RNA interference (RNAi) in *B. cinerea* remains blank.

In this doctoral project, four *Botrytis* genes encoding Ago proteins were identified encompassing *Ago1*, *Ago2*, *Ago3* and *Ago4*. Phylogenetic analysis showed that *Ago1*, *Ago3* and *Ago4* belong to the clade of quelling and *Ago2* falls into the group of MSUD in *Botrytis cinerea*. The expression pattern indicated that *Botrytis* suppressed endogenous *Ago2* expression in response to early- and late-stage infection on tomatoes, suggesting a potential function of *Ago2* in the cross-talk of fungal-hosts interaction. Through phenotypical analyses with homokaryotic deficient mutants disrupting *Botrytis Ago1*, *Ago2*, *Ago3* and *Ago4*, I observed that loss of *Ago* genes had no impact on mycelial morphology, conidial size and conidiation, implicating that *Ago* genes are not required for *Botrytis* development and growth in the vegetative phase. Furthermore, *Ago2* loss-of-function mutants displayed impaired virulence compared to WT and complementation of *Ago2* restored reduced pathogenicity, demonstrating that *Ago2* contributes to pathogenicity in *Botrytis* during infection on tomato. The abundance of sRNAs were elevated in *Ago2* and *Ago3* mutation strains, which suggests the role of mRNA degradation for *Ago2* and *Ago3* instead of stabilization in post-transcriptional gene silencing (PTGS). Meanwhile, transcripts of retroelement LTR2 was significantly increased in *Ago1* or *Ago2* loss-of-function mutant and LTR1 was down-regulated in *Ago3* loss-of-function mutant, indicating that *Ago2* might be a dominant slicer in *B. cinerea*, whereas *Ago3* is likely a minor slicer competing with *Ago2* binding with sRNAs and interfering RNAi, and *Ago4* may not involve in PTGS. Notably, mRNA-seq from *Ago2* loss-of-function mutants showed that eight differentially expressed genes (DEGs) enriched in cellular component and three DEGs (*BCIN_16g04050* encoding a glutamate dehydrogenase, *BCIN_09g04410* encoding a galactose oxidase and *BCIN_03g04090* encoding glycerol kinase) enriched in the KEGG pathway were identified, which played a role in arginine biosynthesis, galactose metabolism and lipid metabolism, respectively. sRNA profiling derived from these identified genes uncovered that 24-28-nt sRNAs, probably microRNA-like RNAs, dramatically lost in *Ago2* mutation strains. Taken together, *Ago2* positively regulates pathogenicity, possibly via

Functionally distinct *Botrytis cinerea* Argonaute proteins in plant-microbe interaction

regulation on these genes enriched in GO or KEGG pathway that might be the targets of 24-28-nt miRNAs forming a positive feedback loop in *B. cinerea*.

Keywords: RNAi, cross-kingdom RNAi, *Botrytis cinerea*, tomatoes, small RNAs, virulence

List of figures

Figure 1.1 Illustration of <i>B. cinerea</i> life cycle (Figure strongly adapted from (Shiu et al., 2001))	17
Figure 1.2 Signalling pathway involving in distinct developmental stages in <i>B. cinerea</i> (Figure from (Williamson et al., 2007))	17
Figure 1.3 Protein structure of Dicer in <i>Giardia intestinalis</i> (Figure from (Macrae et al., 2006))	22
Figure 1.4 Illustration of PTGS model in <i>N. crassa</i> (Figure modified from (Chang et al., 2012; Xue et al., 2012))	28
Figure 1.5 Crystal structure of full-length Argonaute proteins in <i>Kluyveromyces polysporus</i> (Figure from (Nakanishi et al., 2012))	30
Figure 1.6 Illustration of gene silencing pathway in <i>A. thaliana</i> (Figure from (Rogers & Chen, 2013))	33
Figure 3.1 Ago protein features in <i>B. cinerea</i> .	47
Figure 3.2 Phylogeny, gene structure and protein domain architecture of Argonaute proteins in representative filamentous fungi.	48
Figure 3.3 Expression of <i>Ago</i> genes in <i>B. cinerea</i> in different vegetative tissues	49
Figure 3.4 Expression pattern of <i>Agos</i> in <i>Botrytis</i> WT from culture and infected <i>S. lycopersium</i> and <i>A. thaliana</i> .	50
Figure 3.5 Strategy for construction of <i>Botrytis</i> Δago deletion mutants.	51
Figure 3.6 Schematic diagram of <i>Botrytis</i> <i>Ago</i> genes disruption.	52
Figure 3.7 <i>Ago</i> genes expression in Δago deletion mutants.	52
Figure 3.8 Morphology of <i>Botrytis</i> WT and Δago deficient mutants.	53
Figure 3.9 Phenotyping of <i>B. cinerea</i> WT and Δ deletion mutants on tomatoes.	55
Figure 3.10 Colonization of <i>B. cinerea</i> on tomatoes.	55
Figure 3.11 Generation of <i>cAgo2</i> complementary strains in <i>Ago2</i> mutation background.	56
Figure 3.12 Morphology of <i>Botrytis</i> WT and <i>cAgo2</i> complementary strains.	57
Figure 3.13 Pathogenicity assay of WT and complementary strain <i>cAgo2</i> on tomato.	58
Figure 3.14 Subcellular localization of <i>Ago1</i> and <i>Ago2</i> .	59
Figure 3.15 Characterisation of small RNAs in WT and Δago deletion mutant.	61
Figure 3.16 small RNA profiling from distinct RNA species.	62
Figure 3.17 Number of DEGs in WT and Δago ko mutants	64
Figure 3.18 Differentially expressed genes in Δago ko mutants compared to WT in <i>B. cinerea</i> .	64
Figure 3.19 DEGs that enriched in cellular component in <i>Ago2</i> loss-of-function mutant.	65
Figure 3.20 sRNA profiling of DEGs enriched in GO in $\Delta ago2$.	66
Figure 3.21 sRNA profiling derived from three gene loci and relative expression in Δago compared to WT.	67
Figure 4.1 A proposed scenario for functionally distinct Ago proteins in <i>B. cinerea</i>	70

Supplemental figures

Supplemental figure 1 Alignment of MID-PIWI motif of Ago protein sequences.....	72
Supplemental figure 2 Expression pattern of <i>Botrytis Rdr</i> genes from infected <i>S. lycopersicum</i> and <i>A. thaliana</i>	73
Supplemental figure 3 Expression pattern of <i>Botrytis Dcl</i> genes from infected <i>S. lycopersicum</i> and <i>A. thaliana</i>	73
Supplemental figure 4 Western blot of <i>Botrytis</i> WT and GFP labelled strains.	74
Supplemental figure 5 Inoculation assay with WT and Δago deletion mutants.	74
Supplemental figure 6 Total sRNA nucleotide distribution in WT and Δago deletion mutants ..	76
Supplemental figure 7 Sample distance in WT and Δago ko mutants with five replicates for each genotype.	77
Supplemental figure 8 DEGs enriched in cellular component in <i>Ago1</i> loss-of-function mutants (incompletion).....	77
Supplemental figure 9 DEGs enriched in <i>Ago3</i> loss-of-function mutants (incompletion).....	78
Supplemental figure 10 Eleven genes differentially expressed in <i>Ago2</i> loss-of-function mutants and enriched in GO and KEGG pathways.....	79
Supplemental figure 11 Twenty-five downregulated genes differentially expressed in <i>Ago2</i> loss-of-function mutants.	79

List of tables

Table 1 Genes enriched in KEGG that specifically and differentially expressed in $\Delta ago2$	66
Table 2 <i>Botrytis</i> strains used in this study.....	80
Table 3 Accession number of Ago protein sequence in representative Ascomycota fungi.....	80
Table 4 Primers used in this study	82

List of abbreviations

RNAi	RNA interference
ckRNAi	cross-kingdom RNAi
RISC	RNA-induced silencing complex
dsRNAs	Double-stranded RNAs
ssRNAs	Single-stranded RNAs
ATP	Adenosine triphosphate
UTR	Untranslated region
ORF	Opening reading frame
TGS	Transcriptional gene silencing
PTGS	Posttranscriptional gene silencing
nt	Nucleotide
Qde	Quelling defective
Sms	Suppressor of meiotic silencing
Sid	Systemic RNAi-deficient
Sad	Suppressor of ascus dominance
Dim	Defective in methylation
Sgs	Suppressor of gene silencing
Asm	Ascospore maturation
Stu	Stunt
Hen	HUA enhancer
Qip	Qde2-interacting protein
ko	knockout
RdRp/Rdr	RNA-dependent RNA polymerase
Dcr	Dicer
Dcl	Dicer-like
TERT	Telomerase reverse transcriptase
PAZ	PIWI-Argonaute-Zwille
PIWI	P-element-induced wimpy testis

Functionally distinct *Botrytis cinerea* Argonaute proteins in plant-microbe interaction

MID	Middle
MSUD	Meiotic silencing by unpaired DNA
RIP	Repeat induced point mutation
SAM	Shoot apical meristem
RdDM	RNA-dependent DNA methylation
RNase	Endoribonuclease
XRN	Exoribonuclease
EV	Extracellular vesicle
qRT-PCR	Quantitative real-time polymerase chain reaction
Chs	Chalcone synthase DNA
Al	Albino
WT	Wild-type
P body	Processing body
LTR	Long terminal repeat
miRNA	microRNA
milRNA	micro RNA-like RNA
siRNA	small interfering RNA
tasiRNA	transacting small interfering RNA
hc-siRNA	heterochromatic small interfering RNA
tRNA	transfer RNA
mRNA	messenger RNA
rRNA	ribosomal RNA
sn/snoRNA	small nuclear/small nucleolar RNA
hph	Hygromycin phosphotransferase
trpC	Tryptophan synthase
CTAB	Cetyltrimethylammonium bromide
GO	Gene ontology
KEGG	Kyoto Encyclopedia of Genes and Genomes
DDD/H	Aspartate-aspartate-aspartate / Aspartate-aspartate-glutamate

Functionally distinct *Botrytis cinerea* Argonaute proteins in plant-microbe interaction

Dcp	De-capping enzyme
<i>Botrytis cinerea</i>	<i>B. cinerea</i>
<i>Neurospora crassa</i>	<i>N. crassa</i>
<i>Magnaporthe grisea</i>	<i>M. grisea</i>
<i>Aspergillus nidulans</i>	<i>A. nidulans</i>
<i>Drosophila melanogaster</i>	<i>D. melanogaster</i>

1. Introduction

1.1 Life cycle and virulent factors of *Botrytis cinerea*

The genera of *Botrytis* were found as early as two centuries ago, which belongs to a heterothallic filamentous fungal pathogen infecting a wide range hosts over 200 plant species (Aamlid, 1952; Allen et al., 2005; Barkai-Golan et al., 1971; Cooley, 1931; Hopkins, 1921; Humphrey, 1891; McColloch & Wright, 1966; Ogilvie & Munro, 1947; Pawsey, 1969; Peltier, 1912; Schmitt, 1952; Stevens, 1916). *Botrytis cinerea* is categorized in the order Helotiales and family Sclerotiniaceae (Jarvis, 1977). In contrast to *Neurospora crassa* (*N. crassa*) that produce uninucleate conidiospores, *Botrytis* germinates multinucleate conidia containing 3-11 nucleus. Two distinct mating-type loci in *Botrytis* were identified, including mat 1-1 and mat 1-2 (van Kan et al., 2010).

Botrytis spp. consists of 16 chromosomes (Shirane et al., 1989) containing a total of 11688 protein-coding genes according to current genome assembly (van Kan et al., 2017). Its life cycle comprises two stages, conidial stage (*Botrytis cinerea*) and ascigerous stage (*Botryotinia fuckeliana*) (**Figure 1.1**). During vegetative growth, mature mycelium of two opposite mating types 1-1 and 1-2 sporulate and produce conidiospores. When conidia from 1-1 touch the trichogyne generated from sexual structure protoperithecium of 1-2 mating type, the nuclei of mating type 1-1 get into the cell of 1-2. Two haploid nuclei from opposite mating types fuse and get into the stage of karyogamy, wherein sexual reproduction initiates. The diploid nuclei undergo twice meiosis and once mitosis in the common cytoplasm of the ascus, generating 8n haploid nuclei (n=number of parental nuclei), which are segregated into the corresponding number of spindle-shaped ascospores in an ascus. The mature ascospores are multinucleate. Germinated ascospores develop new mycelium and turn into vegetative phase again (Shiu et al., 2001; van Kan, 2006).

Signaling pathways in *Botrytis* control self-development and infection structure formation during infection on hosts (**Figure 1.2**). The early development of the fungi on the plant surface is often associated with the development of adhesiveness of spores, germling and infection structures (infection cushion). Specific components of the fungal cell wall belong to pathogen-associated molecular patterns (PAMPs), which are recognized by plant recognition receptors (PRRs), leading to pattern-triggered immunity (PTI) in planta (Boller & He, 2009). The contact of fungal conidiospores with the host cell surface triggers a series of cellular signalling responses and delivery, initiating the secretion of fungal pathogenesis factors encompassing various enzymes such as pectinase, hemicellulase, cellulase and protease and cutinase, small molecules such as

toxins and small RNA effectors. It seems that the role of enzymes in fungal pathogenicity depends on the proportion of enzymes in distinct filamentous fungi. Infection on the host induced the production of fungal pectinase (Sethi et al., 2016) and enhanced pathogenicity in *Valsa mali* (Wu et al., 2018). Similarly, cutinase contributes to uredospore adhesiveness on the host cell surface and virulence in *Magnaporthe grisea* (*M. grisea*) (Deising et al., 1992; Schafer, 1993; Sweigard et al., 1992). However, cutinase A was reported not functioning in pathogenicity in *Botrytis* during infection on tomato and gerbera (van Kan et al., 1997).

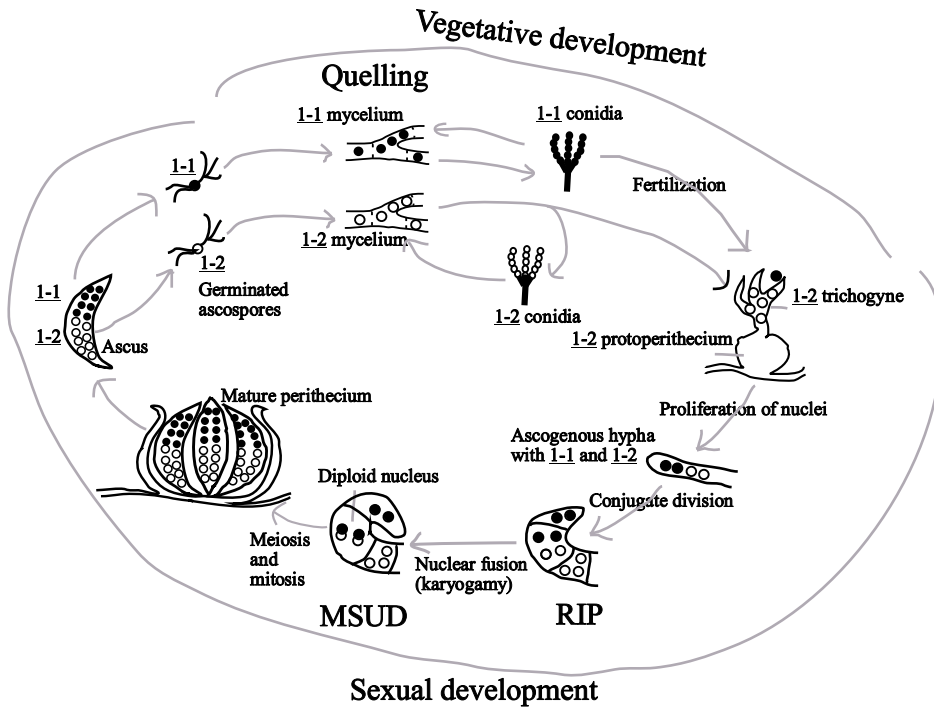


Figure 1.1 Illustration of *B. cinerea* life cycle (Figure strongly adapted from (Shiu et al., 2001))

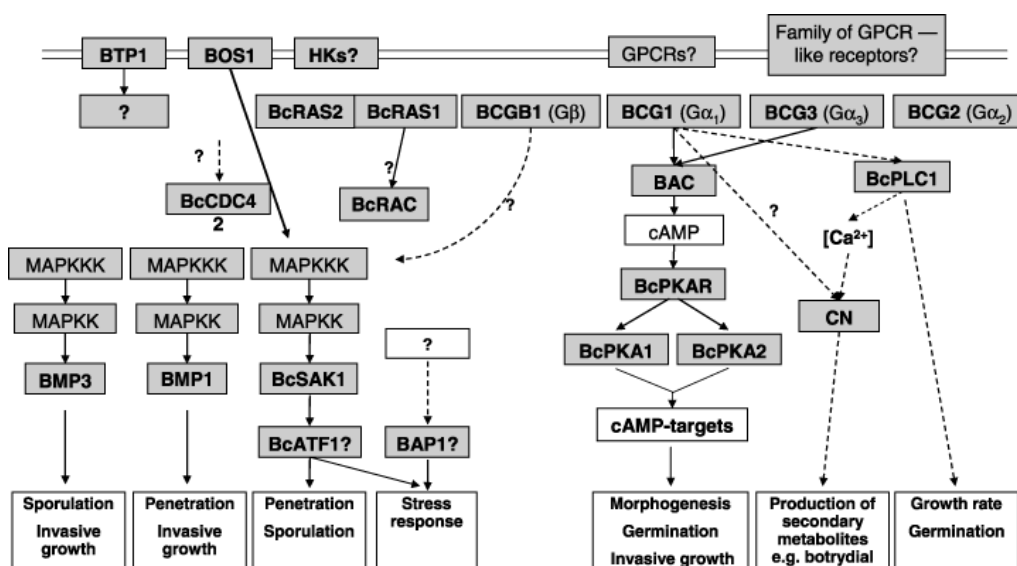


Figure 1.2 Signalling pathway involving in distinct developmental stages in *B. cinerea* (Figure from (Williamson et al., 2007))

1.2 RNA interference in plant-pathogen interaction

1.2.1 The discovery of RNA interference

Studies have shown that RNA interference (RNAi) in animals is equivalent to co-suppression in plants and quelling in fungi transcriptionally or post-transcriptionally. Here, these three silencing pathways were termed RNAi. The phenomenon of RNAi was initially observed in plant in 1990 when plant biologists introduced a chalcone synthase (*chs*) driven by 35s promoter that control the pigmentation of flowers into petunia to enhance the purple color of flowers (Napoli et al., 1990). However, most petunia displayed purple-white or even white petals instead of plants bearing darker purple flowers, which looked like the phenotype of *Chs* mutated plant (Napoli et al., 1990). This was considered a strange phenomenon particularly occurred in petunia and was termed co-suppression at that time. Two years later, a similar phenomenon was observed in filamentous fungus *N. crassa*. Microbiologists introduced an ectopic *al-1* (albino-1) gene which is responsible for the biosynthesis of the carotenoids in *N. crassa* and they found that approximately 30% *N. crassa* appeared white phenotype as the morphology in *al* null mutant (Romano & Macino, 1992). The phenomenon was coined Quelling. In 1993, the first miRNA *lin-4* was found in *Caenorhabditis elegans* (*C. elegans*) and its anti-sense strand was homologous to the 3' UTR region of *lin-14* (Lee et al., 1993). Several assays were subsequently conducted to find out the intermediate that induced gene silencing. In the beginning, anti-sense RNA complementary to *par-1* was injected into *C. elegans* (Guo & Kemphues, 1995). Surprisingly, a similar inhibition efficiency was obtained when injecting both anti-sense and sense (control) RNAs, which was inconsistent with the expectation that anti-sense strand of miRNAs paired with mRNA homologies to suppress translation. The intermediate was confirmed until 1998 by Fire and his colleagues. They observed that the conventional experiment used to prepare single-stranded RNA could produce a small amount of double-stranded RNAs. When dsRNAs (double-stranded RNAs) were removed, anti-sense ssRNA (single-stranded RNAs) lost most interference activity and sense ssRNA lost interference activity completely (Fire et al., 1998). Based on these findings, they uncovered that it was dsRNA induce post-transcriptional gene silencing. The phenomenon was named RNA interference and abbreviated as 'RNAi'.

The earliest evidence provided for the viral defense of RNAi was in 1998. Transgenic plants carrying both sense and anti-sense genes that complementary to the viral genome were much more resistant to virus, which was consistent with the finding that dsRNAs act as the mediator of RNAi (Waterhouse et al., 1998). Since then, studies were further extended regarding RNAi components and their mechanism, crystal

structures of RNAi factors and associated proteins involving in RNAi, RNAi in cross-species and RNAi in distinct organisms. In 1999, Hamilton and his colleagues found 25-nt in length RNA intermediate in PTGS in plants for the first time (Hamilton & Baulcombe, 1999). In 2000, Zamore and Hammond found that exogenous the generation of 21-23nt siRNAs by RNase III enzyme (Dicer) depended on ATP in *Drosophila Melanogaster* (*D. melanogaster*) in vitro. RNAi has also evolved in mice (Wianny & Zernicka-Goetz, 2000), humans (Elbashir, Harborth, et al., 2001a), oomycete (Asman et al., 2016; Vetukuri et al., 2012; Vetukuri et al., 2011), archaea and most bacteria. However, archaea and bacteria possess a non-canonical RNAi machinery based on CRISPR/Cas system (Hale et al., 2009; Marraffini & Sontheimer, 2010).

Surprisingly, the silencing signal is diffusible and spreads in planta and propagates between host and graft. Direct experimental evidences were provided, suggesting the mobility of sRNA molecules within the cells and transmission in a long distance via vascular phloem (Palauqui et al., 1997; Voinnet & Baulcombe, 1997; Voinnet et al., 1998). Likewise, RNA silencing transmission intercellularly was also found in *C. elegans* in a manner dependent or independent on Sid-1 (systemic RNAi-deficient-1) gating channel (Feinberg & Hunter, 2003; Jose et al., 2009; Winston et al., 2002). Interestingly, RNAi is heritable from parent to offspring in *C. elegans* (Bucher et al., 2002; Buckley et al., 2012; Xu et al., 2018). However, systemic silencing was not found in *D. melanogaster* and human (Roignant et al., 2003). Two dominant types of gene silencing mediated by dsRNAs compass transcriptional gene silencing (TGS) (Cernilogar et al., 2011; Liu et al., 2018; Sigova et al., 2004; Verdel et al., 2004; Volpe et al., 2002) and post-transcriptional gene silencing (PTGS) (Diederichs & Haber, 2007; Engels & Hutvagner, 2006; Fei et al., 2013; Forrest et al., 2004; Hoffer et al., 2011; Klahre et al., 2002; Lai, 2002; Makeyev & Bamford, 2002b; Morel et al., 2002; Nolan et al., 2008; Pal-Bhadra et al., 2002; Sigova et al., 2004). A certain correlation between two silencing pathways exists and the PTGS pathway is the most deeply characterized and the most applied in practice.

1.2.2 RNAi mechanism

RNA interference (RNAi) silencing machinery belongs to an ancient conserved defense machinery against viral infection, transposons or retrotransposons mobilization to maintain endogenous genome stability, which has been found in prokaryote and eukaryote, even though RNAi machinery in prokaryote differs from eukaryote (Duran-Figueroa & Vielle-Calzada, 2010; Hale et al., 2009; Padeken et al., 2021; Tabara et al., 1999). Numerous proteins involve in RNAi in distinct organisms while the functional mechanism is similar. Although different organisms comprise distinct RNAi factors associating proteins, three main RNAi components are pervasive in plants, fungi and

animals composing RNA-dependent RNA polymerase (RdRp), Dicer (Dcr)/Dicer-like (Dcl) proteins and Argonaute (Ago) proteins. The canonical RNAi pathway consists of three steps:

- the biogenesis of small non-coding RNA duplexes
- the incorporation process of sRNA duplexes into Ago proteins
- the recognition and cleavage of cytoplasmic mRNA targets directed by guide sRNAs

RNA-dependent RNA polymerases (RdRp) initially catalyze the synthesis of sense RNAs that are homologous to RNA template from 5' to 3' orientation (Cogoni & Macino, 1997; Dalmay et al., 2000; Makeyev & Bamford, 2002a). Synthesized long dsRNAs are recognized and precisely processed into 21-25nt short siRNA duplexes by ribonuclease III (Bernstein et al., 2001; Hutvagner et al., 2001) named Dicer or Dicer-like proteins (Dcl) that contain a helicase domain, a PAZ domain, two RNase III domain (endoribonuclease and exoribonuclease) and an RNA binding domain. Some siRNA classes are independent of Dcr/Dcl such as Piwi-interacting RNAs in mammals and secondary siRNAs in *C. elegans*. Alternatively, pre-miRNA hairpin precursors are processed by Dicer proteins directly, generating miRNA/miRNA* duplex. Different Dicer proteins produce small RNAs in distinct lengths, which will be further discussed in RNAi pathway in specific organisms below. Afterward, short RNAs are assembled to Argonaute proteins, with the ejection of passenger sRNAs, forming RNA-induced silencing complexes (RISCs) (Park & Shin, 2015). Anti-sense sRNAs guide RISC (RNA induced silencing complex) to target mRNAs by binding to 3' untranslated region (UTR) (Lai, 2002; Lee et al., 1993) that perfectly or imperfectly homologous to sRNAs causing mRNA degradation and translational inhibition post-transcriptionally (Chen, 2004; Montgomery & Fire, 1998; Ngo et al., 1998; Tuschl et al., 1999; Zeng et al., 2003) or chromatin remodeling transcriptionally (Sasaki et al., 2012). In the following parts I will introduce the development and protein structures of RdRp and Dcl and for the information regarding Agos is introduced in the Ago section.

1.2.2.1 RNA-dependent RNA polymerases

RdRp was initially purified in Chinese cabbage (Astier-Manificier & Cornuet, 1971) and then isolated in tomato (Schiebel et al., 1998). Homologs were subsequently cloned and identified such as *Qde-1* in *N. crassa* (Cogoni & Macino, 1997). *Ego-1/Rrf-1* in *C. elegans* (Simmer et al., 2002; Smardon et al., 2000), *Sgs2/Sde1* in *A. thaliana* (Dalmay et al., 2000; Mourrain et al., 2000) and *Rdr1* in *S. pombe* (Tabara et al., 1999). RdRps are classified into three categories comprising RDR α , RDR β and RDR γ . RDR α exists in plants and animals, whereas RDR β is present in animals and fungi. RDR γ exclusively

exists in fungi (Bollmann et al., 2016). However, no homologs were found in *S. cerevisiae*, *D. melanogaster* and Vertebrates. Strikingly, recent studies found RdRp substitutes in humans such as TERT (telomerase reverse transcriptase) catalytic subunit and Pol II (RNA polymerase II). TERT can combine with the non-coding RNA component of RMRP (mitochondrial RNA processing endonuclease), forming the smallest catalytic unit with RdRp activity (Maida et al., 2009). Although Pol II is a DNA-dependent RNA polymerase, it is capable of catalyzing dsRNA synthesis using ncRNA (B2 RNA) as a template (Wagner et al., 2013). RdRp proteins function as homodimer in *Neurospora crassa*, *Thielavia terrestris* and *Myceliophthora thermophila* in vitro and the catalyzation activity vary in each organism (Qian et al., 2016).

Studies in plants have uncovered that silencing signal can be systemically spread and amplified (Allen et al., 2005; Palauqui et al., 1997; Voinnet & Baulcombe, 1997; Yoo et al., 2004). The secondary mRNA silencing is mediated by 22-nt miRNAs (Allen et al., 2005; Yoshikawa et al., 2005) and triggered by either one or two miRNA complementary sites on mRNA substrates (Allen et al., 2006). The cleaved mRNA fragments (one side cleavage) are catalyzed by Rdr6 producing long dsRNAs with the protection of a silencing suppressor called Sgs3 (Mourrain et al., 2000) in an unprimed-synthesis manner (Petersen and Albrechten, 2005). The newly synthesized dsRNA molecules are processed by Dcl4 and give rise to trans-acting siRNAs (tasiRNAs) every 21-nt, which are assembled to Ago1 protein forming RISC complex, targeting homologous mRNA molecules and strongly raising degradation efficiency to 40-fold in the molar ratio (Allen et al., 2005). Silencing amplification is also present in *C. elegans* and *D. melanogaster* independent of Dicer because amplified sRNAs are short enough in these two organisms to be directly recognized and assembled to Ago proteins (Pak & Fire, 2007; Sijen et al., 2007). By contrast, no secondary sRNAs have been found in humans.

1.2.2.2 Dicer/Dicer-like proteins

A study in *D. melanogaster* has revealed that sRNAs are processed from long dsRNAs by an endoribonucleolytic enzyme named Dicer (Bernstein et al., 2001). Dicer proteins belong to RNase III enzyme and typically compass a DExD box, a DUF283 domain, a PAZ (PIWI-Argonaute-Zwille) domain, two RNase III (endoribonuclease III) domains and a dsRBD (double-stranded RNA binding domain) (Collins & Cheng, 2005). Dicer proteins chop dsRNA every 21-23-nt to make short sRNAs dependent on energy generating by ATP hydrolysis. These resulting sRNAs contain specific structures with 2-nt 3' overhangs of hydroxyl termini and 5' monophosphate group (Bernstein et al., 2001; Collins & Cheng, 2005; Elbashir, Harborth, et al., 2001b; Elbashir, Lendeckel, et al., 2001; Zamore et al., 2000).

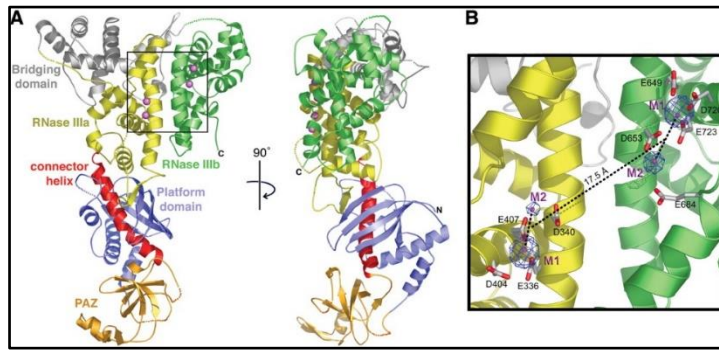


Figure 1.3 Protein structure of Dicer in *Giardia intestinalis* (Figure from (Macrae et al., 2006))

The architecture of Dicer protein looks like a hatchet. The dual RNase III domains form the blade and the PAZ domain forms the basis of the handle (Macrae et al., 2006) (**Figure 1.3 A**). DExD box, an RNA helicase, is highly conserved in Dicer proteins. The N terminus of this domain contains ATP-related binding motifs Q, I and II, ATP hydrolysis motif III and RNA binding motifs Ia and Ib. The C terminus consists of RNA binding motifs IV, V and VI (Sengoku et al., 2006). These subunits are utilized for unwinding dsRNAs in an ATP-dependent manner (Cordin et al., 2006). The PAZ domain is an RNA binding motif present in both Dicer and Ago proteins. PAZ domain in Ago proteins adopts an OB (oligonucleotide and oligosaccharide-binding)-fold that recognizes and binds 3' 2-nt overhang of sRNAs. A similar folding manner is present in Dicer proteins in *G. intestinalis*, whereas the PAZ domain in Dicer contains an extended loop contributing to RNA recognition which is absent in Ago proteins (Macrae et al., 2006). The C terminal of Dicer comprises dual RNase III and a dsRBD. Dicer proteins act as a ruler to precisely process dsRNAs into 21-23-nt sRNAs as the consequence of the unique structure of the RNase III domain. Each RNase III domain consists of two catalytic activities capable of cleaving phosphodiester bonds and chops dsRNA into short RNAs with 2-nt 3' overhangs (Collins & Cheng, 2005), but each RNase III domain provides sole catalytic center nonetheless (Zhang et al., 2004). The distance between two active catalytic centers is 25-bp giving rise to the precise generation of 21-23-nt in length sRNAs by alteration the distance between two RNase III domains (Blaszczyk et al., 2001). Thus, Dcr functions as a homodimer, generating sRNAs with 5' phosphate group, 3' hydroxyl termini and 2-nt 3' overhangs (Blaszczyk et al., 2001).

1.2.3 RNAi in plant, plant development and immunity

After identifying *Qde-2* in *N. crassa* in 1998, plant biologists isolated *Arabidopsis* $\Delta ago1$ mutants through mutagenesis and T-DNA insertion into the native location. *Ago1* is an ortholog of *Qde-2*. Hypomorphic mutation in *Ago1* gave rise to abnormal leaf development (Bohmert et al., 1998). Shortly after the screening of $\Delta ago1$ mutants, *Ago1* was revealed to play an essential role in PTGS and contributing to viral defense similar to Sgs2 and Sgs3 (Elmayan et al., 1998; Fagard et al., 2000b; Morel et al., 2002).

Several bacterial ribonucleases, particularly RNase III and RNase HI involved in RNA maturation and gene regulation (Nicholson, 1999), hinting that these ribonucleases might participate in the RNAi pathway. Importantly, Argonaute, an RNase H-like protein and the core component of RISC, was firstly demonstrated in *D. melanogaster* facilitating mRNA cleavage guided by 20-25-nt sRNAs (Hammond et al., 2000; Hammond et al., 2001). Hen1 (HUA enhancer1) was vital for sRNA stabilization (Yu et al., 2005) by methylation at 3' OH termini (Z. Yang et al., 2006) preventing them from 3' uridylation (Li et al., 2005) and degradation by exonuclease Sdn1 (Small RNA degrading nuclease) (Ramachandran & Chen, 2008). Meanwhile, biochemical data provided in *Drosophila* have revealed the chopping process of long dsRNAs into 21-23-nt sRNAs (Zamore et al., 2000) and the protein involved in this slicing was the RNase III enzyme (i. e. Dicer) (Bernstein et al., 2001). The essential steps in the RNAi pathway had been solved since 2001 and many studies had started to focus on identifying the homology of RNAi factors.

RNAi functions in diverse biological processes in plants. As the core compound in RNAi, Ago proteins play an eminent role in plant development, floral timing control, shoot apical meristem differentiation and immunity. Reports have shown that Ago1 necessitated for plant growth and development during vegetative and sexual life cycle from juvenile to mature stage and *Ago1* mutation lines displayed severe deficiency in reproduction (Bohmert et al., 1998; Jover-Gil et al., 2012; Lynn et al., 1999; Miyashima et al., 2009; Sorin et al., 2005; L. Yang et al., 2006). Ago10 functioned in timing control of floral stem cells (Ji et al., 2011), SAM and leaf development through regulating miR165 and miR166 (Liu et al., 2009; Xue et al., 2017; Zhou et al., 2015; Zhu et al., 2011). In addition, hypomorphic Δ *ago1* mutants regulated *Arabidopsis* leaf Morphology (Bohmert et al., 1998; Morel et al., 2002). Meanwhile, Ago1 involves in antiviral defense (Qu et al., 2008; Zhang et al., 2006) and regulates downstream signaling transduction (Li et al., 2012). Similar roles were also found in other Ago proteins (Ago2, Ago4, Ago5 and Ago7), which contributed to viral defense (Ando et al., 2021; Brosseau et al., 2016; Brosseau & Moffett, 2015; Qu et al., 2008; Zhang et al., 2006). However, *Arabidopsis* Ago7, also named ZIPPY (Sturani et al.), has been documented previously, showing a significant role in timing control during plant development rather than transgene silencing (Hunter et al., 2003). In addition, Ago4 involved in plant resistance against oomycetes and bacteria (Agorio & Vera, 2007). In addition, Ago2-miRNA393* complex regulated innate immunity by targeting a Golgi-localized SNARE gene *MEMB12* in response to bacteria (Zhang et al., 2011).

1.2.4 RNAi in fungi and fungal pathogenesis

Filamentous fungi generally contain less than 10% repetitive elements and a majority of them are silenced for genome stability maintenance. In this case, distinct silencing defense machinery has evolved in fungi. Three silencing surveillances have been discovered in *N. crassa* encompassing Quelling (RNAi) that occurs in the vegetative phase (Romano & Macino, 1992), meiotic silencing by unpaired DNA (MSUD) that occurs during karyogamy in prophase I of meiosis (Aramayo & Metzberg, 1996; Shiu et al., 2001) and repeat-induced point mutation (RIP) that occurs prior to meiosis in haploid dikaryotic phase (Selker et al., 1987; Selker & Stevens, 1985). In the following section, I will introduce Quelling and MSUD, while detailed information on RIP will not be discussed further. RIP is a fungal unique genome defense machinery occurring prior to nuclear fusion in the stage of sexual reproduction through rearranging multiple G-C to A-T pairs which Dim-2 subsequently methylates in duplicated sequences (Galagan & Selker, 2004; Grayburn & Selker, 1989; Mautino & Rosa, 1998; Selker, 1990, 2002; Selker et al., 1987).

1.2.4.1 Genes involving in Quelling

After the finding of quelling phenomenon in asexual growth of *N. crassa* by Cogoni and Macino in 1992, they confirmed that this gene inactivation belongs to post-transcriptional silencing as the abundance of *al-1* (*albino-1*) mRNA precursor in quelled strains was similar to that in unquelled strains (Cogoni et al., 1996). Furthermore, the efficiency of quelling in *N. crassa dim-1* (*defective in methylation*) deletion mutant that defects in cytosine methylation was similar to wild-type (Cogoni et al., 1996). Likewise, mutation of *Dim-5* in *N. crassa* crosses encoding a Lys9H3 methyltransferase unaffected biosynthesis of dsRNAs (Tamaru & Selker, 2001). Moreover, *Dim-2*, a DNA methyltransferase, whose deletion mutants contained an insignificant methylated LINE-like transposable element Tad (Nolan et al., 2005). These works indicate that DNA methylation functions independently with RNAi in *N. crassa*. It was exciting that the first RNAi components quelling defective (*Qde*) genes were isolated in *N. crassa* in 1997 including *Qde-1*, *Qde-2* and *Qde-3* by mutagenesis on stable strains of *al-2* (*albino-2*) containing distinct copies of *Albino* transgenes (Cogoni & Macino, 1997). Δqde deficient mutant recovered the quelled phenotype of *al-2*, displaying orange phenotype with the presence of endogenous *Albino* gene and high copies of *Albino* transgenes. Later on, *Qde-1* was demonstrated homologous to RNA-dependent RNA polymerase in tomato (Cogoni & Macino, 1999b; Schiebel et al., 1998) and required for PTGS by catalyzing the synthesis of dsRNAs in *N. crassa* (Cogoni & Macino, 1999a; Makeyev & Bamford, 2002b). Unlike *Qde-1* in *Tribulus terrestris* and *Methanosarcina thermophila* independent on primer to initiate short dsRNA biogenesis, *N.*

crassa Qde-1 synthesizes dsRNAs either de novo or relying on primer (Makeyev & Bamford, 2002b; Qian et al., 2016). In addition, overexpress *Qde-1* increased the production of dsRNAs and silencing efficiency (Forrest et al., 2004).

Qde-2 was identified homologous to Ago1 in *A. thaliana* and Rde-1 in *C. elegans* (Fagard et al., 2000a). Qde3 is an ortholog of RecQ DNA helicase in *Escherichia coli* and humans and loss of *Qde-3* abrogated quelling in *N. crassa* (Cogoni & Macino, 1999c), whereas its paralog *RecQ-2* not involved in regulation on quelling pathway but played a role in DNA repair together with *Qde-3* (Kato et al., 2004; Pickford et al., 2003). However, many studies show that DNA helicase functions in DNA replication, DNA transcription, DNA repair and DNA recombination, giving us a hint that the regulation of *RecQ* in RNAi might be a consequence of impaired transcription. The production of short dsRNAs was dependent on *Qde1* and *Qde3*, whereas *Qde2* not necessitated for siRNAs production despite it was required for quelling (Catalanotto et al., 2002), indicating that Qde-2 should be downstream of sRNA production, which was consistent with another document in *D. melanogaster* (Williams & Rubin, 2002). Direct evidence was further provided revealing that Qde2 cleaved passenger strand of sRNA duplex associating with Qip, a Qde-2-interacting protein that possesses exonuclease activity contributing to the degradation and removal of nicked passenger strands (Maiti et al., 2007; Xue et al., 2012). This slicing characteristics of Qde-2 on sense sRNAs strongly supports previous in vitro studies in *D. melanogaster*, showing that orthologous Ago2 binds with sRNA duplex and slices anti-guide strand as it conducts cleavage on mRNAs (Matranga et al., 2005; Meister & Tuschl, 2004; Miyoshi et al., 2005; Rand et al., 2005). Likewise, a study in fission yeast also confirmed that Ago proteins are required for sRNA maturation (Buker et al., 2007).

Dcl proteins were the last identified key component of RNAi factors in the quelling pathway in *N. crassa*. *N. crassa Dcl1* and *Dcl2* functioned redundantly in processing dsRNAs into short sRNAs in vivo and in vitro and $\Delta dcl1dcl2$ double deletion mutant blocked silencing in vegetative growth (Catalanotto et al., 2004). Strains with mutation on *Dcl1*, *Dcl2* and *Dcl1Dcl2* displayed normal mycelial growth and conidial development. By contrast, homozygous crosses of $\Delta dcl2$ mutants showed normal morphology in the sexual life cycle, while homozygous crosses of $\Delta dcl1$ mutants produced small and abnormal fertilized female sexual structures (perithecia) without asci inside (Alexander et al., 2008). So far, no evidence has been provided on the subcellular localization of RNAi components in vegetative growth in *N. crassa*.

1.2.4.2 Genes involving in MSUD

N. crassa is a haploid, heterothallic ascomycete containing two mating types (A and a) (Glass et al., 1988). Its sexual structure named protoperithecia can be formed by

nitrogen starvation on culture medium. Protoperithecia can also be artificially fertilized with an opposite mating type vegetative cell, normally conidia, to produce sexual fruiting body perithecium. Apart from silencing machinery in the fungal vegetative phase, gene silencing also exists during meiosis named MSUD. MSUD was initially called meiotic transvection (Aramayo & Metzenberg, 1996). The experimental idea in the study of Aramayo and Metzenberg originated from a forward genetic screen in *Aspergillus nidulans* (*A. nidulans*), in which some mutants defective in conidial development were isolated by observation on conidiophore morphology. One of the mutants loss of *stu-1* developed short and abnormal sterigma, producing very few conidia but unaltered mycelial growth rate (Clutterbuck, 1969). If we could identify a gene essential for *N. crassa* development and morphology, it would be an attractive candidate to investigate the silencing mechanism in the sexual reproductive cycle simply by observing the appearance of mutants and complementary strains. Luckily, the geneticists found *Asm-1* (ascospore maturation 1), an ortholog of *Stu-A* (*Stunted-A*) of *Aspergillus nidulans* (*A. nidulans*). Mutation of *Asm-1* failed to form female sexual structure in cross-culture medium and yielded inviable ascospores and displayed an ‘ascus-dominance’ phenomenon while crossing *asm-1* mutation strain and wild-type, which could be explained by the hypothesis that alleles must be in pair for being expressed or would be inactivated (Aramayo & Metzenberg, 1996). The proposal was reexamined with an additional experimental set-up by crossing two opposite mating-type strains carrying two copies of *Asm-1* at the native locus and ectopic position of *His-3* by Shiu and his colleagues. Their work demonstrated that unpaired DNA in meiosis resulted in the silencing of all homologous DNA, including genes paired, which indicates that alleles must not be unpaired during meiotic growth to prevent degradation (Shiu et al., 2001). Since then, the term of meiotic transvection was changed to MSUD.

Several mutants have been isolated involving in the MSUD pathway in *N. crassa*. Shiu et al. found a semi-dominant cross mutant *sad-1^{UV}* that repressed ascus dominance resulting from mutation of *Asm-1* (Shiu et al., 2001). *Sad-1* is a suppressor of ascus dominance encoding an RNA-dependent RNA polymerase and the vegetative growth of its mutation strains was normal as wild-type (Shiu et al., 2001). The finding of MSUD and *Sad-1* trigger microbiologists to discover other components in the silencing pathway in *N. crassa* sexual phase. In 2003, Lee et al. identified a paralog of *Qde-2* coined *Sms-2* which null mutants had no defects in mycelial growth and conidial development during the vegetative phase. By contrast, the phenotype of crosses of homozygous *sms-2^{RIP}* resembled the phenotype of homozygous crosses of *sad-1^{UV}*, producing inviable ascospores, indicating the necessity of *Sms-2* in MSUD (Lee et al., 2003; Shiu et al., 2001). Three years later, Shiu et al. isolated another meiotic suppressor named *Sad-2*. Homozygous crosses of the recessive *sad-2^{RIP}* mutant inactivated meiotic

prophase I of unpaired alleles and Sad-2 recruited Sad-1 for perinuclear colocalization, suggesting that *Sad-2* is required for the MSUD pathway (Shiu et al., 2006). Shiu and his colleagues had conducted a lot of genetic researches on MSUD machinery in *N. crassa* since 2001 when they added an experimental set-up for the guided work of Aramayo and Metzenberg and found MSUD. The PTGS components in sexual growth (including Sad-1 (RdRp), Sad-2 (meiotic suppressor), ReQ (helicase), Sms-2 (Ago-like), Qip (exonuclease) and Dcl1 (RNase III enzyme)) were proposed by Shiu's laboratory showing the interaction of all these proteins in the perinuclear region via BiFC approach (Alexander et al., 2008; Decker et al., 2015; Shiu et al., 2006). Notably, it seems that Sad-2 is vital for perinuclear localization by other MSUD partners as MSUD factors lose their localization on perinuclear in the absence of Sad-2 (Shiu et al., 2006). However, the experimental data they provided were unable to address that if the process of MSUD does not occur before colocalization of RNAi factors in the nuclear periphery or it functions normally in the cytoplasm. Meanwhile, at present, no evidence has shown the interaction of RdRp, Dcr/Dcl and Ago proteins in vivo in other organisms such as fruit flies, worms and animals with an exception for the interaction of Rde1, Rde4 and Dicer in *C. elegans*.

Currently, the generally believed model of PTGS in *N. crassa* is illustrated in **Figure 1.4**. During sexual reproduction at the stage of karyogamy, the whole genome is scanned spontaneously in *N. crassa* searching for unpaired alleles in non-sister chromatid, which will be silenced through the MSUD pathway. Sad-1 is responsible for synthesizing aberrant long dsRNAs interacting with Sad-2 and Sad-3 in the cytoplasm or nuclear periphery. Long dsRNAs are processed by Dcl-1, producing 20-25-nt siRNA duplexes, which are incorporated into Ago-like protein Sms-2. With the help of exonuclease activity from Qip, passenger strand of siRNA duplexes is sliced and released by Sms-2, forming an activated RISC-like complex and initiating guide siRNA-directed recognition on completely or partially complementary mRNA targets for degradation (Chang et al., 2012; Hammond et al., 2011; Quoc & Nakayashiki, 2015). In contrast, aberrant RNAs from discrete loci are catalyzed by Qde-1 forming long dsRNAs during vegetative growth. The resulting dsRNAs and miRNA precursors are diced by Dcl-1 or Dcl-2 generating 20-25nt (siRNAs) and 18-28nt (miRNAs) (Lee et al., 2010) in length sRNA duplexes, respectively. sRNA duplexes subsequently are loaded into Qde-2, recruiting Qip to remove passenger strand siRNA. Activated RISC complex target cognate mRNAs complementary to guide sRNAs resulting in degradation or translational repression (Chang et al., 2012; Quoc & Nakayashiki, 2015; Xue et al., 2012).

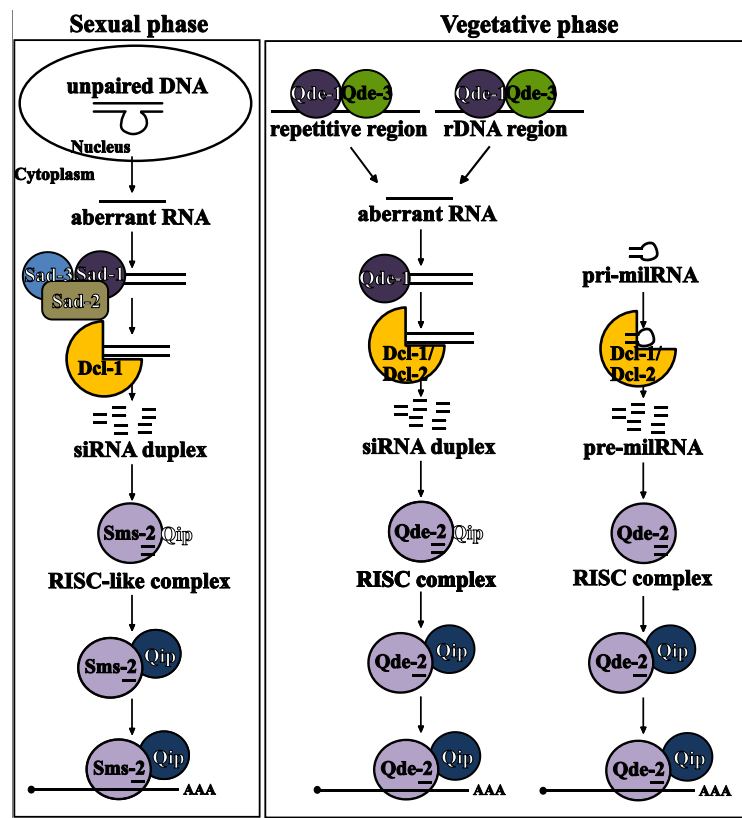


Figure 1.4 Illustration of PTGS model in *N. crassa* (Figure modified from (Chang et al., 2012; Xue et al., 2012))

The left panel shows the process and proteins involving in gene silencing in the MSUD pathway. The right panel shows the process and components functioning in quelling in the vegetative cycle.

1.2.5 Cross-kingdom RNAi

RNAi has been generally believed a machinery particularly for viral defense and numerous previous works have focused on RNAi in plant or pathogen in response to virus (Baumberger et al., 2007; Brosseau & Moffett, 2015; Derrien et al., 2018; Duan et al., 2012; Garcia-Ruiz et al., 2015; Morel et al., 2002; Neupane et al., 2019; Schott et al., 2012; van Rij et al., 2006; Wu et al., 2017; Zhang et al., 2006). Until 2007, a study showed that RNAi also played a role in anti-bacterial response. Loss-of-function mutant $\Delta ago4$ reduced *Arabidopsis* pathogenicity to *Pst* DC3000 (Agorio & Vera, 2007). Another study revealed that Ago4-miR393* complex contributes to plant immunity against *Pst* Dc3000 by regulating a SNARE gene, *MEMB12* to increase the release of PR protein from a cell (Zhang et al., 2011). RNAi also contributes to anti-fungal defense in host plants. Evidence were provided showing that RNAi in *Arabidopsis* is necessary for defense against multiple vascular fungi in the genera of *Verticillium* (Ellendorff et al., 2009). TasiRNA mediated RNAi also regulates nodulation in *Lotus japonicus* via auxin and ethylene signaling pathway (Li et al., 2014). Intriguingly, with more and more in-depth research on the biological function of the RNAi pathway, RNAi

mechanism is found not only an endogenous genome maintenance machinery but also act as a defense weapon traveling cross species and hijacking enemy's immune genes, which is called cross-kingdom RNAi (ckRNAi) and has been discovered among diverse organisms and their interacting hosts. Report revealed that *Botrytis* LTR1-derived sR3.1, siR3.2 and siR5 loaded into host Ago1 and targeted plant immune-related genes *PRXIIIF*, *MAK1/MAK2* and *WAK*, respectively, impairing immunity in planta (Weiberg et al., 2013). *Botrytis* siR37 inhibited *Arabidopsis* *WRKY7*, *PMR6* and *FEI2* to enhance the host's susceptibility (Wang et al., 2017). Rhizobia sRNAs derived from tRNA competed binding to legume Ago1 to regulate nodulation (Ren et al., 2019). Cross-kingdom RNAi also exists in oomycetes. Studies showed that a phytophthora effector PSR2 targeted tasiRNAs in *Arabidopsis* significantly enhancing the susceptibility of planta (Hou et al., 2019) and *Hyaloperonospora arabidopsidis* used host Ago1 to silence host immune genes (Dunker et al., 2020). The observation of cross-kingdom RNAi indicates the existence of the sRNAs secretion pathway in organisms. Some *Arabidopsis* tasiRNAs and miRNAs translocated to *Botrytis* via extracellular vesicles during plant-pathogen interaction. For example, *Botrytis* siR483 derived from TAS1c loci and siR453 originated from TAS2 loci inhibited *Arabidopsis* *VPS51/DCTN1* and *SAC1*, respectively by cross-kingdom RNAi, impairing plant immunity during plant-pathogen interaction (Cai et al., 2018). Likewise, various secondary sRNAs bound with Ago proteins were secreted to the extracellular environment by exosome-like extracellular vesicles in the gastrointestinal nematode *Heligmosomoides bakeri* (Chow et al., 2019). However, whether *Botrytis* adopts a similar approach delivering sRNAs via EVs into host plants remains obscure.

1.3 Argonaute proteins

1.3.1 Crystal structure and mechanism

Argonaute (Ago) proteins are the core component in RISCs and critical for RNA-mediated gene silencing, which exists in many prokaryotes, archaea and eukaryotes. In contrast to eukaryotic Ago proteins that recognize RNAs, most bacterial Ago proteins were reported association with guide DNAs giving rise to DNA interference (Hegge et al., 2019; Kuzmenko et al., 2020; Kuzmenko et al., 2019; Makarova et al., 2009; Sheng et al., 2014; Swarts et al., 2015; Swarts et al., 2014), whereas Ago from a bacteria *Rhodobacter sphaeroides* was also found binding with guide RNAs and targeting base-paired DNAs (Miyoshi et al., 2016). Although Ago sequences share low homology in prokaryote and eukaryote, the architecture of Agos is rather conserved in archaea and prokaryote and eukaryote (flies, mammals, plants and fungi). Crystallographic studies

on Ago proteins have shown that the overall protein structure looks like a bilobal architecture (**Figure 1.5**) comprising one lobe with amino-terminal domain and a PAZ domain binding 3'-end of anti-sense sRNAs, the other lobe with a middle (Mid) domain that adopts a Rossman-like fold, sensing and offering a binding pocket for 5'-phosphate anti-sense sRNAs and a PIWI (P-element-induced wimpy testis) domain that belongs to ribonuclease H and possess endonucleolytic activity in some Ago proteins, e.g., Human Ago2 (Matranga et al., 2005) and fission yeast Ago1 (Liu et al., 2004).

The crystal structure of the PAZ domain has been solved in archaea *Pyrococcus furiosus* (Song et al., 2004) and *Thermococcus thioeducens* (Wang et al., 2008), bacteria *Aquifex aeolicus* (Rashid et al., 2007) and animals encompassing *Drosophila melanogaster* (Lingel et al., 2003), *Homo sapiens* (Rashid et al., 2007) and *Mus musculus* (Simon et al., 2011) and yeast *Kluyveromyces polysporus* (Nakanishi et al., 2012). PAZ domain adopts an OB-like fold (Song et al., 2004). The binding of PAZ domain has no sRNA sequence bias, showing similar binding affinity in distinct small RNA classes. Nevertheless, the PAZ domain strongly reduced binding affinity to sRNA molecules that were in the absence of 2-nt 3' overhangs (Lingel et al., 2004), which is consistent with the sRNA products of Dicer (5' phosphate and 3' hydroxyl) (Zhang et al., 2004). Two aromatic residues Phenylalanine (codon: F) are critical for RNA binding to 3' 2-nt overhang of guide RNAs (Lingel et al., 2003; Song et al., 2003; Song et al., 2004).

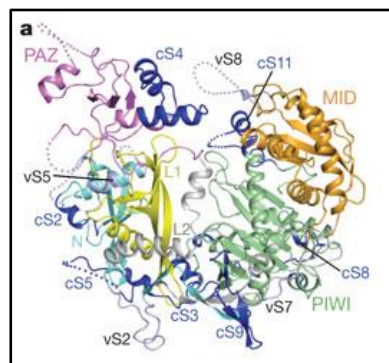


Figure 1.5 Crystal structure of full-length Argonaute proteins in *Kluyveromyces polysporus* (Figure from (Nakanishi et al., 2012))

The crystal structure of MID domain has been solved in animals *H. sapiens* (Frank et al., 2010) and *M. muscus* (Cora et al., 2014), fungus *N. crassa* (Boland et al., 2011) and plant *A. thaliana* (Frank et al., 2012). The architecture of MID domain adopts traditional nucleic acid binding fold, i.e., Rossman-like fold. MID domain is unable to bind sRNAs in the absence of PIWI, whereas the PIWI domain alone can bind with guide sRNAs at a reduced affinity in *N. crassa* (Boland et al., 2010). By contrast, *Arabidopsis* Ago1 Mid domain resembles the binding affinity of PIWI domain, indicating a more significant role of the Mid domain in sRNA binding in *A. thaliana* (Zha et al., 2012).

The crystal structure of the PIWI domain has been available in archaea *Pyrococcus furiosus* (Song et al., 2004) and *Archaeoglobus fulgidus* (Ma et al., 2005; Parker et al., 2004), bacteria *Aquifex aeolicus* (Yuan et al., 2005), fungi *Neurospora crassa* (Boland et al., 2011) and *Kluyveromyces polysporus* (Nakanishi et al., 2012), animals *Homo sapiens* (Tian et al., 2011), *Bombyx mori* (Matsumoto et al., 2016) and *Drosophila melanogaster* (Yamaguchi et al., 2020). The architecture of the PIWI domain adopts an RNase H fold with a conserved active site aspartate-aspartate- aspartate motif (DDD) in *N. crassa* that is less common than aspartate-aspartate-glutamate (DDH) (Buddhika et al.) (Buddhika et al., 2020) in most eukaryotic Agos (Nakanishi et al., 2012). However, endoribonuclease activity is not a global property for Agos even if they contain DDD/H motif. In human, Ago2 exclusively cleave target mRNAs (Liu et al., 2004). Likewise, evidence have been demonstrated that Ago1, Ago2, Ago4, Ago7 and Ago10 possess catalytic activity in *A. thaliana* (Baumberger & Baulcombe, 2005; Carbonell et al., 2012; Ji et al., 2011; Montgomery, Howell, et al., 2008; Qi et al., 2005; Qi et al., 2006; Zhu et al., 2011). Ago proteins cleave guide sRNA/mRNA hybrids at the phosphodiester bond between 10 and 11 nucleotides from 3' terminus of guide RNA, releasing a 9-nt 5' product with 5' phosphate and a 12-nt 3' product with 3' hydroxyl termini (Martinez & Tuschl, 2004). In most cases, 3' cleavage products of mRNA are degraded by 3' exosome after deadenylation (Chekanova et al., 2007), while uncapped 5' cleavage products of mRNA undergo degradation by 5'-exoribonuclease (XRN1/XRN4/EIN-5) (Olmedo et al., 2006; Orban & Izaurralde, 2005; Souret et al., 2004). For miRNAs (most plant and mammalian miRNAs) that are incompletely complementary to RNA transcripts, gene silencing is achieved by inhibiting the translation of the target mRNAs instead of mRNA cleavage, following by mRNA decay (Brodersen et al., 2008; Chen, 2004; Cho et al., 2017; Djuranovic et al., 2012; Eulalio et al., 2008; Hou et al., 2016; Huntzinger et al., 2013; Iwakawa & Tomari, 2013; Li et al., 2013; Yang et al., 2021). Consistent with the RNase H enzyme, Ago proteins also need divalent metal ions as cofactors binding to DDD/H motif to complete the cleavage reaction. For example, Magnesium combined with the DDH motif was found in the crystal of *P. furiosus* Ago2 (Rivas et al., 2005).

The amount of Agos varies considerably in each organism. Many Agos and homologs were cloned and identified in distinct organisms two decades ago such as Qde-2 in *N. crassa* (Cogoni & Macino, 1997), Rde1 in *C. elegans* (Tabara et al., 1999) and PIWI in *D. melanogaster* (Pal-Bhadra et al., 2002). The seed region 5' 2-8-nt of miRNA is vital for mRNA target recognition and binding (Czech et al., 2008; Lewis et al., 2005; Lewis et al., 2003).

1.3.2 Subcellular localization

The subcellular location of Ago proteins has been described in plants, animals and fungi. Ago proteins are associated with mRNA degradation or translational inhibition and processing bodies (P bodies) are a vital compartment for non-translated mRNA decay and storage. A report has shown that mRNA turnover occurred in cytoplasmic P bodies (Sheth & Parker, 2003), which was consistent with previous findings demonstrating that mRNA degrading enzymes Dcp1/2 (de-capping enzyme) and XRNI (exonuclease) resided in cytoplasmic foci in human cells (Ingelfinger et al., 2002; van Dijk et al., 2002). Likewise, human Ago2 localized in cytoplasmic granules where mRNA degradation and translational repression occur, but sRNA binding was not required for localization of cytoplasmic bodies (Sen & Blau, 2005). Instead, RNAs were necessary for the formation of P bodies (Sen & Blau, 2005), which was confirmed by another study, revealing that RNAs were necessary for P bodies assembly (Teixeira et al., 2005). By contrast, report showed that human Ago2 resided in P bodies and the localization of mRNAs for degradation was dependent on miRNAs (Liu et al., 2005). Moreover, Ago2 localized in P granules and resided in cytoplasm and stress granules (Leung et al., 2006). Similarly, *C. elegans* Alg-1 (Ago) localized in cytoplasmic P bodies (Ding et al., 2005) and *Arabidopsis* Ago1 resided in the endoplasmic reticulum and associated with Amp1 directed by miRNAs to cause mRNA translational inhibition (Li et al., 2013). Further, Agos locate in cytoplasm and P bodies in *M. oryzae* (Nguyen et al., 2018) and *Arabidopsis* Ago1 could export mature miRNAs from the nucleus to the cytoplasm (Bajczyk et al., 2019; Bologna et al., 2018; Pare et al., 2009).

Unlike animal cells that the biogenesis of mature sRNA molecules by RNase III enzyme (Drosha and Dcr) localizes in both nucleus (Drosha) and cytoplasm (Dcr), plant sRNA duplexes are generated by Dcl in the cytoplasm. By fluorescence tagging and tracking on Ago proteins in plant cells, studies uncovered that different Ago proteins localize in distinct cellular compartments depending on their functions as shown in **Figure 1.6**. *Arabidopsis* Ago4 resembled with hc-siRNAs (heterochromatin siRNAs) in the cytoplasm and translocated to the nucleus in Cajal body nearby nucleolus for heterochromatin regulation (Li et al., 2008; Li et al., 2006; Ye et al., 2012). Likewise, the mobilization of Ago1-mature miRNA complex from the nucleus to the cytoplasm was required for RNAi (Bologna et al., 2018). Ago1 also functioned in the endoplasmic reticulum, giving rise to translational inhibition in *A. thaliana* (Li et al., 2013). In contrast, Ago7 localized in cytoplasmic siRNA bodies different from processing bodies (P bodies) for tasiRNA generation. (Jouannet et al., 2012), whereas mammalian Ago2-sRNA complex localized in P bodies (Sen & Blau, 2005).

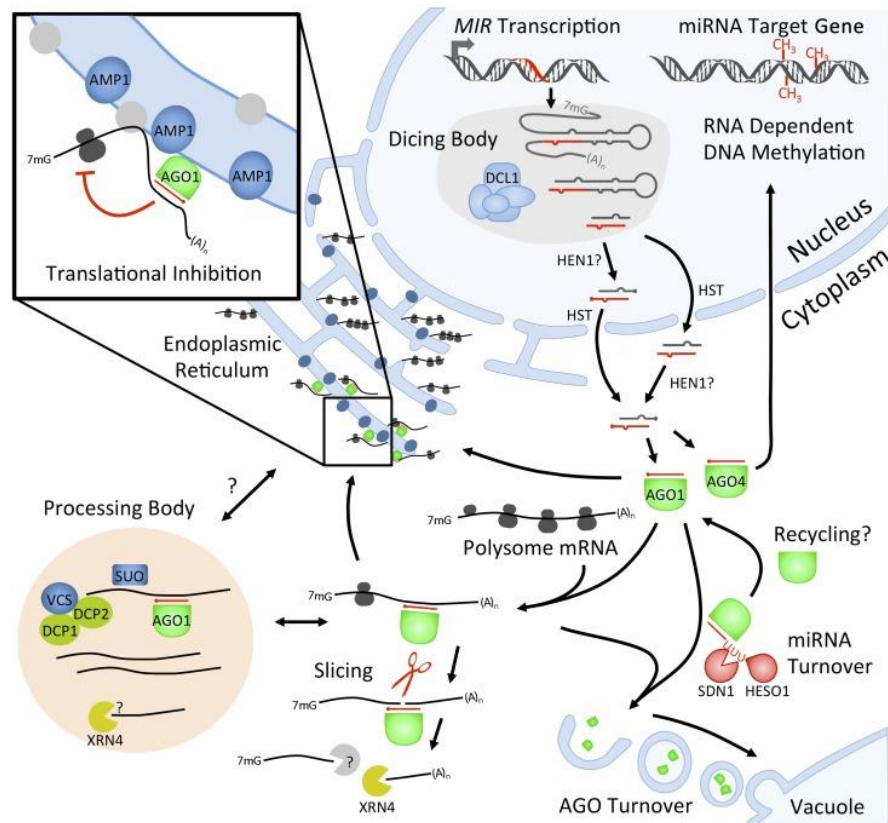


Figure 1.6 Illustration of gene silencing pathway in *A. thaliana* (Figure from (Rogers & Chen, 2013))

1.3.3 Agos in fungi

N. crassa comprises two paralogous Ago proteins (*Qde-2* and *Sms-2*). *Qde-2* was isolated in *N. crassa* by mutagenesis on stable strains of *al-2* (*albino-2*) containing distinct copies of *Albino* transgenes (Cogoni & Macino, 1997). Δqde deficient mutant recovered the quelled phenotype of *al-2* and displayed orange phenotype with the presence of endogenous *Albino* gene and high copies of *Albino* transgenes. *Qde-2* was homologous to *Ago1* in *A. thaliana* and *Rde-1* in *C. elegans* (Fagard et al., 2000a). The production of short dsRNAs was dependent on *Qde1* and *Qde3*, whereas *Qde2* not necessitated for siRNAs production despite it was required for quelling (Catalanotto et al., 2002), indicating that *Qde-2* should be downstream of sRNA production, which was consistent with another document in *D. melanogaster* (Williams & Rubin, 2002). Direct evidence further revealed that *Qde2* cleaved passenger strand of sRNA duplex associating with *Qip*, a *Qde-2*-interacting protein that possesses exonuclease activity contributing to the degradation and removal of nicked passenger strands (Maiti et al., 2007; Xue et al., 2012). This slicing characteristics of *Qde-2* on sense sRNAs strongly supports previous in vitro studies in *D. melanogaster*, showing that orthologous *Ago2* bound with sRNA duplex and slices anti-guide strand as it conducted cleavage on mRNAs (Matranga et

al., 2005; Meister & Tuschl, 2004; Miyoshi et al., 2005; Rand et al., 2005). Likewise, a study in fission yeast also confirmed that Ago proteins were required for sRNA maturation (Buker et al., 2007). *Colletotrichum higginsianum* $\Delta ago1$ and $\Delta ago2$ deletion mutants affected vegetative growth and conidial shape and *Ago1* mutation strain suppressed sporulation (Campo et al., 2016). *Agl-2* null mutant reduced the mycelial growth rate and *Agl-4* mutation strain unaltered vegetative morphology in *Sclerotinia sclerotiorum* (Neupane et al., 2019). *M. oryzae* contains three Ago proteins. Ago1 and Ago3 functioned redundantly in RNAi and Ago2 negatively regulated retroelement (MAGGY)-triggered silencing machinery (Nguyen et al., 2018).

1.3.4 Agos in *A.thaliana*

1.3.4.1 Agos categories

A. thaliana encompasses 10 Ago proteins which are divided into three groups. Ago1, Ago5 and Ago10 belong to the same clade; Ago2, Ago3 and Ago7 belong to the same clade; Ago4, Ago6, Ago8 and Ago9 fall into the same clade (Morel et al., 2002; Vaucheret, 2008). Among them, Ago1, Ago2, Ago4, Ago7 and Ago10 possess slicing ability (Arribas-Hernandez et al., 2016; Baumberger & Baulcombe, 2005; Carbonell et al., 2012; Ji et al., 2011; Montgomery, Howell, et al., 2008; Qi et al., 2006; Yu et al., 2017; Zhu et al., 2011). *Arabidopsis* Ago genes are differentially expressed in distinct growing stages and plant tissues. The expression of *Ago1*, *Ago4* and *Ago10* were relatively higher than others and *Ago8* was the lowest expressed gene (Mallory & Vaucheret, 2010). Ago1, Ago4, Ago7 and Ago10 are the most characterized Ago proteins in *A. thaliana*. Numerous works have demonstrated that Ago proteins regulate diverse pathways in root growth, shoot apical meristem (SAM) development, flowering in response to biotic stress, abiotic stress, transposition of transposable elements and retroelements. Notably, Ago4 plays a vital role in regulating heterochromatin in the nucleus by RdDM (Qi et al., 2006; Zilberman et al., 2003; Zilberman et al., 2004).

1.3.4.2 Agos and associated sRNAs

It should be noted that only fully paired miRNA-mRNA duplex causing mRNA degradation (Hutvagner & Zamore, 2002). Thus, the complementarity between guide miRNAs and mRNA targets is critical for silencing. Some miRNAs are independent of Ago cleavage activity even if Ago proteins contain endoribonucleolytic activity. These miRNA molecules are partially complementary to mRNA molecules, loading into and generally resulting in translational inhibition to regulate gene expression (Brodersen et al., 2008; Iwakawa & Tomari, 2015). One significant role of Ago proteins is the sorting strategy on distinct sRNA species. RIP-sequencing shows that Ago1 binds with most

21-nt miRNAs whose 5' nucleotide is Uridine (Mi et al., 2008). However, how Ago proteins distinguish different sRNA molecules or how certain types of sRNAs are loaded into specific Ago proteins remain obscure. Some Ago proteins such as Ago4 mainly function in nucleus guided by 24-nt sRNAs leading to TGS through RdDM (RNA-dependent DNA methylation) pathway (Duan et al., 2015; He et al., 2009; Qi et al., 2006; Wang et al., 2011; Zilberman et al., 2003; Zilberman et al., 2004), whereas some Ago proteins such as Ago1 mainly localize in cytoplasm guided by 21-oligomers giving rise to PTGS (Baumberger & Baulcombe, 2005; Fagard et al., 2000b; Ma & Zhang, 2018; Wang et al., 2011). In addition to primary sRNAs, secondary siRNAs were firstly discovered in *C. elegans* (Sijen et al., 2001). These secondary siRNAs are termed trans-acting RNAs (tasiRNAs) in plants as they differ from classic cis-siRNAs that silence genes where they originate. TasiRNAs, ~21-nt in length, are vital for plant growth and development, which has already evolved in the early days (Axtell et al., 2006; Peragine et al., 2004). Four TAS families generating tasiRNAs have been identified in *A. thaliana* encompassing TAS1 (TAS1a, TAS1b, TAS1C), TAS2, TAS3 (TAS3a, TAS3b, TAS3c) (Allen et al., 2005; Howell et al., 2007; Rajagopalan et al., 2006; Vazquez et al., 2004) and TAS4 (Peragine et al., 2004; Vazquez et al., 2004; Wang et al., 2011). Sgs3, Rdr6, Dcl4 and 21-22-nt miRNAs are critical for the biogenesis of tasiRNAs (Allen et al., 2005). Ago1/miR173 (22-mers) complex produce tasiRNAs derived from TAS1 and TAS2 loci and Ago7/miR390 (21-nt) complex generate TAS3-derived tasiRNAs (Allen et al., 2005; Endo et al., 2013; Montgomery, Howell, et al., 2008; Montgomery, Yoo, et al., 2008; Yoshikawa et al., 2005), whereas Ago1/miR826 (21-nt) complex trigger the generation of tasiRNAs from TAS4 loci (Rajagopalan et al., 2006).

Aims of the thesis

RNAi acts as a conserved defense machinery against viruses, bacteria and fungi in prokaryotes and eukaryotes. Agos are the core components of RNAi and play vital roles in diverse cellular processes, development and numerous responses to biotic stresses. ckRNAi is a new intriguing chapter in pathogen-host interaction. *Botrytis* sRNAs used host Ago/RISC to manipulate plant physiology and immunity, which highlights the central function of Agos in ckRNAi. In addition, ckRNAi is bidirectional as plants deliver sRNAs into *Botrytis* to inhibit fungal genes related to virulence. These findings raise the hypothesis that Ago proteins might involve in pathogenicity regulation by controlling fungal virulent genes or pathogen sRNA effectors.

In this doctoral project, *B. cinerea*-tomato was utilized as a pathosystem. With the hypothesis, I aim to employ genetics, molecular biology and transcriptomics approaches to generate *Ago* disruption and complementary mutants for phenotypical and molecular analyses at the level of mRNA and sRNA expression. Thus, the first aim of the thesis was to identify *Botrytis* *Ago* genes involving in the PTGS pathway in response to infection on tomatoes, and the second aim was to shed light on the possibility that translocated host sRNAs might target *Botrytis* *Ago* genes to inhibit virulent genes as a defense mechanism. To fulfill these two goals, I would like to answer five puzzles: I. Do *Ago* genes regulate virulence in *Botrytis cinerea*? II. Do *Ago* proteins stabilize small RNAs in *Botrytis cinerea*? III. Does *Ago*-mediated stabilization on small RNAs associate with *Botrytis* pathogenicity? IV. What are the DEGs associated with virulence in *Ago*-deficient mutants compared to wild-type? V. Are DEGs related to virulence regulated by endogenous sRNAs via *Ago* proteins in *B. cinerea*? Overall, I aim to describe the function of *Botrytis* *Ago* proteins in pathogenicity and ckRNAi, which should provide insights into the interactions between fungi and their hosts.

2. Material and Methods

2.1 Plant materials

Solanum lycopersicum (Cultivar Hanz and money maker) seeds were germinated 5 days in a petri dish covered by two wet filter papers under darkness at 24°C. They then were transplanted to soil and grew in an insect-free binder chamber under controlled condition (16h light/8h dark, 24°C, 58% relative humidity). *Arabidopsis thaliana* Columbia ecotype (Col-0) seeds were treated with coldness at 4°C for 3 days before germinated in the soil in the climate chamber for 7 days. Germinated seedlings were transplanted to soil and grown under short-day conditions (8h light/16h dark, 22°C, 60% relative humidity).

2.2 *Botrytis cinerea* growth

2.2.1 *Botrytis cinerea* strains and maintenance

B. cinerea Pers. Fr. (*Botryotinia fuckeliana* [de Bary] Whetzl) strain B05.10 was firstly isolated from the grape in 1994 (Buttner et al., 1994). This strain was used as transformation recipient in the study. *Botrytis* wild-type strains were cultured on complete media HA agar (Doehlemann et al., 2006). Argonaute gene disruption strains were grown on HA media amended with hygromycin (Roth, 70ug/ml). Complementary strains *cAgo2* were plated on HA media supplemented with nourseothricin (WERNER Bio-Agents, 120µg/ml) as selection. All *Botrytis* strains were cultivated at 20°C under constant irradiation for conidiation or under constant dark condition. Sporulated mycelia of *Botrytis* were eluted with distilled water and filtered by Miracloth (Merck Millipore) to get pure conidial suspensions. Spores were stored in 25% glycerol and kept at -80°C for a long-term storage. Mycelial plugs (Ø=0.4 cm) were collected in distilled water at 4°C for a temporary storage. Mycelia collected from infected tomato leaves were stored for inoculation assay to activate fungal virulent genes. *Botrytis* transgenic strains used in the study are listed in **Table 2**.

2.2.2 Mycelial growth

For observation of the growth rate of *Botrytis* wild-type and transgenic strains, a droplet of a suspension (15µl, 10⁶ spores/ml) with spores in distilled water was pipetted on HA agar media. Petri dishes were incubated for 4 days at room temperature under dark condition. Mycelial growth was determined by measuring the radial growth of colonies

from two independent transformants for each genotype with twelve biological replicates.

2.2.3 Conidium morphology

Conidia were collected from HA media culturing for two weeks under constant light to observe the conidial shape of *Botrytis* wild-type and transgenic strains. Conidium width and length were measured from over 200 spores for each transformant.

2.2.4 Sporulation

Conidia were eluted in 20ml distilled water by stirring sporulated mycelium on media plates. The number of conidia produced was determined by counting the spores microscopically with the hemocytometer (Neubauer improved, Marienfeld). Each genotype had six biological replicates.

2.3 Generation of transgenic *Botrytis cinerea*

2.3.1 Identification and phylogeny of Argonaute proteins

Botrytis cinerea Argonaute proteins were identified by searching the protein databases for homologies of Qde-2 in *Neurospora crassa* using BLAST search (Altschul et al., 1990) under the E-value at 10, word size at 3, with Matrix x Blosum80 and Gap Costs existence 11 extension 1 filtering out low complexity region. The rooted phylogenetic tree was constructed with amino acid sequences of filamentous fungal Argonaute proteins in phyla of Ascomycota by RAXML method with JTT model. Fungal species and their accession number were listed in **Table 3**. The alignment was performed by MAFFT and bootstrap was calculated based on 1000 replicates. The phylogenetic tree was built at CIPRES (Miler et al., 2010) and gene structure was illustrated at Gene Structure Display Server (GSDS) (Hu et al., 2015). Protein conserved domains were identified by searching at Pfam database under the E-value at 10.

2.3.2 Vector construction

Plasmids were constructed based on the Golden Gate toolkit (Binder et al., 2014) and were propagated in *Escherichia coli* strain Top10. For the Δago knockout (ko) constructs, 5' and 3' homologous arms flanking *Ago1*, *Ago2*, *Ago3* and *Ago4* were amplified using genomic DNA of wild-type as a template and fused with hygromycin phosphotransferase (*hph*) cassette amplified from pCSN44 with the tryptophan synthase (*trpC*) promoter from *Aspergillus nidulans* (Carroll et al., 1994). Plasmids harboring

Ago disruption segments were introduced into *Botrytis* wild-type protoplast. BpiI and BsaI cutting sites in *Ago1* and *Ago2* were mutated by overlapping primers before cloning. For the *AGO1_{pro}-3xHA::AGO1* (*cAgo1*) and *AGO2_{pro}-3xHA::AGO2* (*cAgo2*) complementation constructs, *3xHA* was fused to 5' terminus of full *Ago1* or *Ago2* gene with a *nat1* gene cassette which confers nourseothricin resistance (Malonek et al., 2004) under the control of the native promoter. The transformation was conducted under the mutation background of *Ago1* or *Ago2*.

For the *Ago1_{pro}-eGFP:Ago1:3xHA* and *Ago2_{pro}-eGFP:Ago2:3xHA* constructs, I ligated codon-optimized *eGFP* and *3xHA* with complete *Ago2* gene at 5' terminal and 3' terminal, respectively. Transformation for plasmids of GFP labeled *Botrytis* was performed under the wild-type background. *eGFP* and *3xHA* were cloned using respective plasmid *pNAH-OGG* (Schumacher et al., 2012) and *pAMPATp35S:3xHA-CYCLOPS* (Singh et al., 2014). All constructed plasmids were verified using PCR amplification and sequencing prior to generating transgenic strains. Phusion High-Fidelity DNA Polymerase (Guinebretiere et al.) was used for gene cloning with Cycler (Analytic Jena) at conditions of initial denaturation at 98°C for 30s, then 32 cycles of 98°C for 10s, annealing at 58°C for 30s and extension at 72°C for 15s-45s (1kb/30s) followed by 5min additional extension at 72°C. Primer oligos used for amplification are listed in **Table 4**.

2.3.3 Protoplast transformation and homokaryotic purification

Linear fragments digested with BpiI from constructed plasmids were introduced into protoplast of wild-type *Botrytis* or $\Delta ago2$ deletion mutant using polyethylene glycol (De Zotti et al.) -mediated protoplast transformation as described before (Hamada et al., 1994) with minor modifications.

Protoplast preparation. Young mycelium was harvested and washed twice by 0.6M KCl and 0.1M NaP for osmotic stabilization. After filtration with sterile miracloth, mycelium was gently suspended in glucanex solution (0.6M KCl, 0.1M NaP, 1% Glucanex (Sigma-Aldrich), 1M KOH) for cell wall digestion, followed by incubation at 23°C on a rocky 3D shaker (TRM50) for 2 hours. The digested suspension was filtered through miracloth and protoplasts were pelleted by centrifugation at 3500rpm for 5 minutes, which were gently washed twice with TMS buffer (1M Sorbitol, 0.01M MOPS, PH=6.3, NaOH) and resuspended in TMS buffer (1M Sorbitol, 0.01M MOPS, 0.05M CaCl₂, PH=6.3, NaOH).

Transformation. A suspension of 100ul aliquot containing at least 2×10^7 protoplasts was maintained on ice for 10 minutes. Next, 15ug linearized fragments in Tris-CaCl₂ (10mM Tris-HCl, 1mM EDTA, 40mM CaCl₂, PH=6.3, NaOH) were gently mixed with

protoplast and incubated on ice for regeneration for 10 minutes. The mixture was then added with 160ul 60% PEG3350 (Merck), incubating for 20 minutes at room temperature in case of PEG precipitation, followed by softly mixing with 680ul TMSC and centrifuged for 5 minutes at 3200rpm. PEG was removed with pipette and pellet was resuspended in 200ul TMSC. Finally, transformed protoplast was softly mixed in 30ml melted SH-agar (45°C) and distributed equally on two petri dishes for regeneration. The protoplast on the media was overlaid with 20ml HA agar embedded with 70µg/ml Hygromycin B or 120µg/ml Nourseothricin on the other day.

Purification. Colonies grown on selectable media were transferred to new HA media with 70µg/ml Hygromycin B or 120µg/ml Nourseothricin. Transformants carried with correct insertion in *Botrytis* genome and verified by genotyping and southern blotting were used for homokaryotic purification. Hyphal tips of transformants were transferred to HA media with a selectable marker. The procedure was conducted several times until homokaryotic transformants were obtained.

2.3.4 Genomic DNA extraction and genotyping

Genomic DNA of pure mycelium or sporulated mycelium was isolated from at least 30 transformants for each construct using CTAB (2% cetyltrimethylammonium bromide, 1% polyvinyl pyrrolidone, 100 mM Tris-HCl, 1.4 M NaCl, 20mM EDTA) according to the previous method (Murray & Thompson, 1980) prior to chloroform/isoamyl alcohol extraction and isopropanol precipitation (Chen & Ronald, 1999) with minor modifications (Allen et al., 2006). Mycelia growing on HA media dishes (10cm) were harvested after cultivation for five to seven days in constant light or overlaid with cellophane for three days under constant dark condition. Six pairs of primers were used for genotyping transgenic transformants for each genotype of *B. cinerea*. GoTaq G2 DNA Polymerase (Promega) and homemade Tap Polymerase were used for genotyping with cyclical condition initiated at 95°C for 2min, then 30 cycles of denaturation at 95°C for 30s, annealing at 58°C for 30s and extension at 72°C for 20s-180s (1kb/min), followed by 5min extension at 72°C. Primer oligos used for genotyping were listed in **Table 4**.

2.3.5 Integration verification by southern blotting

Genomic DNA of putative *Ago* deletion mutants was extracted using Phenol/Chloroform/Isoamyl alcohol as described previously (Chen & Ronald, 1999). Probes were cloned with oligonucleotides (**Table 4**) and labeled with Digoxigenin by amplification using Probe labeling Kit Pcr DIG Probe Synthesis Kit (Roche). The amplification profile was initiated with pre-denaturation at 94°C for 5 minutes, followed by 40 cycles PCR of 30s at 94°C, 30s at 58°C and 1min at 72°C with 5 min additional extension at

the final step. Integration of constructed fragments was examined using southern blot as previously described (Southern, 1975) using DIG high prime kit II (Roche) with minor modifications. 20µg of gDNA was digested by implicated restriction enzymes (**Figure 3.6**) in a 37°C water-bath (Medingen) overnight and separated by 0.8% agarose gel at 30 voltage for 16 hours. After denaturation and neutralization, gDNA was subsequently transferred to positively charged nitrocellulose membrane (Merck) overnight by upward capillary approach, followed by fixation using Stratalinker 1800 (Stratagene) with exposure at 1200 microjoules (x100) for 25-50s. The membrane was then transferred in a hybridization tube and prehybridized for 1 hour and incubated with a denatured DIG-labeled probe overnight. On the other day, the hybridized membrane was washed twice using less stringency solution for 5min each time and then stringency solution for 20min per wash. The membrane was washed once using washing buffer, followed by blocking for 30min, incubation with the anti-DIG antibody for 30 minutes and then washing twice with washing buffer for 15min each time. After equilibration for 5min in detection buffer, the membrane was incubated with CSPD for 10min in a 37°C incubator for chemiluminescence and exposed using the equipment (Fusion-SL 3500). Primers used for probe cloning were listed in **Table 4**.

2.3.6 Western blot

Botrytis genetically modified strains were grown for three days on HA media overlaid with cellophane under constant dark condition. Fresh Mycelia (200mg) were homogenized by mortar and pestle and suspended in 1ml lysis buffer according to the previous method (50mM Tris-HCl PH7.5, 100mM NaCl, 5mM EDTA, 1% Triton X-100, 2mM PMSF) (Yin et al., 2018) with 10µl of cOmplete™ Protease Inhibitor Cocktail (Merck) (25X). The lysate was incubated on a vertical wheel and centrifuged for 5 min at 4°C. The crude proteins were separated with 6% SDS-polyacrylamide gel at 80 voltages for 30min and 120 voltage for 1.5-2 hours and transferred to PVDF membrane (Immobilon-FL) using Bio-Rad casting apparatus overnight at 4°C. The primary monoclonal α-HA antibody (3F10, Roche) and α-GFP antibody were used at respective 1:1000 dilution and 1:5000 dilution, incubating with PVDF immobilized protein for 1.5 hours. This was followed by incubation overnight at 4° with secondary antibody α-rat IRdye800 (LI-COR, 1:15000 dilution) or α-mouse IRdye800 (LI-COR, 1:15000 dilution). Proteins were detected with the Odyssey imaging system (LI-COR). All procedures were manipulated on ice or at 4°C condition.

2.4 Gene expression

2.4.1 Total RNA extraction

Total RNA was extracted by CTAB buffer as described in pine tree (Chang et al., 1993) with minor modifications (2% CTAB, 2% PVP, 100mM Tris-HCl (pH=8.0), 25mM EDTA (pH=7.5), 2M NaCl, a spatula PVPP (Merck, added prior to use), TCEP (0.5M, Sigma-Aldrich, added before use). For qRT-PCR analysis, *Botrytis* strains were grown on HA media for seven days under constant light for sporulation or cultured on HA plates overlaid with cellophane for three days in dark condition. Total RNAs were isolated by 1 volume of Chloroform/Isoamyl alcohol (24:1) and precipitated with 1 volume of Lithium Chloride (6M) for six hours at 4°C, which was followed by centrifugation for 20 minutes at 4°C, 15000 rpm. Pellet was cleaned by pre-cooled 70% ethanol and dissolved in 100 ul DEPC water. Total RNA was then precipitated in 70% ethanol (0.1 volume NaAc (3M, PH=5.2) and 2.5 volume 100% ethanol) overnight. After centrifugation for 20 minutes at 4°C, 15000 rpm, total RNA was cleaned by pre-cooled 70% ethanol and dissolved in 20ul RNase-free water. Concentration and intact of total RNAs were examined by nanodrop and 1% agarose gel electrophoresis. Good quality of total RNAs were used for qRT-PCR or stem-loop RT-PCR.

For small RNA library and mRNA library construction, total RNAs were isolated by 1 volume Phenol/Chloroform/Isoamyl alcohol (25:24:1) and precipitated with 1 volume Lithium Chloride (6M) for six hours at 4°C, followed by centrifugation for 20 minutes at 4°C, 15000 rpm. Pellet was dissolved in 400 ul RNase-free water. Total RNA was then re-isolated by 1 volume Chloroform/Isoamyl alcohol (24:1), followed by precipitation in 70% ethanol (0.1 volume NaAc (3M, PH=5.2) and 2.5 volume 100% ethanol) overnight. Other steps are the same as before. Concentration and intact of total RNAs were examined via Bio-analyzer (Agilent). Good quality of total RNAs were used for small RNA separation.

2.4.2 Quantitative RT-PCR (qRT-PCR)

Four-week-old tomatoes were treated with conidial suspension (2×10^5 spores/ml) of *Botrytis* wild-type and $\Delta ago2$ deletion strain using a versatile sprayer (Roth). Tomato leaf discs were collected after 20 hours and 30 hours of treatment using a spray nozzle (Roth). Six leaf discs ($\varnothing=0.4$ cm) were collected as a biological replicate. *Botrytis* wild-type and genetically modified strains were cultivated on HA plates overlaid with cellophane for three days in the dark or grown on HA media for seven days under constant light for sporulation. Mycelia from the same plate were collected as a biological replicate. After total RNA extraction, genomic DNA was removed from 1 μ g total RNA

sample with DNase I (Thermo Fischer Scientific) treatment for 30 minutes at 37°C. The reaction was stopped by 1µl 50 mM EDTA at 37°C for 10 minutes. DNA-free total RNAs were used for first-strand cDNA synthesis with oligo (dT) and SuperScript III reverse transcriptase (Thermo Scientific) according to the manufacturer's instructions. RT reactions were diluted 10 folds with ddH₂O prior to performing qRT-PCR using SYBR Green (Invitrogen, Thermo Fischer Scientific). *B. cinerea Actin* (*BCIN_16g02020*) was used as a reference gene to normalize mRNA. Relative transcripts were calculated by $2^{-\Delta\Delta Ct}$ based on the previous method (Livak & Schmittgen, 2001) using qPCR cycler (Quantstudio5, Thermo Fisher Scientific). Primer sequences were listed in **Table 4**.

2.4.3 Stem-loop RT PCR

DNA-free total RNAs (1µg) were used for a first-strand cDNA synthesis reaction with specific stem-loop RT primer and reverse transcription was carried out as described previously (Varkonyi-Gasic et al., 2007) with minor modifications. A mixture of 0.25µl dNTP mix (10mM), 0.5µl RT primer (1uM), 3.5µl DNA-free total RNA and 2.45µl DEPC-treated water were denatured 5 minutes and cooled on ice prior to cDNA synthesis. The resultant solution was gently mixed with 2ul First-strand buffer (5X), 1µl DTT (0.1M), 0.1µl Ribolock RNase Inhibitor (Thermo Scientific, 40 units/ul) and 0.2µl SuperScript III RT (Thermo Scientific, 200 units/µl). The reaction was conducted in a thermocycler with incubation for 30min at 16°C, followed by 60 cycles of 30°C for 30s, 42°C for 30s and 50°C for 1s and 5 minutes additional incubation at 85°C. The resultant cDNA was directly used for amplification using GoTaq DNA Polymerase (Promega) on a thermo cycler initiated with 95°C for 2min, then 30 cycles of denaturation at 95°C for 30s, annealing at 58°C for 30s and extension at 72°C for 20-180s (1kb/min), followed by 5min extension at 72°C. PCR products were visualized with 10% non-denaturing PAGE gel. Oligonucleotides were provided in **Table 4**.

2.5 Inoculation test

2.5.1 Infection assay with conidial suspension or mycelial plugs

For infection assay with spores, conidia were eluted from sporulated *Botrytis* of different genotypes with 1% malt extract (Doehlemann et al., 2006) suspension buffer. A droplet of 5µl and 10µl (10^5 spores/ml) conidial suspension were inoculated on four-weeks old detached tomato leaves. Inoculation assay with mycelial plugs ($\varnothing=0.4$ cm) was performed according to the previous method (Stein, 1985). Mycelia on agar plates of *Botrytis* were inoculated on four-weeks old detached tomato leaves after cultivation

for three to four weeks in constant light. The lesion area was measured using ImageJ. For quantifying mycelial colonization of *Botrytis*, discs from three infected detached leaves were collected for genomic DNA extraction and qRT-PCR by using SYBR Green (Thermo Scientific) and GoTaq G2 polymerase (Promega) with qPCR cycler (CFX96, Bio-Rad).

2.6 Transcriptomics analysis

2.6.1 Small RNA library cloning, sequencing and profiling analysis

Small RNAs of mycelia from WT and Δago ko mutants were isolated for high throughput sequencing according to the previous method (Weiberg et al., 2013). Each genotype has two replicates. 20 μ g extracted total RNAs (non-DNase treatment) were used for separation 20-30-nt in length small RNAs. Electrophoresis was conducted in 0.5XTAE buffer at 150 voltage for 3 hours 30 minutes with 14% urea-polyacrylamide gel (16.8g Urea, 18.67ml Polyacrylamide (30%), 400 μ l 50XTAE (pH=8.0), 150 μ l 10% APS, 15 μ l TEMED). Small RNAs were cut out and eluted from RNA gel using 0.3M NaCl. Small RNA library was cloned following manufacturer's instructions (NEBNext Multiplex Small RNA Library Prep Set for Illumina(set1)) and sequenced on an Illumina HiSeq1500 platform. Raw data were demultiplexed into fastq files using the Je-Demultiplex-Illu tool ((Girardot et al., 2016), Galaxy version 1.2.1). 5' adaptor was removed by fastp tool ((Chen et al., 2018), Galaxy version 0.12.5.0) and reads between 19-30-nt were obtained using Filter FASTQ tool with a minimum quality at 20 (Blankenberg et al., 2010), Galaxy version 1.1.1)). The resultant reads were mapped to the *B. cinerea* (B05.10) genome (ASM83294v1.41) (van Kan et al., 2017) with Bowtie algorithm (Galaxy version 1.1.0) allowing for 0 mismatch (-v=0). Ribosomal RNAs (rRNAs) were subsequently removed from reads mapped to the *Botrytis* genome with Bowtie algorithm (Galaxy version 1.1.0) allowing for 3 mismatches (-v=3). Ribosomal removed reads were mapped to messenger RNAs (mRNAs), transfer RNAs (tRNAs), Long terminal repeats (LTR-RTs) to determine the category of small RNA species.

2.6.2 RNA library cloning, sequencing and preprocessing

Extracted total RNAs of mycelia from WT and Δago ko mutants (five replicates for each genotype) were used for mRNA library cloning with prime-seq method as previously described (Geuder et al., 2021) based on single cell RNAseq method (Bagnoli et al., 2018). mRNA libraries were sequenced by paired end sequencing on an Illumina HiSeq1500 platform. Raw data were demultiplexed into fastq files using the deML (Renaud et al., 2015) and processed using the zUMIs pipeline (2.9.6, (Parekh et al.,

2018)) with STAR (2.6, (Dobin et al., 2013)). Processed reads were mapped to current *B. cinerea* (B05.10) genome assembly (ASM83294v1.41) (van Kan et al., 2017).

2.6.3 DistHeatMap and Principal component analysis (PCA) plot visualization and clustering

Raw read counts were transformed using the DESeq2 Bioconductor package (Love et al., 2014). The regularized logarithm transformation (rlog) was used to transformed reads prior to visualization. Euclidean distance was used for DistHeatMap to calculate the distance within samples.

2.6.4 Differentially expressed genes (DEGs) identification, GO term (incompletion) and KEGG analysis

DESeq2 (Love et al., 2014) was used to identify differentially expressed genes in wild-type and Δago deletion mutants based on raw read counts. Reads in WT were used as a control comparing to reads in each Δago ko mutants. $\text{Log}_2\text{FoldChange} \geq 1.0$ or ≤ -1.0 and adjusted P-value (padj) ≤ 0.05 were considered as DEGs. GO and KEGG enrichment analysis were performed using clusterProfiler package (Yu et al., 2012) by Benjamin-Hochberg method with p-value cutoff at 0.01 and q-value cutoff at 0.05.

2.7 Fluorescence microscopy

GFP labeled *Botrytis* strains were grown on HA medium for 14 days under constant light to stimulate sporulation. Conidia were eluted from sporulated plates with 1% malt extract solution filtered by one-layer miracloth (Merck Millipore). A droplet of 100 μ l spore suspension was incubated on the microscope slide under the humid condition at RT for 14-16 hours. Subcellular localization of *Botrytis* Ago1 and Ago2 were observed using fluorescence microscopy (Leica).

2.8 RNA-immunoprecipitation

Botrytis strains expressing 3xHA tagged *Ago1* were cultivated on HA agar with cellophane for four days in dark condition. Proteins of *Botrytis* strains were extracted as previous description (Zhao et al., 2012) with minor modifications. Briefly, 5g mycelia were finely grounded in liquid N₂ by mortar and pestle quickly and lysed in 20ml IP extraction buffer (20mM Tris-HCl, 300mM NaCl, 5mM MgCl₂, 0.5% (v/v) NP40, 5mM DTT, 1 tablet/50ml protease inhibitor (cOmplete, Merck), Ribolock RNase inhibitor (Thermo Scientific) 20 μ l, make up to 50 ml with DEPC-treated water). The IP extraction buffer containing samples was incubated on ice for 10 minutes and thawing

in a roller shaker for 20min at 4°C. The cell debris was removed by centrifugation at 4°C, 12000g for 10 minutes and supernatant was transferred through a pluriStrainer (1µm, pluriSelect). 50µl HA antibody coupled affinity gel (Ezview Red, Sigma-Aldrich) was used for incubation with crude proteins for 2 hours in a vertical wheel at 4°C. α -HA affinity gel was collected by centrifugation for 1 minute at 4°C, 3000g. Gel was gently cleaned four times with 1ml washing buffer (20mM Tris-HCl, 300mM NaCl, 5mM MgCl₂, 0.5% (v/v) Triton X-100, 5mM DTT, 1 tablet/50ml protease inhibitor (cOmplete, Merck), Ribolock RNase inhibitor (Thermo Scientific) 20ul, make up to 50 ml with DEPC-treated water) and was collected by centrifugation for 30s at 4°C, 3000g. α -HA affinity gel was resuspended in 400ul washing buffer. 25% gel suspension was separated for immunoblotting and 75% was used for RNA extraction according to previous method (Carbonell et al., 2012).

To extract RNA from 3xHA-Ago1 protein bound with α -HA affinity gel, 75% gel was resuspended in ½ RNA release buffer (225mM Tris-HCl, 10mM EDTA, 300mM NaCl, 2% SDS, 1µg/ul Proteinase K (Thermo Scientific)). RNA was released at 65°C and 300 rpm for 10 minutes on a Thermo shaker followed by isolation with 1 volume Phenol, 1 volume Phenol/Chloroform/Isoamyl alcohol (25:24:1) and 1 volume Chloroform/Isoamyl alcohol (24:1) twice. The water phase containing RNA was precipitated in 70% ethanol and 1ul Glycogen RNA grade (Thermo Scientific). Extracted RNAs were used for sRNA library construction. Immunoblotting with 25% α -HA affinity gel bound Ago1 was resuspended in 1XSDS loading buffer and was denatured at 95°C for 5 minutes prior to SDS-PAGE. The primary antibody used was α -HA antibody (3F10, Roche) and the secondary antibody used was α -rat IRdye800 (LI-COR, 1:15000 dilution).

3. Results

3.1 Identification of Argonaute proteins in *B. cinerea*

Genes encoding four paralogous Ago proteins were identified in the *B. cinerea* genome (Ago1, Ago2, Ago3 and Ago4) by searching for orthologs of *N. crassa* Qde-2 and Sms-2 using blastp (**Figure 3.2**). We found a premature stop codon exists in *Ago4* (B05.10) nucleic acid sequence (**Figure 3.1**), while *Ago4* in *Botrytis T4* strain was a complete sequence without the premature stop codon. All Ago proteins comprised a PAZ domain that binds to 3' end of guide sRNAs (Lingel et al., 2004), a Mid domain that recognizes and provides a binding pocket for 5' phosphate guide sRNAs (Boland et al., 2010) and a PIWI domain guided by sRNA facilitating cleavage on mRNA substrates (Liu et al., 2004) (**Figure 3.1**). It is known that Ago proteins in the absence of Mid domain impaired sRNA binding affinity in *N. crassa* (Boland et al., 2010). We found that Ago1 and Ago2 protein sequences contained a Mid domain, whereas Mid domain was absent in Ago3 and Ago4, suggesting a reduced sRNA binding affinity of Ago3 and Ago4 proteins if these two proteins bind with sRNAs in *B. cinerea* (**Figure 3.2**).

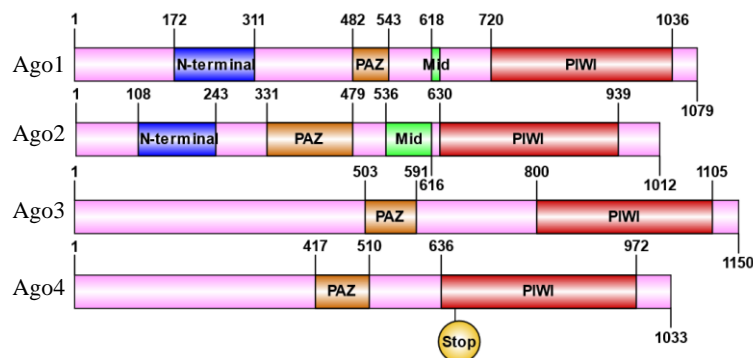


Figure 3.1 Ago protein features in *B. cinerea*.

Schematic representation of the functional domain of *Botrytis* Ago proteins comprising N terminal domain (blue), PAZ domain (orange), Mid domain (green) and PIWI domain (Red). A premature stop codon resides in the orf of *Ago4* labelled with a yellow circle shape tag.

To explore the evolutionary relationship of Ago proteins in *Botrytis* and representative ascomycetes, a maximum likelihood neighbor-joining tree was constructed and rooted by *Arabidopsis* Ago1. The phylogenetic tree showed that Ago proteins were divided into two subgroups based on the orthologous of Qde-2 and Sms-2 in *N. crassa* (Cogoni & Macino, 1997; Lee et al., 2003). *Botrytis* Ago1 protein fell into the clade of Quelling and Ago2 belonged to the clade of MSUD, while Ago3 and Ago4 were categorized in an unknown group (**Figure 3.2A**), which was consistent with the previous classification of *Botrytis* Ago proteins (Campo et al., 2016). Proteins in the subgroup of MSUD are rather conserved, consisting of an N terminal domain, a PAZ

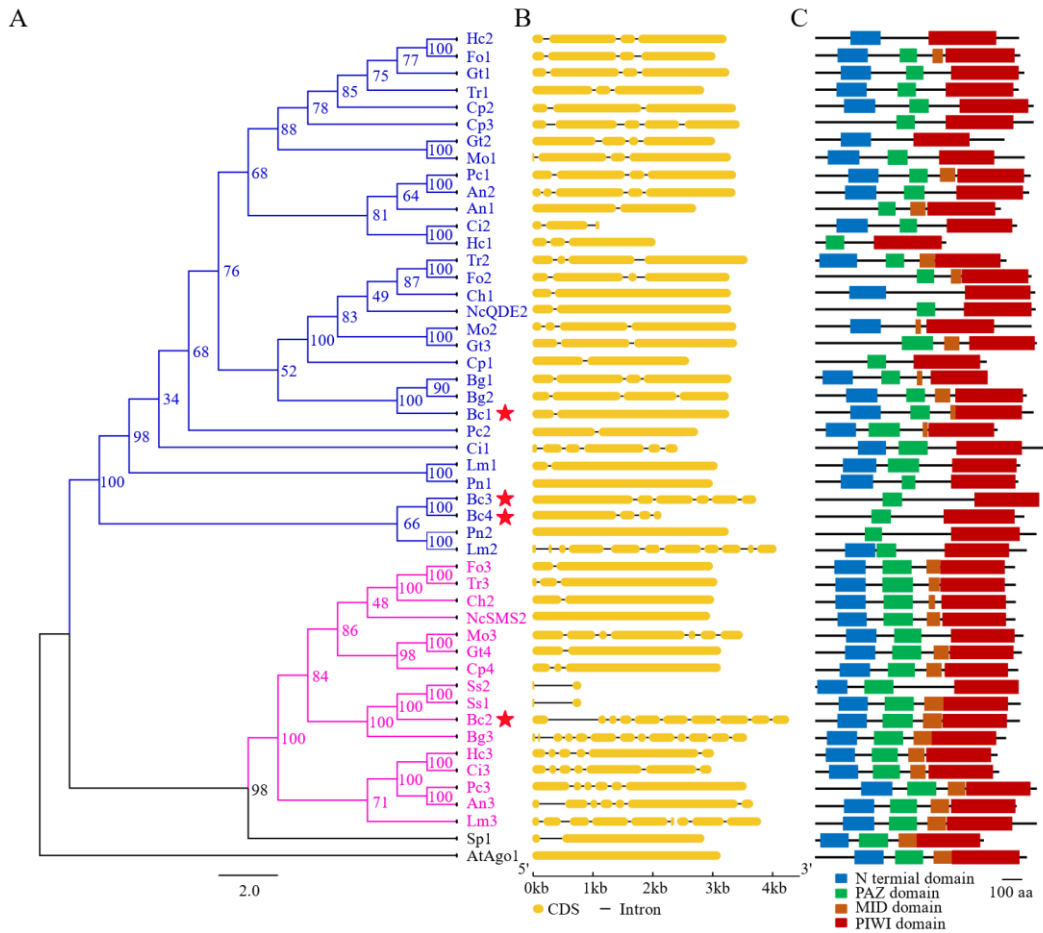


Figure 3.2 Phylogeny, gene structure and protein domain architecture of Argonaute proteins in representative filamentous fungi.

(A) Phylogenetic analysis of full-length Ago protein sequences. Representative fungal species in the phyla of Ascomycota were selected to construct the maximum likelihood neighbour-joining tree using Raxml under the model LG+G+F of amino acid substitution, which was rooted by *A. thaliana* Ago1 (Leotiomycetes, Sordariomycetes, Eurotiomycetes, Dothideomycetes). Two subgroups were labelled, the Quelling pathway and Meiotic-Silencing by Unpaired DNA (MSUD) pathway highlighted in blue and pink. *Botrytis* Ago1, Ago2, Ago3 and Ago4 were labelled with red stars, respectively. Accession numbers used in alignment are in **Table 3**.

domain, a MID domain and a PIWI domain near carboxyl terminus except for Ago2 in *Sclerotinia sclerotiorum* and Ago3 in *Magnaporthe oryzae* which lack a Mid domain (**Figure 3.2C**). Most Ago proteins in Quelling possess a PAZ domain with the exception of Ago1 in *Colletotrichum higginsianum*, Ago2 in *Gaeumannomyces tritici*, Ago2 in *Histoplasma capsulatum* and Ago2 in *M. oryzae*. The MID domain is present in few Argonaute proteins in the Quelling pathway, including Ago1 and Ago2 in *Penicillium chrysogenum*, Ago1 in *Aspergillus niger*, Ago2 in *Trichoderma reesei*, Ago2 in *Blumeria graminis* and Ago3 in *Gaeumannomyces tritici* (**Figure 3.2C**). *Arabidopsis* Ago1 possesses endonucleolytic activity (Baumberger & Baulcombe, 2005) and associates with a majority of sRNAs (Baumberger & Baulcombe, 2005; Wang et al., 2011) and

are vital for tasiRNA generation (Arribas-Hernandez et al., 2016; Montgomery, Yoo, et al., 2008). DDD endonuclease triad is frequent in fungi and the DDH motif is much more common in animals and plants (Choi et al., 2014). In contrast to DDD catalytic tetrad residues existed in *Qde-2* and *Botrytis* Ago1, Ago3 and Ago4 protein sequences, *Botrytis* Ago2 was the single protein containing DDH motif similar to *Arabidopsis* Ago1 (**Supplemental figure 1**), indicating that *Botrytis* Ago2 may have similar functions such as acting as a slicer in RNAi.

3.2 *Ago* expression levels in *B. cinerea* and from infected tomato and *Arabidopsis*

The expression of *Ago* genes differ in distinct vegetative tissues in fungi (Campo et al., 2016) and growing stages in *Arabidopsis* (Mallory & Vaucheret, 2010). To investigate whether *Ago* genes were differentially expressed in different tissues in *B. cinerea*, I quantified relative transcript levels of four *Ago* genes from in vitro vegetative tissues (mycelium and conidia). Totally all *Ago* genes were significantly higher expressed in conidia compared to pure mycelium. *Ago1*, an ortholog of *Qde-2*, was the highest expressed gene in *B. cinerea* in both pure mycelium and conidia, over 400-fold than *Ago2*, 200-fold than *Ago3* and 20-fold than *Ago4* in mycelium (**Figure 3.3**). While in conidia,

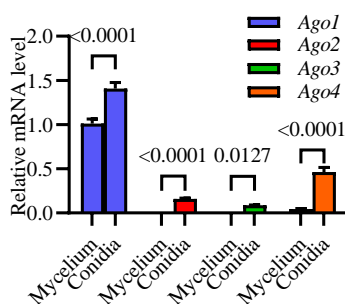


Figure 3.3 Expression of *Ago* genes in *B. cinerea* in different vegetative tissues

Transcripts of *Botrytis* *Ago* genes in mycelium and conidia were examined by qRT-PCR. Values represent mean \pm SD from four biological replicates normalized to the mean of *Actin* and relative to *Ago1* mycelium and conidia, respectively by two-way Anova.

the expression of *Ago1* was 8.5-fold than *Ago2*, 15-fold than *Ago3* and 2.5-fold than *Ago4*. By contrast, *Botrytis* *Ago2* homologous to *Sms-2* involving in MSUD possessed the least transcripts in vegetative tissue in mycelium and was intensely expressed in conidia. Likewise, the expression of *Ago3* and *Ago4* were elevated in conidia compared to pure mycelium. In contrast to *Ago1* expression in conidia which was only 1.2-fold than in mycelium, *Ago2*, *Ago3* and *Ago4* in conidia were nearly 60-fold, 15-fold and 10-fold than in mycelium, respectively (**Figure 3.3**).

We next wondered whether the interaction between *Botrytis* and plants regulated *Ago* genes expression. To address the question, we quantified relative transcripts of *Agos* in *Botrytis* from culture media and tomato or *Arabidopsis* infected by *Botrytis* WT at 24-, 48- and 72-hour time point. We examined that *Botrytis* *Ago1* was induced 5-fold

relative to mycelium after 24 hours infection on tomato during a biotrophic stage, while a 3-fold reduction of *Ago1* transcripts was detected after 72-hour infection on tomato when *Botrytis* turned into necrotrophic stage compared to 20-hour post-inoculation (**Figure 3.4A**). By contrast, *Botrytis Ago2* was suppressed in biotrophic and necrotrophic phases when infecting tomatoes, decreasing 3-fold at 72-hpi. Interestingly, the expression of *Ago* genes was much higher in *Botrytis* in response to *Arabidopsis* than tomatoes. However, the transcripts of *Botrytis Ago1*, *Ago2*, *Ago3* and *Ago4* were relatively stable during infection on *Arabidopsis* compared to in vitro sporulated mycelium of *B. cinerea* (**Figure 3.4B**).

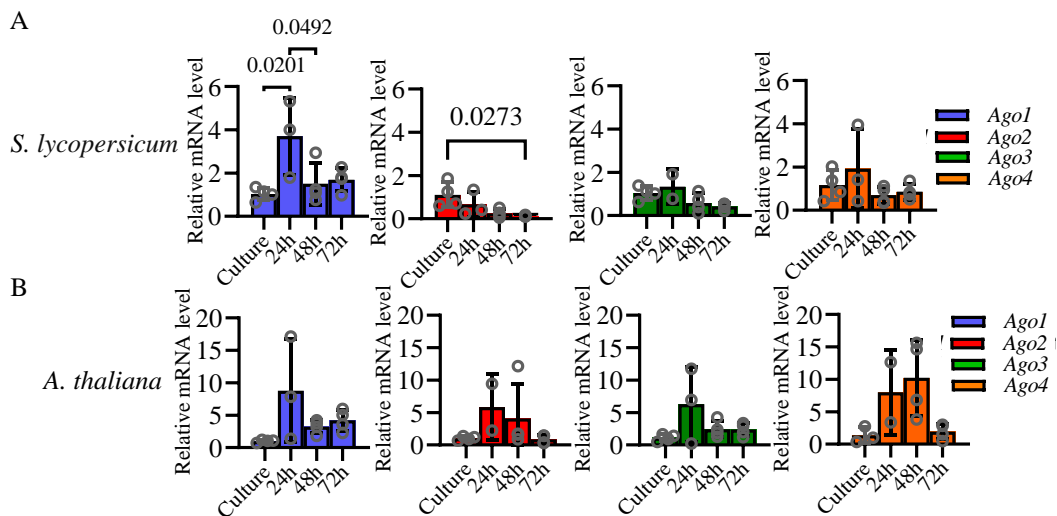


Figure 3.4 Expression pattern of *Agos* in *Botrytis* WT from culture and infected *S. lycopersicum* and *A. thaliana*.

(A) (B) Infected leaves were collected from tomato or *Arabidopsis* after 24-, 48- and 72-hours inoculation by spraying with suspension conidia of WT strain. In vitro sporulated WT mycelium was considered a control. Values refer to mean \pm SD from four biological replicates normalized to the mean of *Actin* as a relative value to in vitro transcripts by two-way Anova.

3.3 Ago proteins-mediated regulation on virulence in *B. cinerea*

3.3.1 Generation of *Ago* loss-of-function mutants by homologous recombination

To explore the function of *Botrytis Ago* proteins in pathogenicity regulation during fungal-plant interaction, I constructed *Ago* deletion plasmids carrying replaced segments of sequences flanking upstream and downstream of specific *Ago* genes and a selectable marker (**Figure 3.5A**), which were introduced into *Botrytis* WT strain (B05.10) by peg-mediated protoplast transformation. Transformants of *Ago* disruption mutants integrated into the native location were selected for further homokaryotic purification after genotyping by PCR with primers examining 5' terminal and 3' terminal

in the genome and the orf region of Ago genes, respectively (**Figure 3.5A, B**). PCR verified transformants were examined by southern blot, demonstrating that four *Botrytis* Ago genes are single copies in the haploid genome. The replaced fragments of *Ago2*, *Ago3* and *Ago4* were inserted in endogenous position with a single copy and a second random integration existed in *Ago1* mutation strains (**Figure 3.6A, B**). We eventually obtained homokaryotic Ago loss-of-function mutants, including two $\Delta ago1$, four $\Delta ago2$, two $\Delta ago3$ and two $\Delta ago4$ through single spore purification.

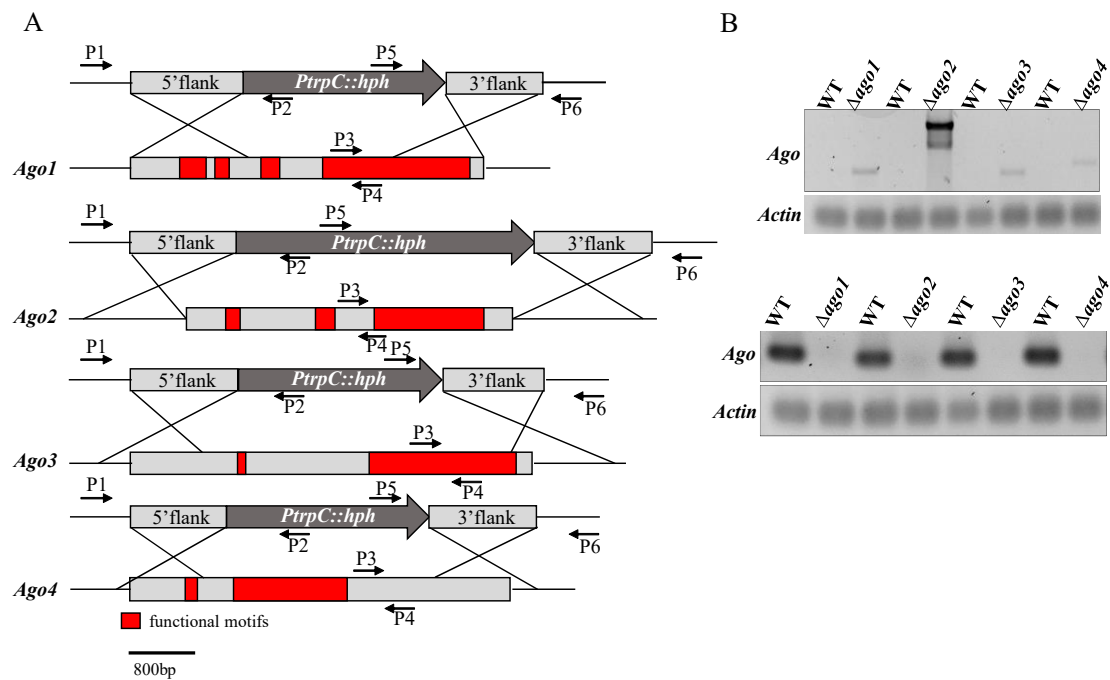


Figure 3.5 Strategy for construction of *Botrytis* Δago deletion mutants.

(A) Red bars refer to functional motifs in *Botrytis* Ago gene sequences. P1 to P6 refer to primers used in genotyping. Scale bar represents 800 bases. (B) Genotyping of Δago ko transformants with PCR using 5' primers (upper panel) and ko primers (lower panel) listed in **Table 4**.

To exclude the possibility of compensated upregulation of other Ago genes in Ago mutation strains in *B. cinerea*, I quantified the relative transcripts of Ago genes. Very low transcripts were detectable in Δago deficient mutants and the deletion of specific Ago genes had no impact on other Ago genes in the same family (**Figure 3.7**), indicating that Ago gene was specifically deleted in *Botrytis*.

Functionally distinct *Botrytis cinerea* Argonaute proteins in plant-microbe interaction

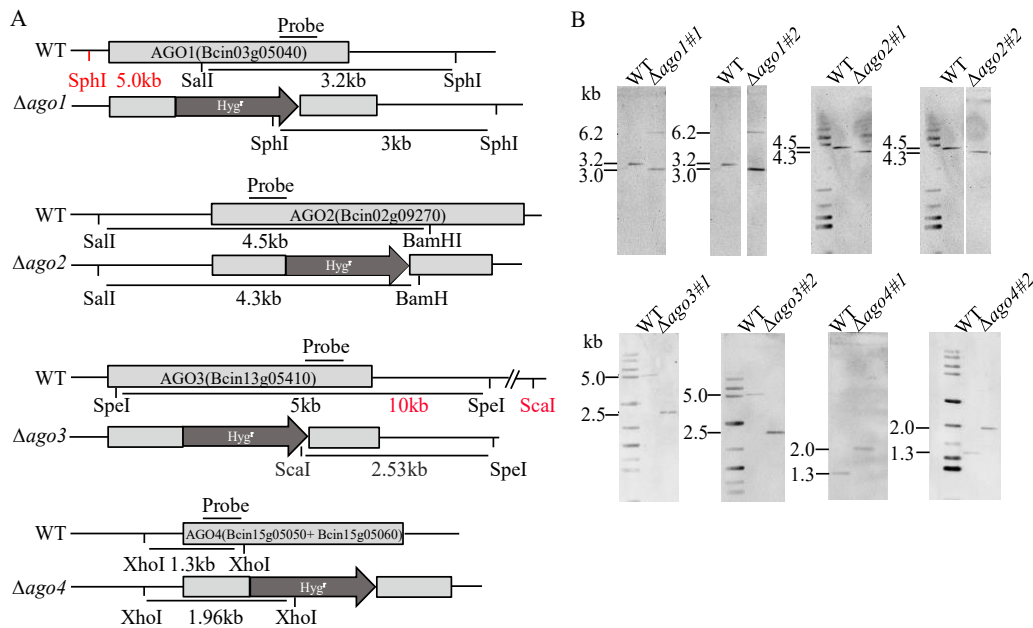


Figure 3.6 Schematic diagram of *Botrytis* Ago genes disruption.

(A) Genome structure of Ago loci in WT and Δago deletion mutant. For *Ago1* disruption, restriction enzymes SalI and SphI, SphI were utilized in gDNA digestion of WT and $\Delta ago1$ deletion mutant (First panel). For *Ago2* disruption, restriction enzymes SalI and BamHI were utilized in gDNA digestion of WT and $\Delta ago2$ deletion mutant (Second panel). For *Ago3* disruption, restriction enzymes SpeI, ScaI and SpeI were utilized in gDNA digestion of WT and $\Delta ago3$ deletion mutant (Third panel). For *Ago4* disruption, restriction enzyme XhoI was utilized in gDNA digestion of WT and $\Delta ago4$ deletion mutants (Fourth panel). (B) Result of southern blot visualized by chemiluminescent. A product at 3.2kb in WT and two products at 3.0kb and 6.2kb in $\Delta ago1$ were detected by southern blotting, indicating a random integration occurred in $\Delta ago1$ ko mutant during protoplast transformation in addition to the insertion in native locus. No product was detected at 5kb in $\Delta ago1$ as WT, showing that $\Delta ago1$ ko mutants are homokaryotic (First panel). Bands at 4.5kb and 4.3kb were detected in WT and $\Delta ago2$ ko mutant by southern blotting, indicating that $\Delta ago2$ ko mutants are homokaryotic (Second panel). Products at 5.0kb and 2.53kb were detected in WT and $\Delta ago3$ by southern blotting. No product was detected at 10kb, indicating that $\Delta ago3$ ko mutants are homokaryotic (Third panel). A single product was examined at 1.96kb in $\Delta ago4$ and 1.3kb in WT strains, indicating that $\Delta ago4$ ko mutants are homokaryotic (Fourth panel).

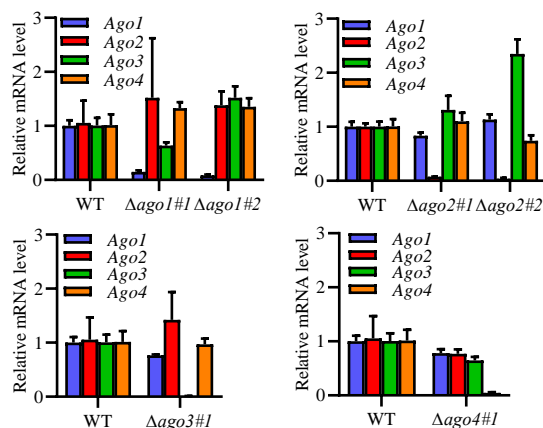


Figure 3.7 Ago genes expression in Δago deletion mutants.

Transcripts of *Botrytis* Ago genes in mycelium and conidia were examined by qRT-PCR. Values represent mean \pm SD from four biological replicates normalized to the mean of *Actin* and relative to *Ago1* mycelium and conidia, respectively by two-way Anova. Results were obtained from three technical replicates.

3.3.2 Loss of *Ago* unalter vegetative morphology in *B. cinerea*

To figure out whether loss of *Ago* genes could influence the growth and development of *Botrytis*, I cultured WT and four Δago ko mutants under continuous lightness or darkness for 14 days. We observed that sporulation, conidia size and colony morphology grew normally in WT and Δago ko mutants under light condition, while darkness stimulated the generation of sclerotia in WT and Δago deletion mutants (**Figure 3.8A, C, D**). Meanwhile, four *Ago* loss-of-function mutants displayed a growth rate similar to WT strain after culturing 2-, 3- and 4- days under continuous lightness (**Figure 3.8B**).

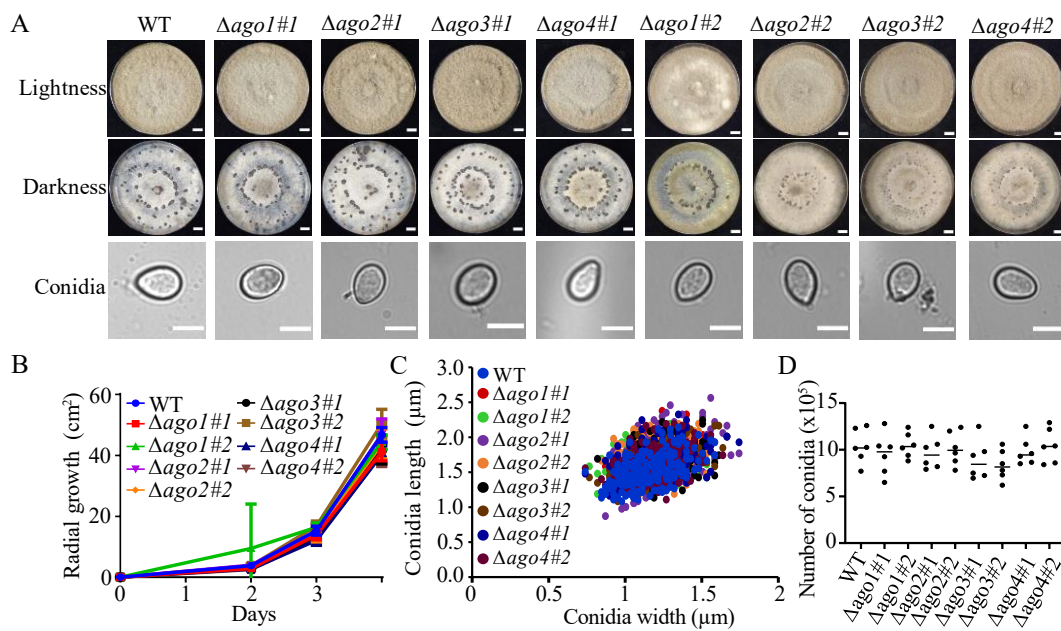


Figure 3.8 Morphology of *Botrytis* WT and Δago deficient mutants

(A) Colony morphology and conidia shape of *Botrytis* WT and Δago ko mutants. *Botrytis* strains were cultured under constant lightness (upper panel) or darkness (middle panel) for two weeks. Scale bar = 1cm. Conidia were collected and observed under light microscope. Scale bar = 10 μ m. (B) The growth rate of WT Δago ko mutants. Conidial suspension (10^6 spores/ml) was cultured on the medium plate for four days. Radial growth of *Botrytis* strains was measured at 2, 3 and 4 days. Result was obtained from six biological replicates for each genotype containing two independent transformants. (C) Conidia size of *Botrytis* WT and Δago ko strains. Conidia were collected from HA medium culturing for two weeks under constant light. Conidium width and length were measured by ImageJ from over 400 conidia for each genotype containing two independent transformants. (D) Sporulation of *Botrytis* WT and $\Delta ago2$ ko strains. Conidia were eluted from medium plates with ddH₂O. Result was achieved from twelve biological replicates for each genotype containing two independent transformants.

These observations demonstrate that loss of *Ago* genes unalters colony morphology and growth rate and *Ago* genes are not required for *Botrytis* growth and development in the vegetative phase. It seems that the morphological phenotype of *Ago* loss-of-function mutants differ in organisms. Previous report showed that *N. crassa Qde-2* (encoding an Ago protein) (Cogoni & Macino, 1997) and *Sms-2* (encoding an Ago protein) (Shiu et

al., 2001) unaffected vegetative growth and development. Likewise, *C. elegans Rde-1* (encoding an Ago protein) mutation strains displaying normal morphology (Tabara et al., 1999). In contrast, *D. melanogaster Ago1* mutation caused defective maternal and zygotic embryos (Kataoka et al., 2001). Furthermore, *Colletotrichum higginsianum* $\Delta ago1$ and $\Delta ago2$ deletion mutants affected vegetative growth and conidial shape and *Ago1* mutation strain suppressed conidiation but not *Ago2* mutation strain (Campo et al., 2016). *Agl-2* mutation strain reduced the mycelial growth rate and *Agl-4* mutation strain unaltered mycelial growth in *S. sclerotiorum* (Neupane et al., 2019). In addition, hypomorphic $\Delta ago1$ mutants regulated *Arabidopsis* leaf Morphology (Bohmert et al., 1998; Morel et al., 2002).

3.3.3 *Ago2* loss-of-function mutants impair pathogenicity in *B. cinerea*

To investigate whether *Botrytis* Ago genes play a role in the modulation of virulence in fungi-plant interaction, I conducted infection assays by dropping conidial suspension of WT and Δago deletion mutants on detached tomato leaves. We observed a significant reduction in virulence in $\Delta ago2$ ko mutant in comparison to WT strain when infecting on tomato even though the expression of *Ago2* is much lower than *Ago1* and *Ago4* (**Figure 3.9B**). No difference of virulence was found in $\Delta ago1$, $\Delta ago3$ and $\Delta ago4$ ko mutants compared to the WT strain (**Figure 3.9A, C, D**). Similar results were obtained by inoculation assay with agar discs of WT, $\Delta ago1$ and $\Delta ago2$ deletion mutants on detached tomato leaves, showing that $\Delta ago2$ deletion mutants were less aggressive compared to WT (**Figure 3.9F**) and the virulence of $\Delta ago1$ unchanged (**Figure 3.9E**). Then we wondered the colonization of *Botrytis*. I quantified the gDNA contents of WT and Δago ko mutants after 0- and 42-hour infection on detached tomato leaves. The gDNA contents of $\Delta ago2$ ko mutant were less examined compared to WT and other Δago deletion strains (**Figure 3.10B**), consistent with the ached tomato leaves. The gDNA contents of $\Delta ago2$ ko mutant were less examined compared to WT and other Δago deletion strains (**Figure 3.10B**), consistent with the reduced virulence of $\Delta ago2$ ko mutant in infection. However, $\Delta ago2$ ko mutants displayed similar pathogenicity to WT strain when infecting *Arabidopsis* (**Supplemental figure 5**). It has been documented that the defense resistance in response to *Botrytis* infection varied in different strawberry cultivars (Lee et al., 2021). Thus, the distinct phenotype between tomato and *Arabidopsis* could be explained by the existence of a more robust defense mechanism in *Arabidopsis* than in tomato. When infecting whole tomato plants with WT and $\Delta ago2$ ko mutant for 30 hours, tomato leaves were more susceptible infected by WT than $\Delta ago2$ (**Figure 3.10A**). gDNA contents $\Delta ago2$ ko mutant were quantified less accumulated than WT (**Figure 3.10B**). These observations implicate that *Botrytis* Ago2 might positively regulate virulence.

Functionally distinct *Botrytis cinerea* Argonaute proteins in plant-microbe interaction

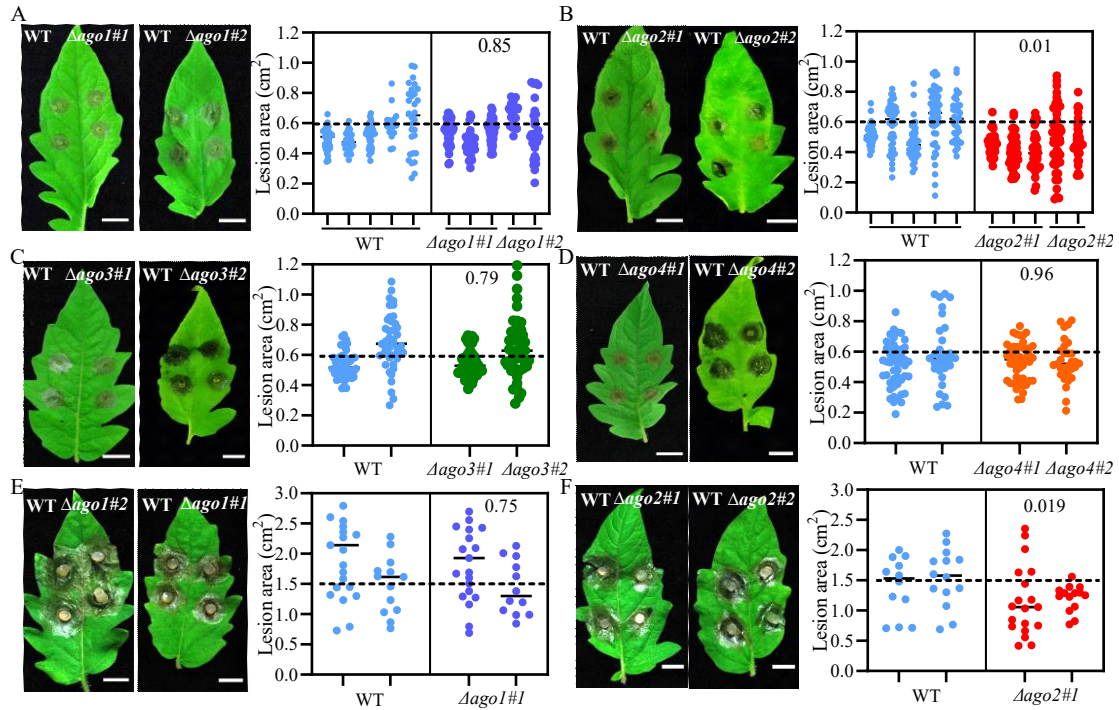


Figure 3.9 Phenotyping of *B. cinerea* WT and Δ deletion mutants on tomatoes.

(A) Infection assay on detached tomato leaves with conidial suspension. A droplet of a suspension with conidia (5 μ l, 10⁵ spores/ml) was pipetted on four-weeks old detached tomato leaves for 2 days. At least 20 leaves from four independent tomato plants were collected for infection assay. Result was obtained from five independent experiments with Δ ago1, two independent experiments with Δ ago3 and Δ ago4 from two independent transformants. Statistics was analysed by nested t-test, n>40. (B) Infection assay *Botrytis* using mycelium of *Botrytis* WT and Δ ago on agar plugs. Four-week-old detached tomato leaves were used for the assay. Result was obtained by two independent experiments with two independent transformants. Statistics was analysed by nested t-test. n \geq 12.

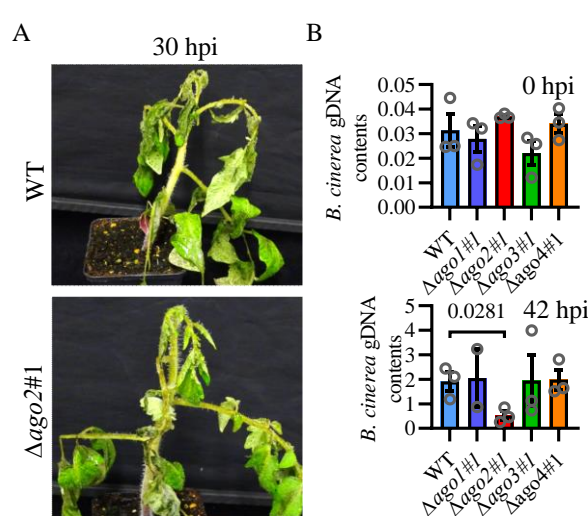


Figure 3.10 Colonization of *B. cinerea* on tomatoes.

(A) Inoculation assay on complete tomatoes with WT and Δ ago2 deletion mutant. Conidial suspension of WT and Δ ago2 deletion mutant were used to inoculate complete tomato plants. Pictures were taken after 30 hours of infection. (B) Colonization of Δ ago deletion mutant from infected detached tomato leaves determined by qRT-PCR. Four-week-old detached tomato leaves were used for the assay. Result was from three biological replicates. Statistics were analysed by two-way Anova.

3.4 Heterokaryon complementation

3.4.1 Introduction a complemented fragment in $\Delta ago2$ unalter vegetative morphology

To confirm the observation of impaired virulence of *Ago2* loss-of-function mutants, I generated heterokaryotic complementary strains *cAgo2*#1/#2 expressing 3xHA-tagged *Ago2* driven by native promoter under the *Ago2* mutation background (**Figure 3.11A, B**). Strains were further verified by southern blot, qRT-PCR and western blot (**Figure 3.11C, D, E**). Results showed that *Ago2* was complemented in $\Delta ago2$ deletion mutants and was unexpectedly overexpressed in two complementary strains in comparison to WT (**Figure 3.11D**). I cultured WT and *cAgo2*#1/#2 in continuous lightness and darkness. We observed no morphological change on mycelial growth, conidia size and sporulation in complementary strains, implicating that the introduction of a 3xHA:*Ago2* segment into *Botrytis* genome unaffected growth, conidial size and production (**Figure 3.12A, B, C, D**).

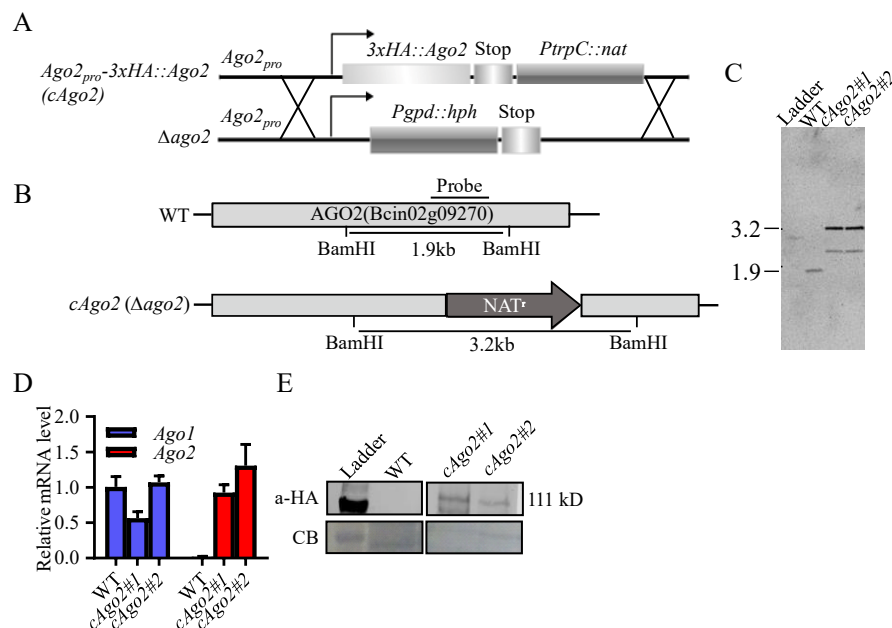


Figure 3.11 Generation of *cAgo2* complementary strains in *Ago2* mutation background.

(A) Illustration diagram of construction for complementation strain *cAgo2*. The *cAgo2* strains harbouring 3xHA-tagged *Ago2* full-length sequence were generated driven by the native promoter under $\Delta ago2$ mutant background. The nomenclature of complementation strain *Ago2_{pro}-3xHA:Ago2* was abbreviated to *cAgo2*. (B) Genome structure of *Ago2* locus in WT and complementary strain. A 452-bp Digoxigenin labelled probe was cloned by PCR with a pair of primers (5'-GTCACCAATAAGACTCCACCC-3' and 5'-GGCCATGGAAGATTGTGGAG-3'), which was used for DNA hybridization. Restriction enzyme BamHI was utilized in gDNA digestion of both WT and *cAgo2* knock-in strains. (C) Bands at 1.9kb and 3.2kb were detected in WT and *cAgo2* knock-in strains by southern blotting in *cAgo2* strains indicates

the heterokaryotic state. (D) Quantification of *Ago2* transcripts in *Botrytis* WT and *cAgo2* strains. Values are means from three technical replicates and normalized to *actin* and relative to *Ago1* expression in WT strain. (E) Western blotting to detect 3xHA-tagged *Ago2* protein in *cAgo2* strains. The expected size was 111 KD labelled with a red arrow.

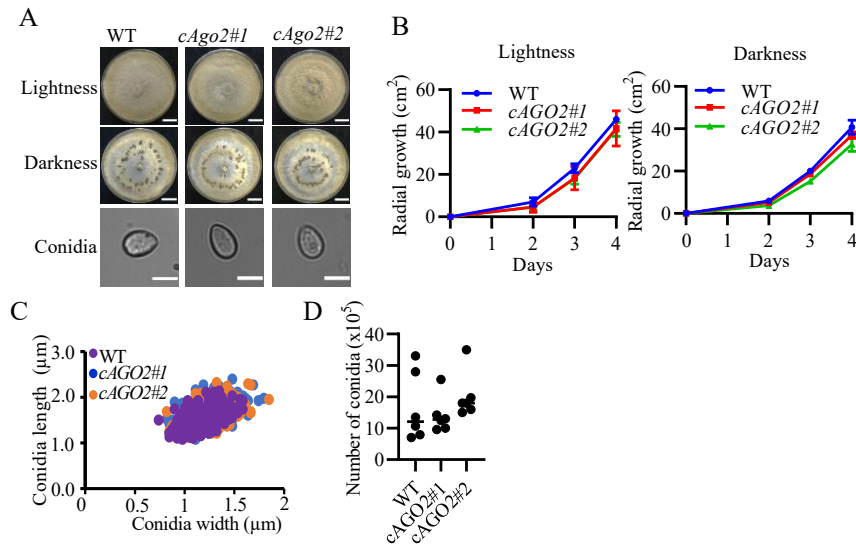


Figure 3.12 Morphology of *Botrytis* WT and *cAgo2* complementary strains.

(A) Colony morphology of *Botrytis* WT and *cAgo2* strains. Pictures were taken after two weeks of culturing in constant light or dark. Scale bar = 1cm (B) Growth rate of *Botrytis* WT and *cAgo2* strains. The conidial suspension (10^6 spores/ml) was cultured on the medium plate for four days. Radial growth was recorded at 2, 3 and 4 days. Result was obtained from six biological replicates for each genotype. (C) Conidia shape of *Botrytis* WT and *cAgo2* strains. Conidia were collected from HA medium culturing for two weeks under constant light. Conidium width and length were measured by ImageJ from over 200 conidia for each genotype. Scale bar = 10um. (D) Sporulation of *Botrytis* WT and *cAgo2* strains. Conidia were eluted from medium plates with ddH₂O. Result was achieved from six biological replicates for each genotype.

3.4.2 Gain of *Ago2* complemented reduced virulence in *B. cinerea*

To verify that whether less pathogenicity of *Botrytis* $\Delta ago2$ deletion strains caused by the absence of *Ago2* gene, I performed infection assay with conidial suspension of WT and complement strains *cAgo2#1/cAgo2#2* by dropping on four-weeks old detached tomato leaves. As expected, reduced virulence in $\Delta ago2$ ko mutants was recovered in

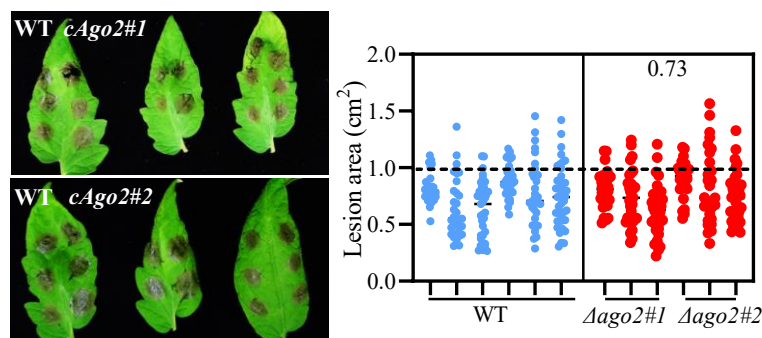


Figure 3.13 Pathogenicity assay of WT and complementary strain *cAgo2* on tomato.

A droplet of a suspension with conidia (5 μ l, 10⁵ spores/ml) was pipetted on four-weeks old detached tomato leaves for 2 days. At least 15 leaves from four independent tomato plants were collected for infection assay. Result was obtained by five independent experiments with two independent transformants. Statistics were analysed by nested t-test, n>40.

cAgo2#1/2 compared to WT (**Figure 3.13**), demonstrating that *Botrytis Ago2* contributes to virulence during infection on tomato.

3.5 Ago1 and Ago2 localize in the cytoplasm and cytoplasmic granules in *B. cinerea*

The cellular localization of Ago proteins implicates the location of their functional process. The most critical role of Ago proteins in PTGS is their endonucleolytic activity slicing excess mRNAs, followed by sRNAs and mRNAs degradation. Another essential role for Ago proteins is independent of the RNase activity. Ago proteins bind with bulged miRNAs and result in translational inhibition. A recent study showed that Ago2 resides in the cytoplasm and cytoplasmic P bodies in *M. oryzae* (Nguyen et al., 2018). However, the subcellular location of Ago proteins remains obscure in a majority of filamentous fungi. To investigate the subcellular localization of Ago1 and Ago2 proteins in *B. cinerea*, GFP and 3xHA were fused to the 5' terminus and 3' terminus of Ago1 and Ago2, respectively. Both replaced segments were driven by the native promoter. The *GFP:Ago1:3xHA* and *GFP:Ago2:3xHA* constructs were transformed into $\Delta ago1$ and $\Delta ago2$ deletion mutants, respectively (**Figure 3.14A**). Result showed that the GFP signal was mainly distributed in the cytoplasm and some GFP signals were concentrated in cytoplasmic granules in fluorescence-labeled *B. cinerea* harboring *GFP:Ago1:3xHA* or *GFP:Ago2:3xHA* constructs. (**Figure 3.14B**). This observation was consistent with previous studies of Ago proteins that reside in cytoplasm and P bodies or stress granules in human cells (Leung et al., 2006; Sen & Blau, 2005), nematodes (Ding et al., 2005), *A. thaliana* (Bajczyk et al., 2019; Bologna et al., 2018; Pare et al., 2009) and *M. oryzae* (Nguyen et al., 2018), respectively.

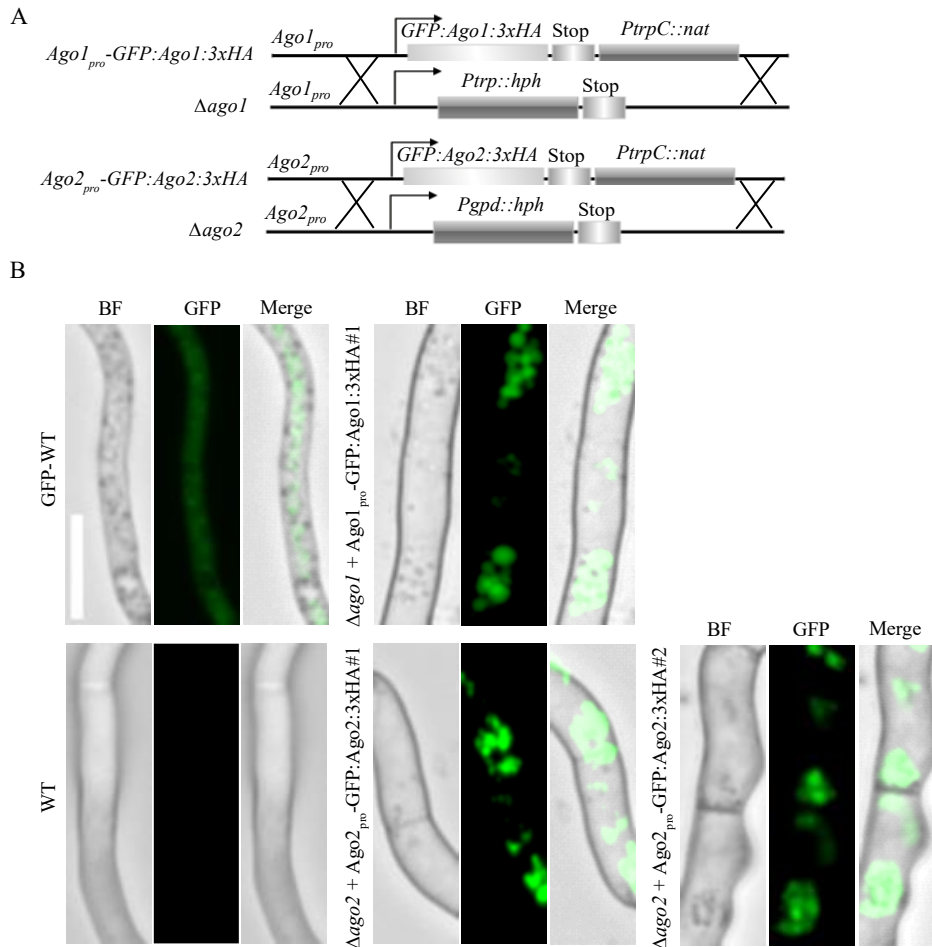


Figure 3.14 Subcellular localization of Ago1 and Ago2

(A) Illustration diagram of complementary constructs harboring GFP and 3xHA fused Ago1 or Ago2 fragment, respectively. Constructs were introduced into *Botrytis* Ago1 or Ago2 mutation strains by protoplast transformation. (B) Subcellular localization of Ago1 and Ago2 in *B. cinerea*.

3.6 Mechanism of Ago-mediated regulation on pathogenicity in *B. cinerea*

3.6.1 22-nt sRNAs are not the cause of reduced virulence in *Botrytis* Δ ago2

Some small RNAs are critical for growth and development in plants and fungi. In *A. thaliana*, defective in tasiRNAs and loss of most siRNAs resulted in alteration on leaf shape in Δ dr6 and Δ dcl2/3/4 mutants (Gascioli et al., 2005; Henderson et al., 2006; Peragine et al., 2004). Furthermore, Homozygous crosses of Δ sms-2 gave rise to lethality in *N. crassa* (Lee et al., 2003; Shiu et al., 2001) and pathogen small RNAs could transfer into the host, targeting *Arabidopsis* Ago1 to suppress host immune genes and vice versa (Weiberg et al., 2013). These gave us a hint that the regulation of sRNAs mediated by Ago2 might influence the virulence of *Botrytis*. Ago proteins have an

impact on the accumulation or biogenesis of sRNAs, and as RNase H members suggest their potential role in generating small RNAs. For example, loss of *Qde2* decreased the accumulation of sRNAs in *N. crassa* (Cogoni & Macino, 1997). Likewise, *Ago4* mutation in *A. thaliana* decreased the accumulation of 25-nt siRNAs (Zilberman et al., 2003). A similar case was found in *Drosophila Ago1* loss-of-function mutant, showing less accumulation of mature miRNAs (Okamura et al., 2004). By contrast, loss of *Ago3* enhanced sRNA levels in *M. oryzae*. Human *Ago2* interacted with Dcr protein (Chendrimada et al., 2005) and influenced miRNA expression post-transcriptionally (Diederichs & Haber, 2007). *C. elegans* ALG-1 (Ago) regulated the synthesis of let-7 (Zisoulis et al., 2012). Furthermore, two Ago proteins (Arb1 and Arb2) in fission yeast and *Ago2* in mice were also required for siRNA and miRNA accumulation, respectively (Buker et al., 2007; Winter & Diederichs, 2011).

As many previous works showed the significance of Ago proteins in regulating sRNA accumulation and *Botrytis Ago2* loss-of-function mutants displayed reduced pathogenicity, we questioned whether reduced virulence in *Ago2* loss-of-function mutants results from the repression of endogenous genes targeted by endogenous sRNAs or host translocated sRNAs. To address the question, I cloned and sequenced sRNAs of WT and Δago deletion mutants. In total, 13282418, 9642954, 18775256, 16917100, 15476435, 16601171, 10005405, 11004839, 12218978 and 12915839 reads were sequenced in WT1, WT2, $\Delta ago1\#1$, $\Delta ago1\#2$, $\Delta ago2\#1$, $\Delta ago2\#2$, $\Delta ago3\#1$, $\Delta ago3\#2$, $\Delta ago4\#1$ and $\Delta ago4\#2$ ko mutants, respectively. Among them, I obtained 11131137, 8198871, 15361092, 13998777, 12307897, 13756299, 8218114, 9015119, 9919857 and 10762097 reads from WT1, WT2, $\Delta ago1\#1$, $\Delta ago1\#2$, $\Delta ago2\#1$, $\Delta ago2\#2$, $\Delta ago3\#1$, $\Delta ago3\#2$, $\Delta ago4\#1$ and $\Delta ago4\#2$ ko mutants mapped to current *Botrytis* genome assembly. sRNA reads were aligned to distinct RNA species comprising ribosomal RNAs (rRNAs), mRNAs (messenger RNAs), tRNAs (transfer RNAs), LTR-RTs (long terminal repeats) and snRNAs/snoRNAs (small nuclear/ small nucleolar RNAs). rRNA-siRNAs are the most abundant sRNA category in WT and *Ago* loss-of-function mutants (**Figure 3.15A**). In *Botrytis* WT1 strain, a total of 15.8%, 2.8%, 8.3% and 2.2% small RNAs were sequenced from mRNAs, tRNAs, LTR-RTs and sn/snoRNAs loci, respectively. In WT2 strain, 14%, 3.3%, 6.9% and 1.9% were mapped to mRNAs, tRNAs, LTR-RTs and sn/snoRNAs, respectively. In $\Delta ago1\#1$ ko mutant, 11.6%, 3.3%, 0.12% and 1.4% were mapped to mRNAs, tRNAs, LTR-RTs and sn/snoRNAs, respectively. In $\Delta ago1\#2$ ko mutant, 13.8%, 2.9%, 0.8% and 2.6% were mapped to mRNAs, tRNAs, LTR-RTs and sn/snoRNAs, respectively. In $\Delta ago2\#1$ ko mutant, 16.9%, 3.5%, 20% and 1.9% were mapped to mRNAs, tRNAs, LTR-RTs and sn/snoRNAs, respectively. In $\Delta ago2\#2$ ko mutant, 15.9%, 2.7%, 19.8% and 1.5% were mapped to mRNAs, tRNAs, LTR-RTs and sn/snoRNAs, respectively. In $\Delta ago3\#1$ ko mutant, 17%, 4.3%,

19.8% and 2.2% of sRNAs were originated from mRNAs, tRNAs, LTR-RTs and sn/snoRNAs, respectively. In $\Delta ago3\#2$ ko mutant, 16.3%, 4.9%, 18.7% and 1.7% of sRNAs were mapped to mRNAs, tRNAs, LTR-RTs and sn/snoRNAs, respectively. In $\Delta ago4\#1$ ko mutant, 14.7%, 4%, 8.4% and 1.7% of sRNAs were derived from mRNAs, tRNAs, LTR-RTs and sn/snoRNAs, respectively. In $\Delta ago4\#2$ ko mutant, 14.1%, 2.7%, 9.5% and 1.8% were sequence from mRNAs, tRNAs, LTR-RTs and sn/snoRNAs, respectively (**Figure 3.15A**). Strikingly, a majority of sRNAs derived from LTR-RTs and mRNAs lost in $\Delta ago1$ deletion mutants, while the absence of *Ago2* and *Ago3* elevated the accumulation sRNAs in LTR-RT and mRNA loci (**Figure 3.15A, B; Figure 3.16A, B, C**). In contrast, deletion of *Ago4* had no effect on sRNA accumulation, suggesting an unfunctional role of *Ago4* in RNAi. 7-8.2% retroelement-derived sRNAs in WT decreased to 0.1-0.8% when deleted *Ago1* gene and 7-8.2% retroelement-derived

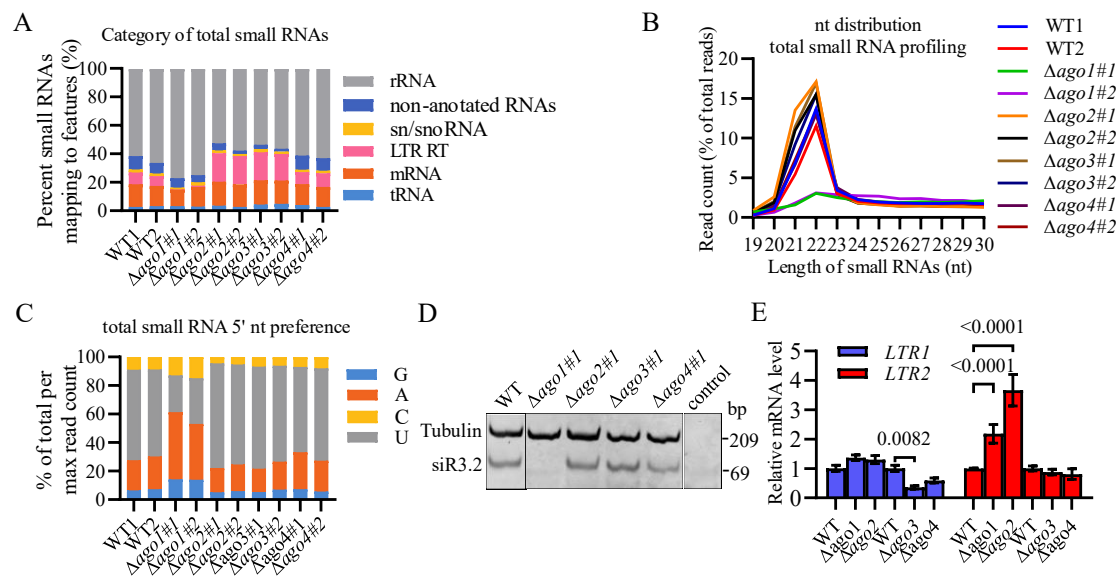


Figure 3.15 Characterisation of small RNAs in WT and Δago deletion mutant.

(A) Category of total sRNAs in WT and $\Delta ago2$ deletion mutant. Bar chart summarizes the annotation of total sRNA population in categories of tRNA-, mRNA-, snRNA- or LTR- derived sRNAs. (B) Size distribution of total sRNAs in WT and $\Delta ago2$ deletion mutant. (C) Total sRNA preference at 5' nt in WT and $\Delta ago2$ ko mutant. (D) *Bc*-siR3.2 accumulation in WT and Δago deletion mutants. siR3.2 was determined by RT-qPCR. (E) Relative mRNA levels of LTR1 and LTR2 in WT and Δago ko mutants.

small RNAs in WT elevated to 20% when deleted *Ago2* or *Ago3* gene in *Botrytis*. This result was confirmed by the semi-quantification of siR3.2 that mapped to retroelement, showing that siR3.2 was undetectable in $\Delta ago1$ ko mutant (**Figure 3.15D**). Total sRNAs were identified enriching at 21-23-nt in length and peaked at 22-nt in *Botrytis* WT and Δago ko mutants (**Figure 3.15B**). In consistent with the total sRNA profiling, sRNAs originated from LTR loci and mRNA-derived sRNAs enriched at 21-23-nt and peaked at 22-nt (**Figure 3.16A**), while 21/22/28/29/30-nt oligomers were most abundant in tRNA-derived small RNAs displaying a double peak pattern at 22- and 29-nt

(Figure 3.16C). The first nucleotide of most sRNAs was uridine in *B. cinerea* (Figure 3.15C; Supplemental figure 6). 97% LTR-derived sRNAs had 5' uridine bias (Figure 3.16D). 47-48% mRNA-originated sRNAs began with 5' uridine and 74-76% tRNA-derived sRNAs started with the first nucleotide uridine at 5' terminus (Figure 3.16E, F). the loss of sRNAs originated from LTR-RT, mRNA and tRNA loci in $\Delta ago1$ ko mutants were also reflected in profiling of specific sRNA categories, showing that the 5' nucleotide sRNAs with uridine were less in $\Delta ago1$ than WT (Figure 3.16D, E, F). The increase of LTR-RT and mRNA derived sRNAs in $\Delta ago2$ and $\Delta ago3$ ko mutants were reflected in profiling of specific sRNA classes, showing that the 5' nucleotide sRNAs with uridine were elevated compared to WT (Figure 3.16D, E).

In summary, these findings demonstrate that a majority of 21-23-nt sRNAs, partic-

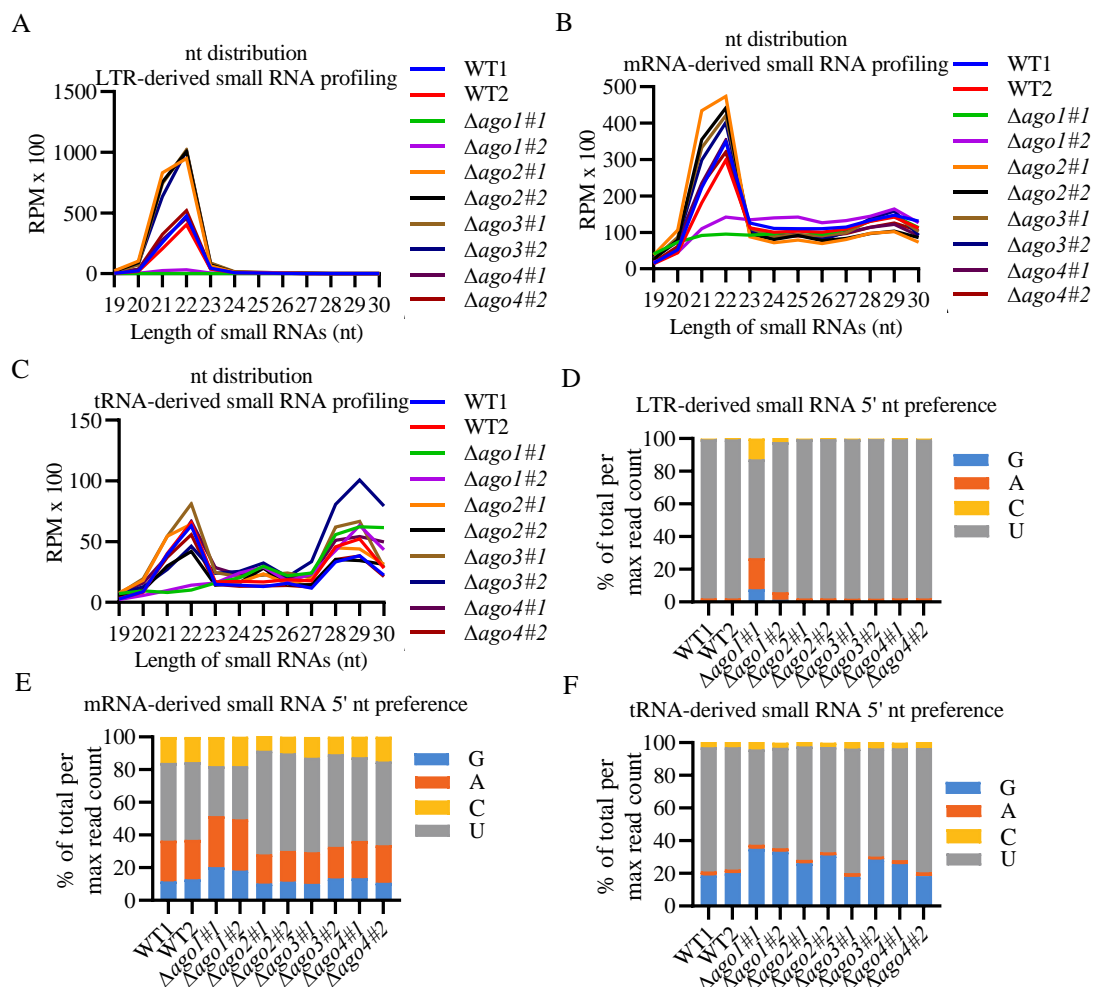


Figure 3.16 small RNA profiling from distinct RNA species.

(A)(B)(C) Size distribution of LTR-derived sRNAs, mRNA-derived sRNAs, tRNA-derived sRNAs in WT and Δago ko mutant, respectively. (D)(E)(F) First nucleotide abundance in LTR-derived sRNAs,

ularly LTR-derived small RNAs, in which the first nucleotide starts with uridine, were abrogated in $\Delta ago1$ ko mutant, indicating either the involvement of sRNA biogenesis

or the stabilization activity independent of RNase activity of Ago1 (if *Botrytis* Ago1 have). On the contrary, 21-23-nt sRNAs, in which the first nucleotide is uridine, were elevated in $\Delta ago2$ and $\Delta ago3$ ko mutants, indicating that Ago2 and Ago3 function in mRNA degradation instead of sRNA stabilization.

I then quantified two *Botrytis* retroelements (LTR1 and LTR2). Result showed that LTR1 was inhibited in $ago3$ ko mutant and no change was observed in $\Delta ago1$, $\Delta ago2$ and $\Delta ago4$ deletion mutants. By contrast, LTR2 was induced in *Ago1* and *Ago2* mutation strains and deletion of *Ago3* and *Ago4* unaffected LTR2 transcripts (**Figure 3.15E**). This result, together with sRNA abundance in $\Delta ago2$ ko mutants, indicates a dominant role of the endonucleolytic activity of Ago2 in *B. cinerea*. The elevation of sRNAs and reduced transcript levels of LTR1 in *Ago3* loss-of-function mutants were consistent with the rise of gene silencing and inhibited transcripts of retroelement (MAGGY) in $\Delta ago2$ deletion mutant in *M. oryzae* (Nguyen et al., 2018), suggesting that *Botrytis* Ago3 might be a minor slicer directed by a small number of guide sRNAs facilitating mRNA cleavage, or Ago3 only binds with some sRNAs independent on cleavage activity if it possesses. These results were unexpected because the loss of sRNAs in $\Delta ago1$ ko mutants unchanged the mycelial growth and virulence of *Botrytis*, which are inconsistent with and seem contradictory to the previous observation that lack sRNAs in $\Delta dcl1dcl2$ double ko mutant slower mycelial growth and impaired pathogenicity in *B. cinerea*, implicating that 22-nt sRNAs in cross-kingdom RNAi are not a big player in *Botrytis* virulence. Furthermore, the reduced virulence in $\Delta dcl1dcl2$ double deletion mutant might be triggered by a series downstream regulation, e. g. impaired vegetative growth, asexual sporulation and infection structure formation when mutated *Dcl1Dcl2* genes in *Botrytis*.

3.6.2 Ago2 regulates genes involving in cellulose-binding domain synthesis, arginine biosynthesis, galactose metabolism and lipid metabolism

To determine the factors mediated by Ago2 protein impairing pathogenicity in *B. cinerea* during infection on tomatoes, we sequenced mRNAs of WT and Δago ko mutants with five replicates for each genotype. The samples were initially examined using the Euclidean distance calculation method. Result showed that samples of WT, $\Delta ago1$, $\Delta ago2$, $\Delta ago3$ and $\Delta ago4$ ko mutants and their duplicates were clustered together respectively, except for one $\Delta ago3$ ko mutant that the distance was far from the other four replicates (**Supplemental figure 7A**). PCA plot showed that samples of $\Delta ago1$ deficient mutants genetically differed from *Botrytis* WT, $\Delta ago2$, $\Delta ago3$ and $\Delta ago4$ ko mutants (**Supplemental figure 7B**). We then wonder the differentially expressed genes (DEGs) in *Ago* loss-of-function mutants. I identified *Botrytis* genes differentially expressed in the loss of *Ago* mutants compared to WT using DESeq2. Among 11688

protein-coding genes, 346 (3%), 256 (2.2%), 1076 (9.2%), 126 (1.1%) genes were identified that were differentially expressed in $\Delta ago1$, $\Delta ago2$, $\Delta ago3$ and $\Delta ago4$ ko mutants using WT as a control, respectively (**Figure 3.17A, B**). 115 (33.2%) genes were up-regulated and 231 (66.8%) genes were down-regulated in $\Delta ago1$ ko mutant in comparison to WT. In $\Delta ago2$ ko mutant, 97 (37.9%) genes were up-regulated and 161 genes were down-regulated. 496 (46.1%) genes were up-regulated and 580 (53.9%) were

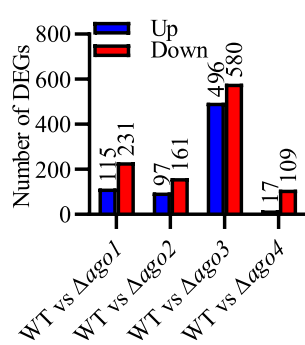


Figure 3.17 Number of DEGs in WT and Δago ko mutants

(A) Identified differentially expressed genes (DEGs) in Δago ko mutants compared to WT. Absolute $\text{Log}_2\text{FC} \geq 1.0$ or ≤ -1.0 and adjusted P-value (padj) ≤ 0.05 were used for DEGs identification.

down-regulated in $\Delta ago3$ deficient mutant. In $\Delta ago4$ deletion mutant, 17 (13.5%) genes were up-regulated and 109 (86.5%) genes were down-regulated (**Figure 3.17A**). Numerous genes were influenced by a mutation on *Ago1*, *Ago2*, *Ago3* or *Ago4*, particularly *Ago3* which affected over 10% of genes (**Figure 3.17**, **Figure 3.18**). DEGs in *Ago* loss-of-function mutants were used for GO enrichment analysis. Result showed that DEGs in $\Delta ago1$ and $\Delta ago2$ enriched in cellular component (CC) pathway (**Figure 3.19**, **Supplemental figure 8**), whereas DEGs in $\Delta ago3$ enriched in molecular function (MF) and biological process (BP) pathways (**Supplemental figure 9**) and DEGs in $\Delta ago4$ do not

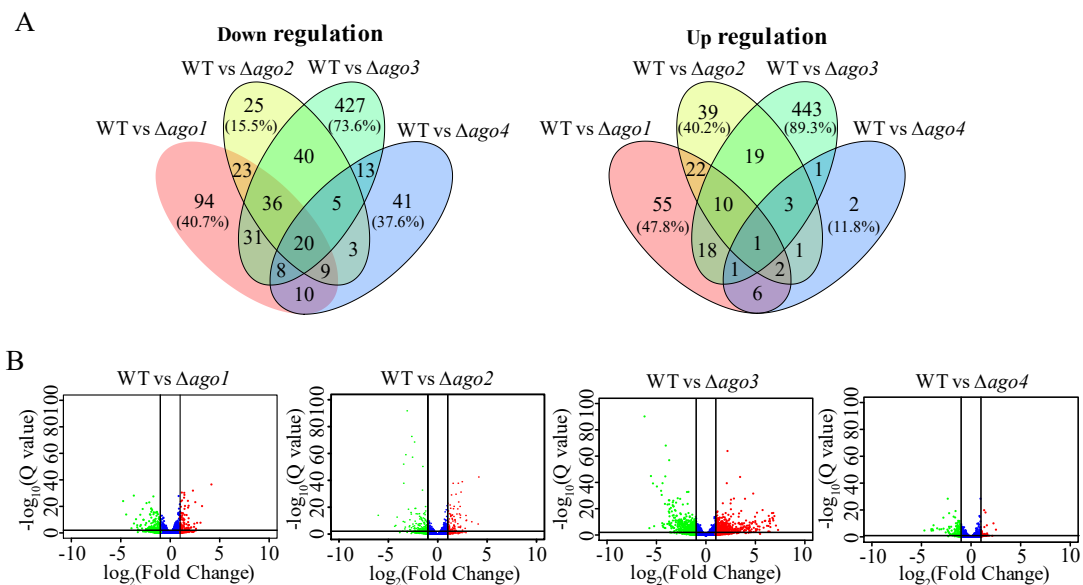


Figure 3.18 Differentially expressed genes in Δago ko mutants compared to WT in *B. cinerea*.

(A) Venn diagram of overlapping DEGs in *ago* ko mutants in comparison to WT. $\text{Log}_2\text{FC} \geq 1.0$ or ≤ -1.0 and adjusted P-value (padj) ≤ 0.05 were considered for DEGs identification. (B) Regulated

genes in Δago ko mutants compared to WT. Volcano plots show regulated genes in Δago ko mutants in comparison to WT. The blue dots refer to non-significant regulated genes. The green dots represent down-regulated DEGs with $\log_2FC \leq -1$ and adjusted $P \leq 0.01$ and the red dots represent upregulated DEGs with $\log_2FC \geq 1$ and adjusted $P \leq 0.01$.

enriched in GO, indicating a distinct role of Ago proteins in *B. cinerea*. Eight DEGs in *Ago2* loss-of-function mutant were enriched in GO. *BCIN_01g09430*, *BCIN_13g02100*, *BCIN_13g05760*, *BCIN_15g03870* encoding extracellular proteins and *BCIN_03g05610*, *BCIN_08g00940*, *BCIN_14g05510* and *BCIN_16g04460* encoding proteins involved in cell wall and external encapsulating structure (**Figure 3.19**). Among them, three genes were downregulated in $\Delta ago2$ ko mutant, including *BCIN_03g05610*, *BCIN_08g00940* and *BCIN_15g03870*. *BCIN_15g03870* encodes a fungal-type cellulose-binding domain (CBD) and the function of *BCIN_03g05610* and *BCIN_08g00940* remain unknown. Many polysaccharide degradation enzymes contain

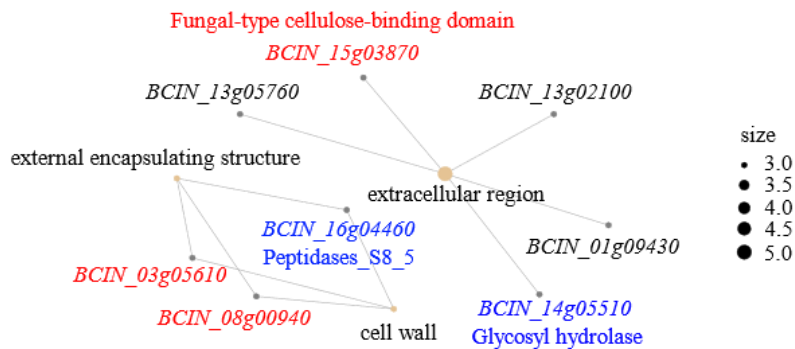
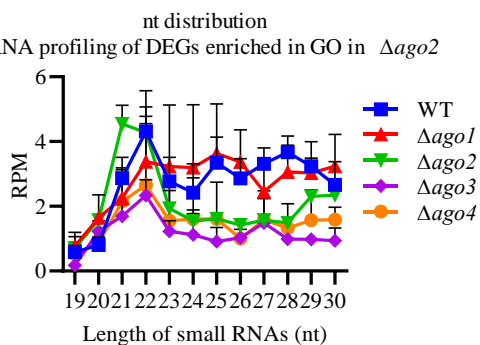


Figure 3.19 DEGs that enriched in cellular component in *Ago2* loss-of-function mutant.

Gene symbols in red refer to downregulated genes and symbols in blue represent upregulated genes that were unique in $\Delta ago2$. Gene symbols in black refer to genes enriched in CC but not unique in $\Delta ago2$.

a cellulose-binding domain (Gilkes et al., 1991) and the introduction of a CBD in *Trichoderma harzianum* suppressed the growth of *B. cinerea* (Limon et al., 2004), which suggests that CBD is vital for the development of *B. cinerea*. sRNAs targeting these eight genes were predicted and sRNA size distribution showed that 21-mers were unexpectedly the most abundant in $\Delta ago2$ ko mutants and 24-28-nt oligomers were significantly less accumulated in $\Delta ago2$, $\Delta ago3$, $\Delta ago4$ compared to WT and $\Delta ago1$ ko mutants (**Figure 3.20**). It is surprised that the abundance of sRNAs derived from eight gene loci showed similar pattern as WT although most sRNAs lost in $\Delta ago1$ ko mutants, indicating that eight genes-derived 24-28-nt sRNAs are probably not dependent on Ago1 in *B. cinerea* (**Figure 3.20**).

sRNA profiling of DEGs enriched in GO in $\Delta ago2$ **Figure 3.20 sRNA profiling of DEGs enriched in GO in $\Delta ago2$.**

Size distribution of sRNAs originated from eight DEGs that enriched in CC in *Ago2* loss-of-function mutants.

Table 1 Genes enriched in KEGG that specifically and differentially expressed in $\Delta ago2$

Kegg ID	Description	BgRatio	P adjust	Definition KO	Gene ID
bfu00220	Arginine biosynthesis	19/2231	0.047	NADP+	<i>BCIN_16g04050</i>
bfu00052	Galactose metabolism	24/2231	0.048	Galactose oxidase	<i>BCIN_09g04410</i>
bfu00910	Nitrogen metabolism	25/2231	0.048	NADP+	<i>BCIN_16g04050</i>
bfu00250	Alanine, aspartate and glutamate metabolism	30/2231	0.048	NADP+	<i>BCIN_16g04050</i>
bfu00561	Glycerolipid metabolism	36/2231	0.048	Glycerol kinase	<i>BCIN_03g04090</i>

25 downregulated DEGs specifically present in $\Delta ago2$ ko mutants were then used for KEGG enrichment analysis. Three genes were identified enrichment in the KEGG pathway, *BCIN_16g04050*, *BCIN_09g04410* and *BCIN_03g04090* (**Table 1**). *BCIN_16g04050* encodes an NADP⁺ (glutamate dehydrogenase), involving in three metabolic pathways comprising arginine biosynthesis, nitrogen metabolism, and alanine/aspartate/glutamate metabolism. *BCIN_09g04410* encodes a galactose oxidase functioning in galactose metabolism and *BCIN_03g04090* encodes a glycerol kinase involving in glycerolipid metabolism. We identified reads homologous to these three genes in *Botrytis* WT and Δago deletion mutants. In contrast to WT and $\Delta ago3$ deletion mutants which sRNAs mapped to three genes enriched between 20-30-nt, the abundance of sRNAs in $\Delta ago1$ ko mutants decreased and displayed a stable distribution pattern between 20-30-nt. However, it is interesting that in $\Delta ago2$ ko mutant sRNAs derived from three identified genes enriched between 20-23-nt and the abundance of sRNAs between 24-30-nt dramatically dropped to the lowest levels compared to other strains (**Figure 3.21B**). Furthermore, these three genes In *N. crassa*, miRNAs distributed between 20-23-nt and 24-27-nt (Lee et al., 2010), suggesting that the loss sRNAs in $\Delta ago2$ ko mutants might belong to miRNAs. Taken together, these results indicate that *Ago2* is likely contributing to pathogenicity by regulating genes that are involved in arginine biosynthesis, galactose metabolism and lipid metabolism, which might be targeted by 24-28-nt sRNAs.

Functionally distinct *Botrytis cinerea* Argonaute proteins in plant-microbe interaction

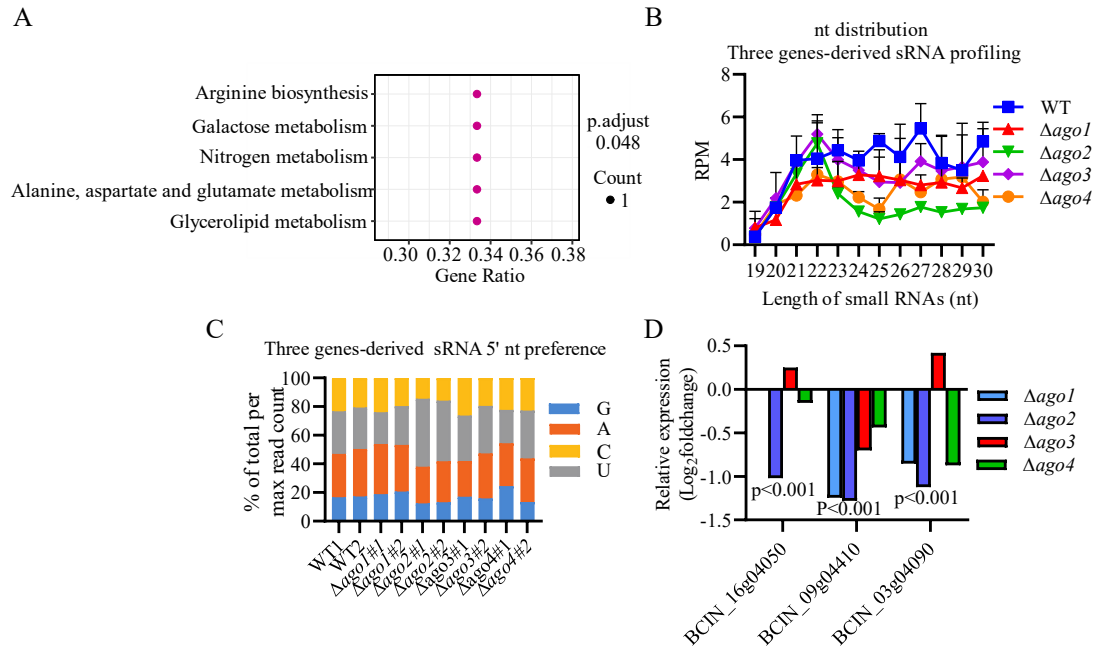


Figure 3.21 sRNA profiling derived from three gene loci and relative expression in Δago compared to WT.

(A) DEGs unique in $\Delta ago2$ enriched in KEGG pathways. (B) Size distribution of sRNAs derived from three identified gene loci in WT and Δago ko mutant. (C) First nucleotide abundance in three genes-derived sRNAs in WT and Δago ko mutant. (D) Relative expression of three genes in Δago ko mutants compared to WT strain. Three genes satisfied $\log_2FC \leq -1$ and adjusted P-value ≤ 0.05 in $\Delta ago2$ ko mutant.

4. Discussion

4.1 Ago2 positively regulate virulence in *B. cinerea*

B. cinerea suppressed endogenous Ago2 expression in both biotrophic and necrotrophic stages and induced the expression of *Ago1* in the biotrophic phase in response to infection on tomato, whereas the transcript levels of *Ago1* and *Ago2* unaltered during infection on *A. thaliana*, suggesting a potential function of Ago1 and Ago2 during *Botrytis*-tomato interaction and that the defense mechanism differs in tomato and *Arabidopsis*. It is surprising that *Ago2* loss-of-function mutants reduced the pathogenicity of *Botrytis*, whereas *Ago1* loss-of-function mutants that blocked the accumulation of most sRNAs had no impact on the vegetative growth and virulence. Previous studies in *N. crassa* revealed that deletion of *Qde-2* and *Sms-2* unaltered mycelial morphology during the vegetative stage but suppressed the efficiency of RNAi (Cogoni & Macino, 1997; Lee et al., 2003). However, no report has shown the abrogation of sRNAs accumulation in Δ *ago* deletion mutants in any organisms to date. Elevated sRNAs in Ago2 mutation strains derived from random loci wherein they generated sRNAs with 5' uridine bias. The deletion of Ago genes unchanged morphological phenotype during the vegetative growth in *B. cinerea*, indicating that reduced virulence in Δ *ago2* deletion strains is not the consequence of morphological alteration. Furthermore, the abundance of 24-28-nt sRNAs was greatly decreased in Ago2 loss-of-function mutants, implicating that it is likely that the phenotype of impaired pathogenicity in *Ago2* loss-of-function mutants results from the regulation of 24-28-nt sRNAs, probably miRNAs.

4.2 24-28-nt sRNAs are likely the intermediary associated with Ago2 regulating pathogenicity in *B. cinerea*

Some small RNAs are critical for growth and development in plants and fungi. In *A. thaliana*, defective in tasiRNAs and loss of most siRNAs resulted in alteration on leaf shape in Δ *rdr6* and Δ *dcl2/3/4* mutants (Gascioli et al., 2005; Henderson et al., 2006; Peragine et al., 2004). Furthermore, the loss of sRNAs in *B. cinerea* Δ *dcl1dcl2* suppressed the growth of mycelium and the formation of infection cushion (Weiberg et al., 2013). However, *Qde1* (encoding an RdRp), *Qde2* (encoding an Ago protein) and *Qde3* (encoding a DNA helicase) mutation that impaired the accumulation of sRNAs unaffected vegetative growth and development in *N. crassa* (Cogoni & Macino, 1997). Similarly, Δ *sad-1* (encoding a RdRp) and Δ *sms-2* (encoding an Ago-like protein) deletion mutant had no obvious impact on asexual development, whereas homozygous crosses of Δ *sad-1* or Δ *sms-2* gave rise to lethality in *N. crassa* (Lee et al., 2003; Shiu et al.,

2001). 24-28-nt oligomers originated from DEGs, which were enriched in GO in $\Delta ago2$ deletion mutants, were greatly less accumulated than WT and other *Ago* mutation strains, implicating that genes enriched in GO and KEGG in $\Delta ago2$ may be targeted by 24-28-nt sRNAs and result in impaired virulence.

4.3 5' nucleotide of mRNA-derived sRNAs is not the sole selection of Agos in *B. cinerea*

In *Botrytis* WT strain, over 97% of LTR-derived sRNAs have 5' uridine bias, which suggests that 5' nucleotide of siRNAs from LTR loci is not the sorting condition for Ago loading. However, only 48% of sRNAs originated from mRNAs begin with 5' uridine. Meanwhile, 24% of mRNA-derived sRNAs start with 5' adenosine and 16% sRNAs from mRNA loci have 5' cytosine. These 5' nucleotide distribution of sRNAs from mRNA loci implicate a more complicated composition of sRNAs than LTR-derived sRNAs. It has been shown that sRNAs were selected by Ago proteins based on seed region structure in *Drosophila*. Ago1 recruited typical miRNA/miRNA* duplexes with mismatches and Ago2 employed most perfectly paired siRNAs (Tomari et al., 2007). A similar finding was found in *Arabidopsis*, demonstrating that the selection of Ago proteins was dependent on the nucleotides at position 2, 6, 9, and 13 rather than simply based on the first nucleotide at 5' terminus (Thieme et al., 2012), which is consistent with our total sRNA profiling in Δago deletion mutants compared to WT strains (**Supplemental figure 6**). In contrast, a report revealed that Ago proteins associated with distinct sRNAs based on 5' nucleotide preference. Ago1 bound with miRNAs starting with 5' uridine, whereas the first 5' nucleotide of sRNAs associating with Ago2 and Ago4 were adenosine and Ago5 mainly employed sRNAs with 5' cytosine (Mi et al., 2008). Another document showed that the structure for 15th nucleotide of miRNA duplex benefited for the selection of Ago proteins (Zhang et al., 2014), which is not the case in *B. cinerea* due to the 15th nucleotide showing no change in Δago deletion mutants in comparison to WT. Thus, 5' nucleotide of mRNA-derived sRNAs is not the sole condition of sorting for Ago proteins in *B. cinerea*.

4.4 Ago proteins are functionally distinct in *B. cinerea*

Three catalytic tetrad DDD/H residues are critical for the RNase activity of Ago proteins. *Botrytis* Ago2 contains a DDH motif similar to *Arabidopsis* Ago1 that haveendonucleolytic activity, and Ago1 and Ago3 comprise a DDD tetrad residues similar to *N. crassa* Qde-2, suggesting the RNase catalysis of Ago1, Ago2 and Ago3 in *Botrytis*. GO term enrichment analysis shows that DEGs in *Ago1* or *Ago2* loss-of-function

mutants are involved in cellular component pathway, while DEGs in *Ago3* deletion mutant associate with molecular function and biological process. A model for distinct function of *Botrytis* Ago proteins is proposed based on the previous works and findings in this study (**Figure 4.1**). Most sRNAs lost in $\Delta ago1$ deletion mutants might result from two possibilities. Conceivably, Ago1 interacts with one of Dcl proteins as $\Delta dcl1dcl2$ double ko mutant was defective in mycelial growth and infection cushion formation (Weiberg et al., 2013) (**Figure 4.1A**). It has been shown that Ago2 interact with Dcr protein in human cells (Chendrimada et al., 2005). Therefore, it is also possible that *Botrytis* Ago2 associates with Dcl1 or Dcl2 protein. Alternatively, Ago might function sequentially and sRNAs might need to load into Ago1 first (**Figure 4.1A**).

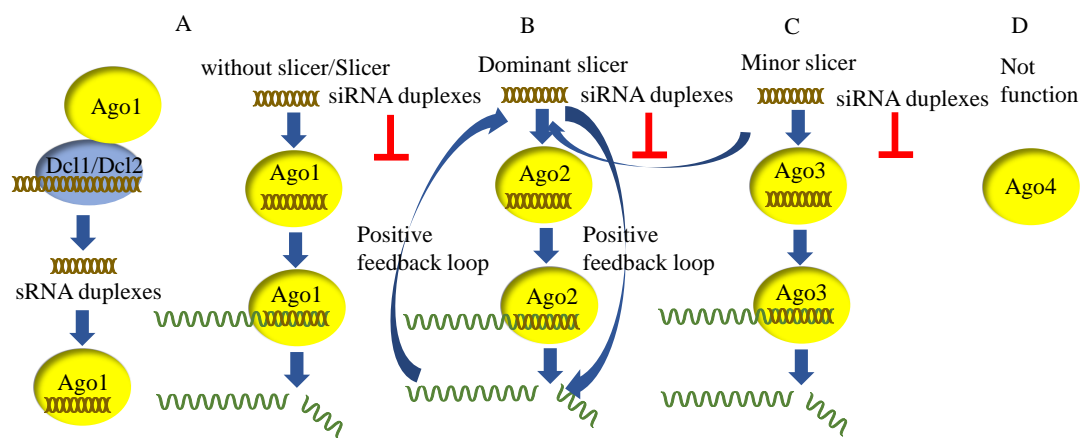


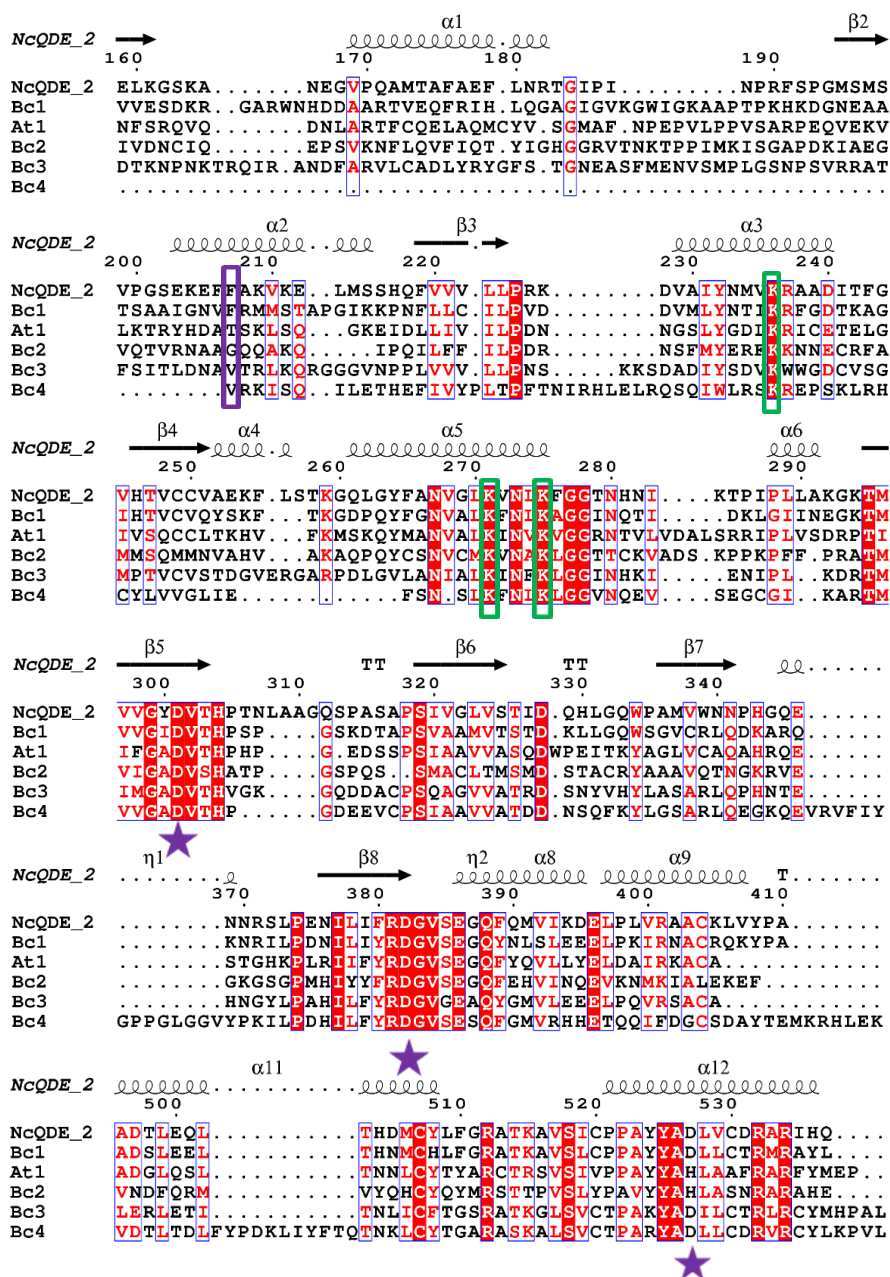
Figure 4.1 A proposed scenario for functionally distinct Ago proteins in *B. cinerea*

Botrytis Ago proteins functionally distinct and function sequentially. Ago1 might interact with one of Dcl proteins to produce sRNA molecules or the initiation of RNAi necessitates Ago1 to transfer sRNAs from nucleus to cytoplasm. Ago2 is a dominant slicer facilitating gene silencing directed by guide sRNAs. Ago3 might be a minor slicer interacting with few sRNAs and Ago4 is a pseudogene not involving in RNAi.

Arabidopsis Ago1 was documented functioning as a vehicle and delivering sRNAs from the nucleus to the cytoplasm (Bologna et al., 2018). In addition, Rde-1 functioned sequentially in *C. elegans*, associating with primary sRNAs to initiate RNAi machinery and other Ago proteins bound with amplified siRNAs to facilitate RNA silencing (Yigit et al., 2006). In this case, *Botrytis* Ago1 might be responsible for exporting sRNAs from nucleus to cytoplasm to initiate RNAi. Meanwhile, $\Delta ago1$ deletion mutants suppressed endogenous transcription (**Supplemental figure 7**). This indicates the function of Ago1 in nucleus. It is known that Ago proteins are capable of slicing passenger strand of sRNA duplex for releasing and negatively regulate sRNA duplex accumulation (Matranga et al., 2005; Meister & Tuschl, 2004; Rand et al., 2005). dsRNAs are more stable than ssRNAs that are easily degraded by exoribonuclease. Transcript level of retroelement LTR2 was greatly increased in $\Delta ago2$ deletion mutant, suggesting the

slicing ability of Ago2 rather than the role of stabilization. Ago2 is likely a dominant slicer because the expression level of LTR2 in $\Delta ago2$ deletion mutant was almost 2-fold higher than LTR2 transcripts in $\Delta ago1$ deletion mutant and sRNAs were increased in Ago2 mutation strains. sRNA molecules and mRNAs form a positive feedback loop (**Figure 4.1B**). By contrast, loss of Ago3 suppressed the transcript level of LTR1 and other Ago loss-of-function mutants unaltered LTR1 expression, which was consistent with *M. oryzae* Ago2 that negatively regulated PTGS (Nguyen et al., 2018). Considering the elevation of sRNAs in $\Delta ago3$ deletion mutants similar to the pattern in $\Delta ago2$, these findings implicate that Ago3 might be a minor slicer and Ago3 might compete with Ago2 for interacting with sRNA molecules (**Figure 4.1C**). However, no changes were observed in sRNA profiling and LTR1/LTR2 expression in $\Delta ago4$ deletion mutants and Ago4 was not required for LTR1 and LTR2 control, indicating that Ago1, Ago2, and Ago3 conduct most RNase complex work and Ago4 might have no function in RNAi in *B. cinerea* (**Figure 4.1D**).

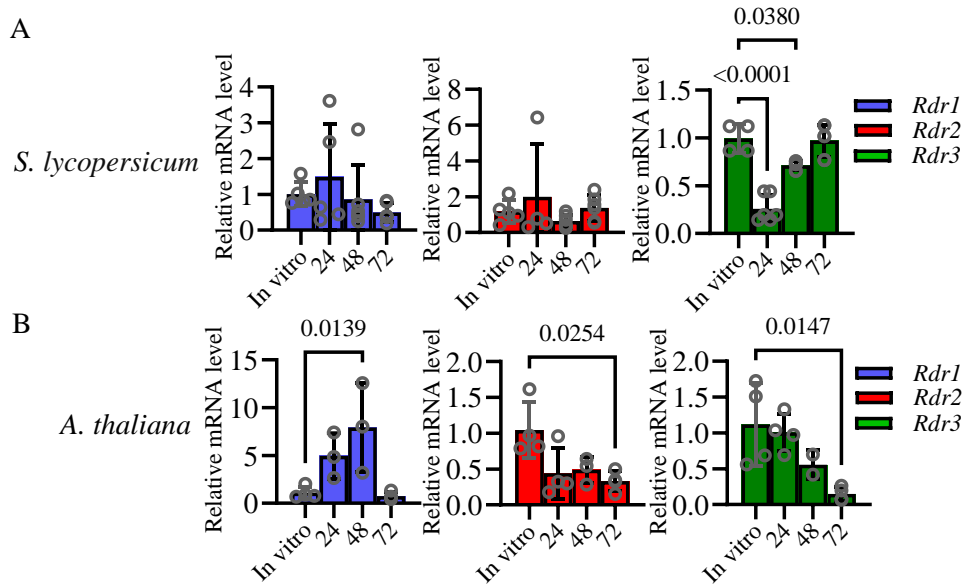
Supplemental figures and tables



Supplemental figure 1 Alignment of MID-PIWI motif of Ago protein sequences.

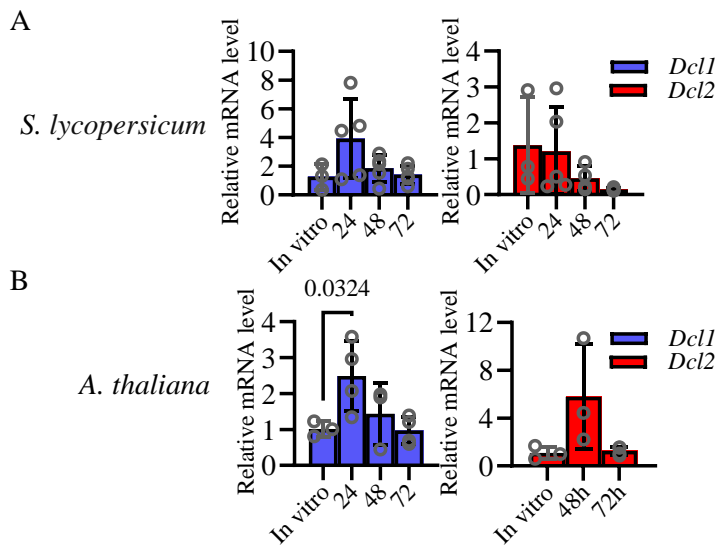
Ago Protein sequence alignment in *B. cinerea*, *N. crassa* and *A. thaliana*. The secondary structures are illustrated above the alignment, such as α -helices and β -strands (arrow). Purple boxes indicate mRNA binding site of the 5' m7GpppN cap (Kiriakidou et al., 2007). The red box refers to residues influence the allosteric regulation of mRNA binding. Green boxes represent residues that coordinate the two sulfate ions. Identical residues are in red shadow with white letters and conservative substitutions are in red letters with blue boxes.

Functionally distinct *Botrytis cinerea* Argonaute proteins in plant-microbe interaction



Supplemental figure 2 Expression pattern of *Botrytis Rdr* genes from infected *S. lycopersicum* and *A. thaliana*.

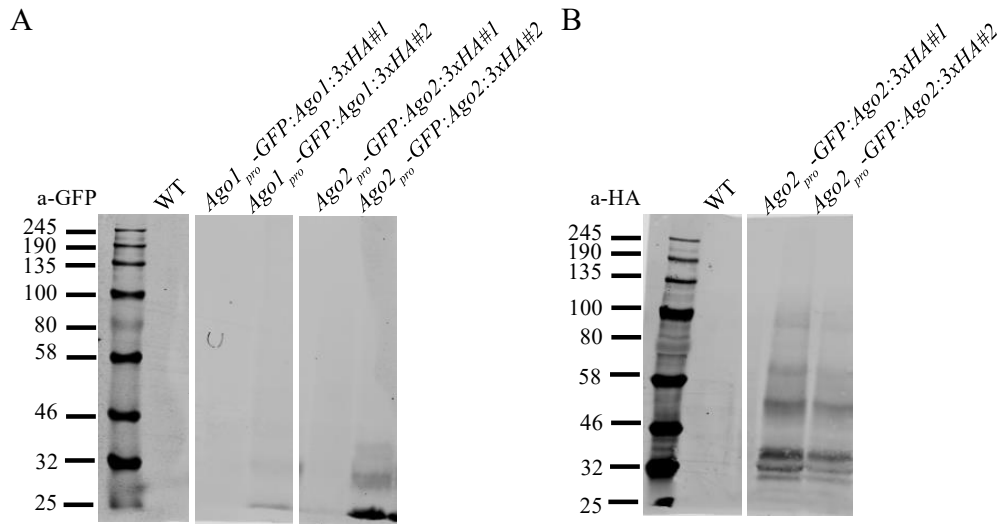
(A) (B) Infected leaves were collected from tomato or *Arabidopsis* after 24-, 48- and 72-hours inoculation by spraying with suspension conidia of WT strain. In vitro sporulated WT mycelium was considered a control. Values refer to mean \pm SD from four biological replicates normalized to the mean of *Actin* as a relative value to in vitro transcript by two-way ANOVA.



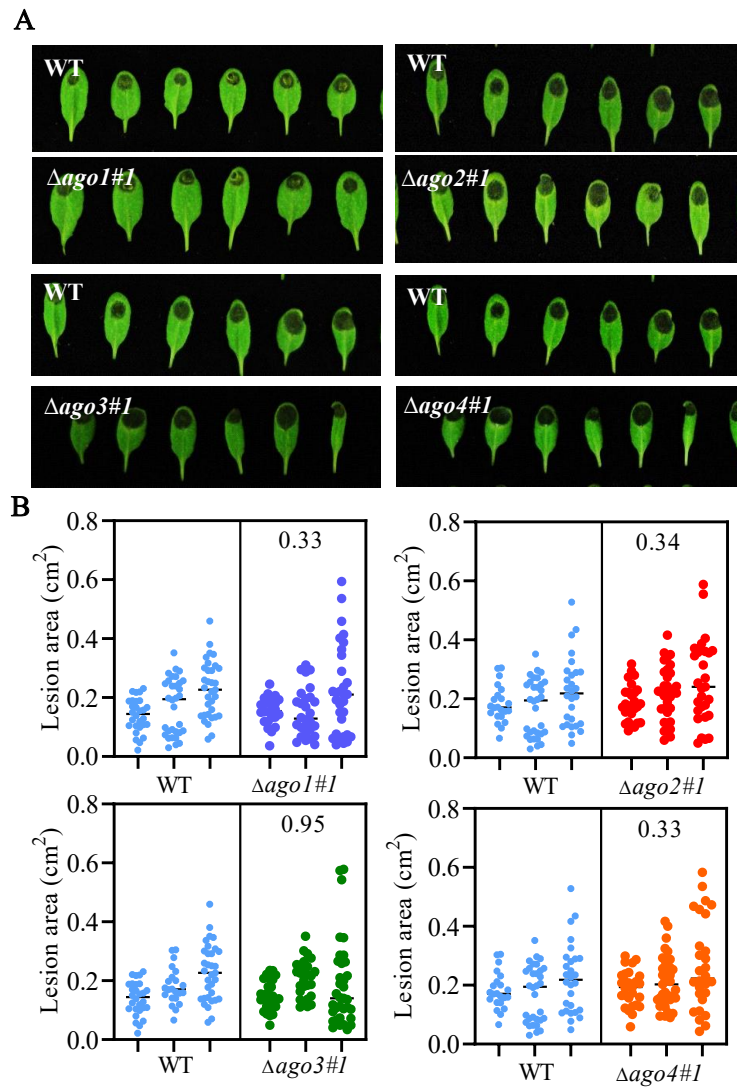
Supplemental figure 3 Expression pattern of *Botrytis Dcl* genes from infected *S. lycopersicum* and *A. thaliana*.

(A) (B) Infected leaves were collected from tomato or *Arabidopsis* after 24-, 48- and 72-hours inoculation by spraying with suspension conidia of WT strain. In vitro sporulated WT mycelium was considered a control. Values refer to mean \pm SD from four biological replicates normalized to the mean of *Actin* as a relative value to in vitro transcript by two-way ANOVA.

Functionally distinct *Botrytis cinerea* Argonaute proteins in plant-microbe interaction

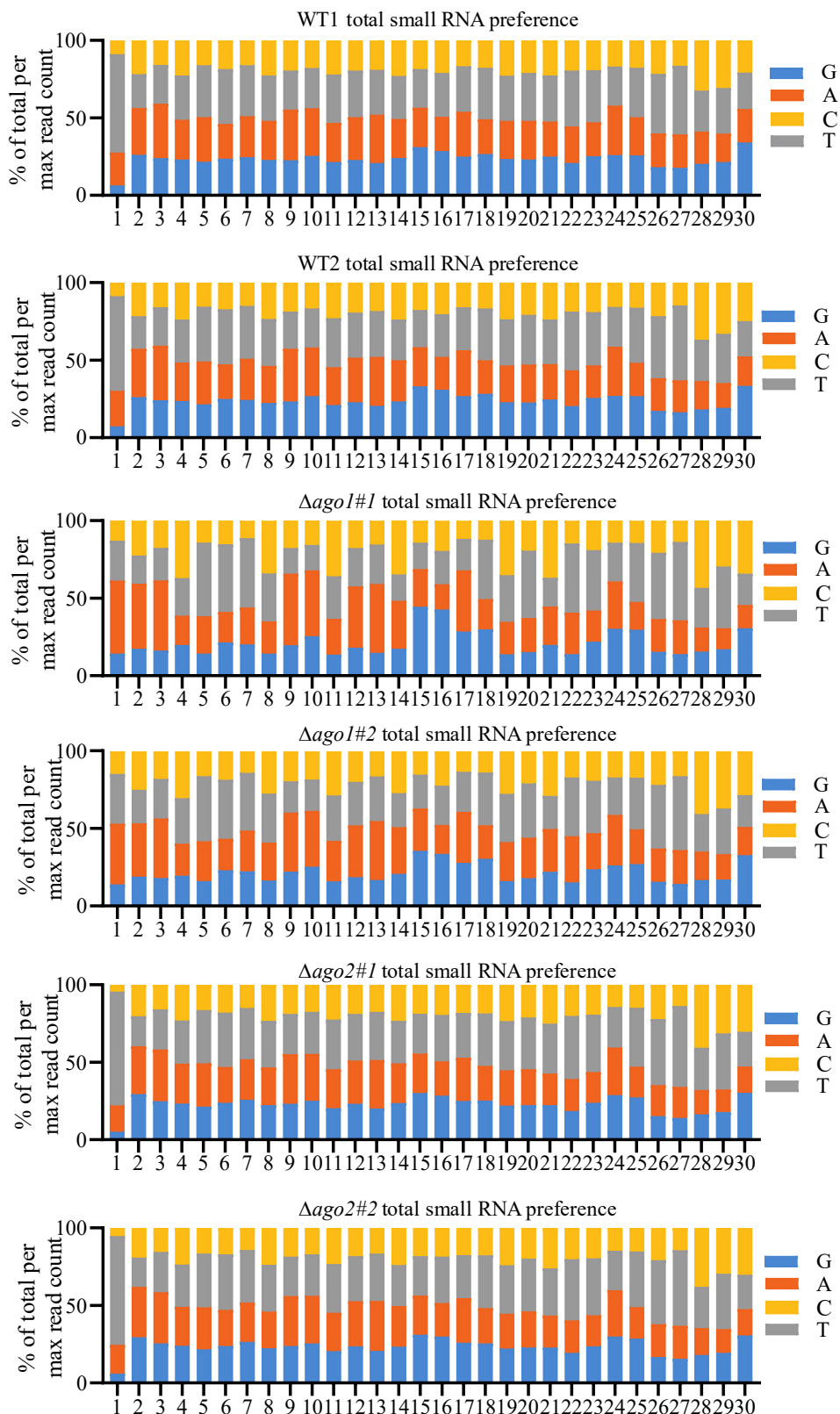


Supplemental figure 4 Western blot of *Botrytis* WT and GFP labelled strains.

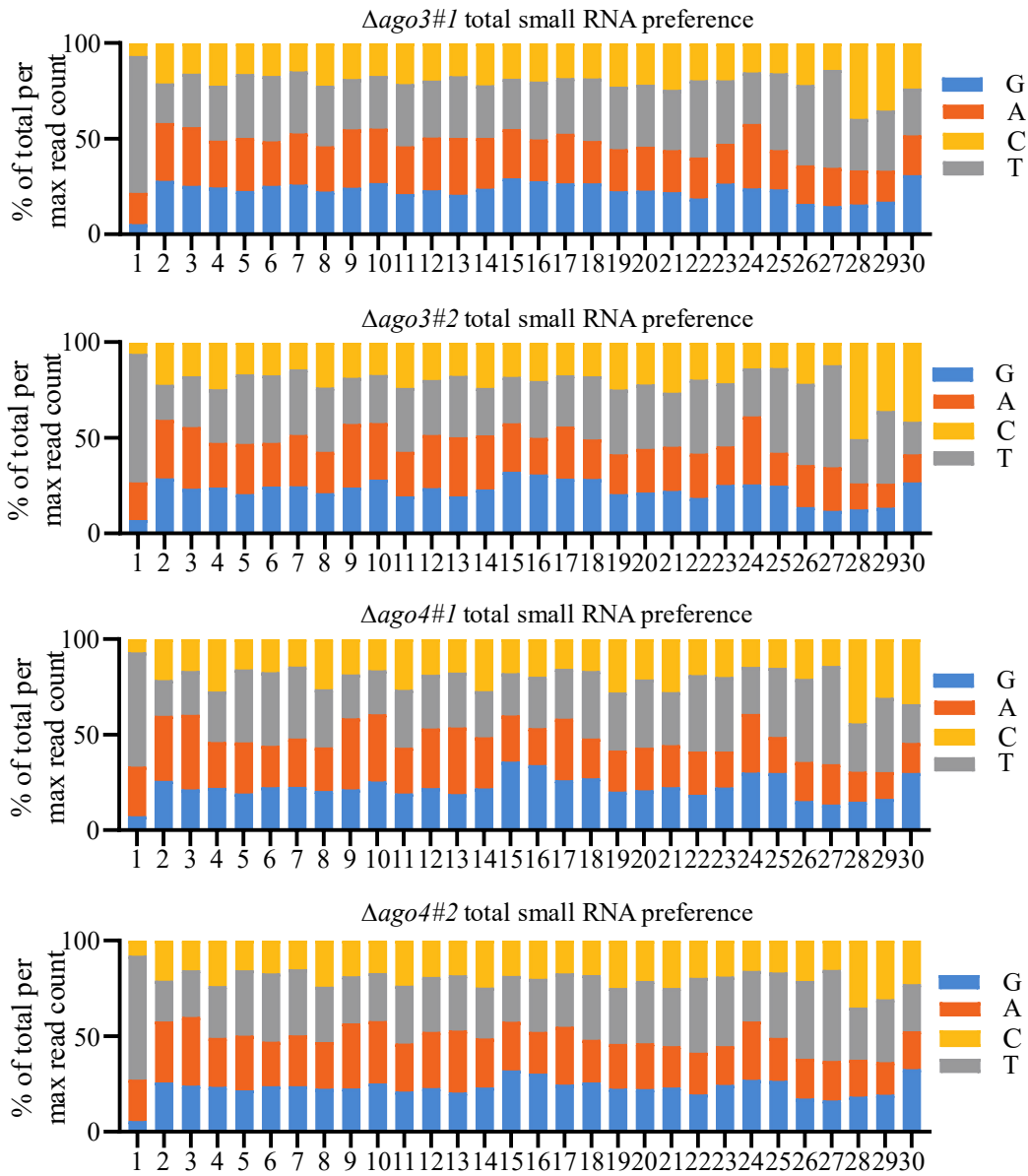


Supplemental figure 5 Inoculation assay with WT and Δago deletion mutants.

Functionally distinct *Botrytis cinerea* Argonaute proteins in plant-microbe interaction

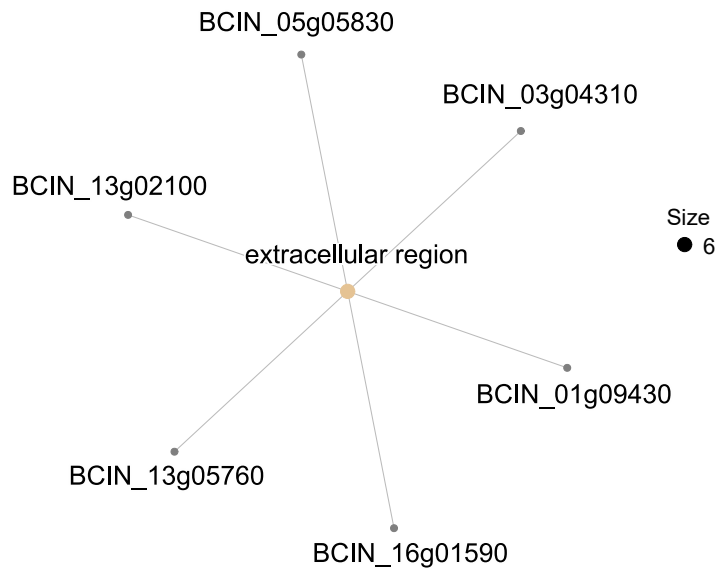
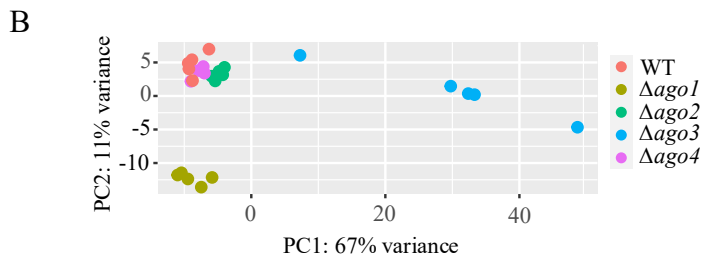
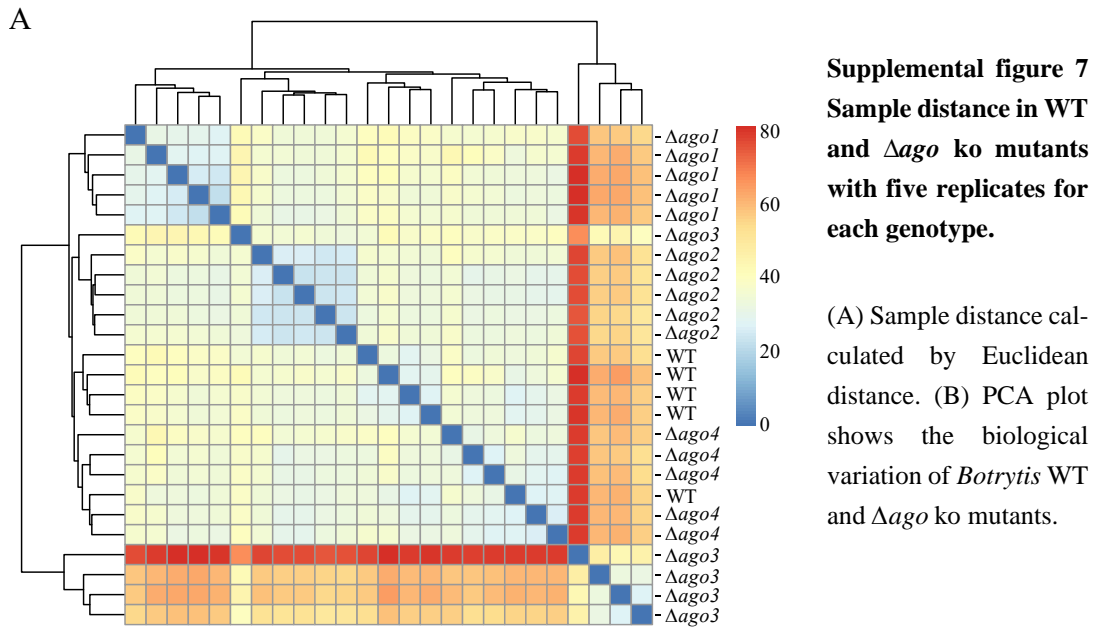


Functionally distinct *Botrytis cinerea* Argonaute proteins in plant-microbe interaction



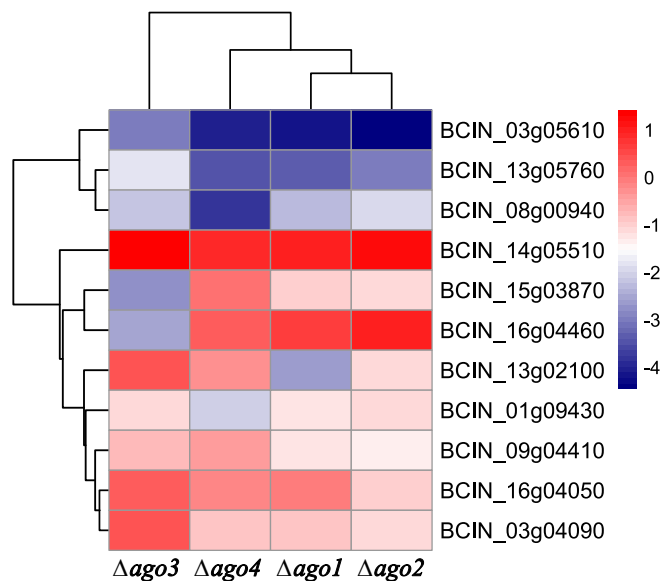
Supplemental figure 6 Total sRNA nucleotide distribution in WT and Δago deletion mutants

Functionally distinct *Botrytis cinerea* Argonaute proteins in plant-microbe interaction

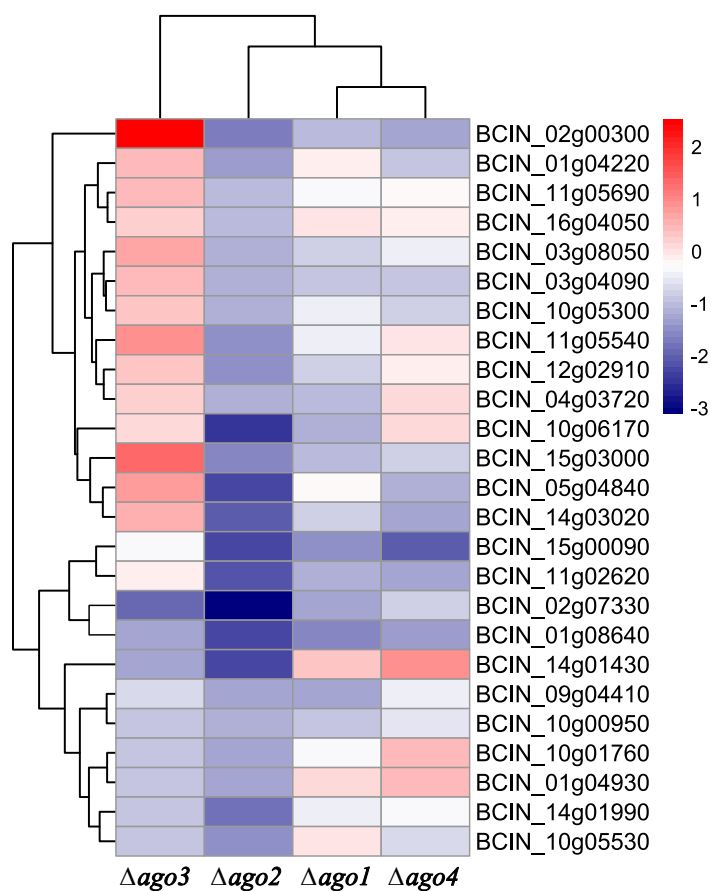


Supplemental figure 8 DEGs enriched in cellular component in *Ago1* loss-of-function mutants (incompletion).

Functionally distinct *Botrytis cinerea* Argonaute proteins in plant-microbe interaction



Supplemental figure 10 Eleven genes differentially expressed in *Ago2* loss-of-function mutants and enriched in GO and KEGG pathways.



Supplemental figure 11 Twenty-five downregulated genes differentially expressed in *Ago2* loss-of-function mutants.

Table 2 *Botrytis* strains used in this study

<i>Botrytis</i> strains	Plasmid	Selectable marker	Received strains
Wild-type (B05.10)	-	-	-
$\Delta ago1\#1/\#2$ (homokaryon)	5'flank-Hph-3'flank	Hygromycin	WT
$\Delta ago2\#1/\#2$ (homokaryon)	5'flank-Hph-3'flank	Hygromycin	WT
$\Delta ago3\#1/\#2$ (homokaryon)	5'flank-Hph-3'flank	Hygromycin	WT
$\Delta ago4\#1/\#2$ (homokaryon)	5'flank-Hph-3'flank	Hygromycin	WT
<i>cAgo2</i> #1/#2 (heterokaryon)	<i>Ago2_p-3HA::Ago2</i>	Nourseothricin	$\Delta ago2$
GFP (heterokaryon)	<i>Ago1_p-GFP::Ago1::3HA</i>	Nourseothricin	$\Delta ago1$
GFP (heterokaryon)	<i>Ago2_p-GFP::Ago2::3HA</i>	Nourseothricin	$\Delta ago2$

Table 3 Accession number of Ago protein sequence in representative Ascomycota fungi

Genus / Fungal species	Accession number
Sordariomycetes	
<i>Colletotrichum higginsianum</i> (IMI 349063)	Ch1: CCF47147
	Ch2: CCF38692
	Cp1: ACY36939
<i>Cryphonectria parasitica</i> (EP155)	Cp2: ACY36940
	Cp3: ACY36941
	Cp4: ACY36942
	Mo1: XM_003714169
<i>Magnaporthe oryzae</i> (70-15)	Mo2: XM_003717456
	Mo3: XM_003716656
	Nc_Qde-2: NCU04730
<i>Neurospora crassa</i> (OR74A)	Nc_Sms-2: NCU09434
	Tr1: ETS02811
<i>Trichoderma reesei</i> (RUT C-30)	Tr2: ETS00705
	Tr3: ETS02384
	Fo1: EXK27157
<i>Fusarium oxysporum</i> f. sp. <i>melonis</i> (26406)	Fo2: EXK33907
	Fo3: EXK48584
	Gg1: XM_009227279
<i>Gaeumannomyces graminis</i> var. <i>tritici</i> (R3-111a-1)	Gg2: XP_009218161

Functionally distinct *Botrytis cinerea* Argonaute proteins in plant-microbe interaction

	<i>Gg3</i> : XP_009216045
	<i>Gg4</i> : XP_009221516
Eurotiomycetes	
	<i>An1</i> : EHA21073
<i>Aspergillus niger</i> (ATCC 1015)	<i>An2</i> : EHA21487
	<i>An3</i> : CAL00657
	<i>Pc1</i> : XM_002557180
<i>Penicillium chrysogenum</i> (Wisconsin 54-1255)	<i>Pc2</i> : XM_002564321
	<i>Pc3</i> : XM_002559301
	<i>Ci1</i> : XM_001241131
<i>Coccidioides immitis</i> (RS)	<i>Ci2</i> : XM_001243611
	<i>Ci3</i> : XM_001244355
	<i>Hc1</i> : XP_001538593
<i>Histoplasma capsulatum</i> (NA _m 1)	<i>Hc2</i> : XP_001544570
	<i>Hc3</i> : XP_001536454
Leotiomycetes	
	<i>Bc1</i> : XP_024547764
<i>Botrytis cinerea</i> (B05.10)	<i>Bc2</i> : XP_024547409
	<i>Bc3</i> : XP_024552695
	<i>Bc4</i> : XP_024553502 +XP_001546217
	<i>Ss1</i> : APA14427
<i>Sclerotinia sclerotiorum</i> (1980 UF-70)	<i>Ss2</i> : XP_001586694
	<i>Bg1</i> : CCU75107
<i>Blumeria graminis f.sp.hordei</i> (DH14)	<i>Bg2</i> : CCU79215
	<i>Bg3</i> : CCU74167
Dothideomycetes	
	<i>Lm1</i> : XP_003843925
<i>Leptosphaeria maculans</i> (JN3)	<i>Lm2</i> : XP_003842164
	<i>Lm3</i> : XP_003841784
	<i>Sn1</i> : XP_001796933
<i>Stagonospora nodorum</i> (SN15)	<i>Sn2</i> : XP_001800812
<i>Arabidopsis thaliana</i> (Col-0)	<i>AtAgo1</i> : NP_175274
<i>Schizosaccharomyces pombe</i>	<i>Sp1</i> : NP_587782

Table 4 Primers used in this study

Purpose	Primer Name	Sequence (5' to 3')
Loss-of-function mutant	<i>Bc</i> -ago1-5'flank-F	ACGGTCTCTGCGGATGTCTTTTGACCCGGCTGCA
Loss-of-function mutant	<i>Bc</i> -ago1-5'flank-R	ACGGTCTCACCTTAGCTGTGGAGAAGTGTCTATTG
Loss-of-function mutant	<i>Bc</i> -ago1-3'flank-F	ATGGTCTCATGAGGACAATCGATAAGCTTGGGA
Loss-of-function mutant	<i>Bc</i> -ago1-3'flank-R	CAGGTCTCTGACATTAGATCCAAAACATCGAGTC
Loss-of-function mutant	<i>Bc</i> -ago2-5'flank-F	CAGGTCTCAGCGGCACTTGATTGCTGGCTCAC
Loss-of-function mutant	<i>Bc</i> -ago2-5'flank-R	CGGGTCTCACCTTGATGTGCGATTTTGGTGGCGTC
Loss-of-function mutant	<i>Bc</i> -ago2-3'flank-F	CAGGTCTCATGAGGTACTTCTATTACTTCATCACCA
Loss-of-function mutant	<i>Bc</i> -ago2-3'flank-R	CGGGTCTCAGACA AAGTGAT- TACATTCATGGCTGCTG
Loss-of-function mutant	<i>Bc</i> -ago3-5'flank-F	TAGGTCTCAGCGGTATTTTGCTAAAAGCTCAAG
Loss-of-function mutant	<i>Bc</i> -ago3-5'flank-R	ATGGTCTCACCTTAGAGTCGAAACTAGGATCTA
Loss-of-function mutant	<i>Bc</i> -ago3-3'flank-F	ATGGTCTCATGAGCACACCAGCGAAATATGCAG
Loss-of-function mutant	<i>Bc</i> -ago3-3'flank-R	ATGGTCTCAGACACGCGTGATAGTTTTTCTATC
Loss-of-function mutant	<i>Bc</i> -ago4-5'flank-F	ATGGTCTCAGCGGTCTTCACAAAGCTTGTGGTAT
Loss-of-function mutant	<i>Bc</i> -ago4-5'flank-R	ATGGTCTCACCTTAGGTACAAACCCTTCGGACT
Loss-of-function mutant	<i>Bc</i> -ago4-3'flank-F	ATGGTCTCATGAGTGAATGCTGGAAGTATCATC
Loss-of-function mutant	<i>Bc</i> -ago4-3'flank-R	ATGGTCTCAGACAATCAAATACTGAAAGATGAG
KO genotyping	<i>Bc</i> -ago1-po-F	CGTATGTAGATAAGATGTAT
KO genotyping	<i>Bc</i> -ago1-po-R	ACGAACAATCGGCATGGTTGA
KO genotyping	<i>Bc</i> -ago1-ko-F	ACAGGAGACTTGCCCCAATG
KO genotyping	<i>Bc</i> -ago1-ko-R	ATTGCTCGACTGTCCTAGCC
KO genotyping	<i>Bc</i> -ago2-po-F	TGATTTAATAGCTCCATGTC
KO genotyping	<i>Bc</i> -ago2-po-R	GAGATCAAAGTCCTAAGAAGTG
KO genotyping	<i>Bc</i> -ago2-ko-F	ACGTTGAAACATCACGGCAA
KO genotyping	<i>Bc</i> -ago2-ko-R	TGGCATTAAACCATCAGCGG
KO genotyping	<i>Bc</i> -ago3-po-F	CGTATGTAGATAAGATGTAT
KO genotyping	<i>Bc</i> -ago3-po-R	TTGTCTAGTATGACGGCACGGA
KO genotyping	<i>Bc</i> -ago3-ko-F	ACACCGAGGTATGCATGAGT
KO genotyping	<i>Bc</i> -ago3-ko-R	CCGACGCCATCACGATAGAA
KO genotyping	<i>Bc</i> -ago4-po-F	CGTATGTAGATAAGATGTAT
KO genotyping	<i>Bc</i> -ago4-po-R	TGGTCGGTACTAGGTACGAGA
KO genotyping	<i>Bc</i> -ago4-ko-F	TACCGAGATGGAGTGAGCGA
KO genotyping	<i>Bc</i> -ago4-ko-R	CGGTTTCCATTTCTCACC GC
qRT-PCR	<i>Bc</i> -Ago1-RT-F	AGGCAATTGGACATCTGGCA
qRT-PCR	<i>Bc</i> -Ago1-RT-R	TGCGGGATACTTCTGACGAC

Functionally distinct *Botrytis cinerea* Argonaute proteins in plant-microbe interaction

qRT-PCR	<i>Bc-Ago2-RT-F</i>	AAGGCACCCTCTAGCCAAAC
qRT-PCR	<i>Bc-Ago2-RT-R</i>	ACCACATGCCATTACGAAGC
qRT-PCR	<i>Bc-Ago3-RT-F</i>	ACCTTCCTGCCACATTCTC
qRT-PCR	<i>Bc-Ago3-RT-R</i>	TGATGGCGCTTTCCTACCAC
qRT-PCR	<i>Bc-Ago4-RT-F</i>	TTGTAGTCCACTAGGCACGG
qRT-PCR	<i>Bc-Ago4-RT-R</i>	GACAGAGAGGGCTTTGGAGG
qRT-PCR	<i>Bc-Actin-RT-F</i>	CATTGTTATGTCTGGTGGAACCAC
qRT-PCR	<i>Bc-Actin-RT-R</i>	AGAACCACCAATCCAGACGGAGTA
Gain-of-function mutant	<i>Bc-Ago1-5UTR-F</i>	ACGGTCTCAGCGGCCAAGCGTTTCTCTGTTGC
Gain-of-function mutant	<i>Bc-Ago1-5UTR-R</i>	ACGGTCTCTGACAGGTATGGCTCAAGAGGGTTC
Gain-of-function mutant	<i>Bc-Ago1-3UTR-F</i>	ACGGTCTCAGCGGACATTTTGATGTGTACTGG
Gain-of-function mutant	<i>Bc-Ago1-3UTR-R</i>	ACGGTCTCTGACAGGAATATCCAATTGCCCTA
ORF cloning (point mutation)	<i>Bc-Ago1_ORF-F_outer</i>	TCGAAGACAGTACGGGTCTCNC ACCTCTTTTGACCCGGCTGCA
ORF cloning (point mutation)	<i>Bc-Ago1_ORF-R_outer</i>	TCGAAGACGACAGAGGTCTCNCC TTGATCCAAAACATCGAGTCTG
ORF cloning (point mutation)	<i>Bc-Ago1_ORF-R_inner1</i>	TCGAAGACTCGATCTCTGTAAAGCGTATTAG
ORF cloning (point mutation)	<i>Bc-Ago1_ORF-F_inner1</i>	TCGAAGACGTGATCCTAATTATCCAGCAGAAG
ORF cloning (point mutation)	<i>Bc-Ago1_ORF-R_inner2</i>	TCGAAGACACGTCCCTCCCTTCGTTTCGC
ORF cloning (point mutation)	<i>Bc-Ago1_ORF-F_inner2</i>	TCGAAGACACGGACGATCCACATGAAAATG
ORF cloning (point mutation)	<i>Bc-Ago1_ORF-R_inner3</i>	TCGAAGACGAGCCTTCTGTTTGCGAAATC
ORF cloning (point mutation)	<i>Bc-Ago1_ORF-F_inner3</i>	TCGAAGACTCAGGCCAGAGCCCAACGCAAT
Gain-of-function mutant	<i>Bc-Ago2-5UTR-F</i>	ACGGTCTCAGCGGCACTTGATTGCTGGCTCAC
Gain-of-function mutant	<i>Bc-Ago2-5UTR-R</i>	ACGGTCTCTGACAGATGTGATTTGGTGGCGTC
Gain-of-function mutant	<i>Bc-Ago2-3UTR-F</i>	ACGGTCTCAGCGGTACTIONTATTACTTCATCACCA
Gain-of-function mutant	<i>Bc-Ago2-3UTR-R</i>	ACGGTCTCTGACAAAGTGAT- TACATTCATGGCTGCTG
ORF cloning (point mutation)	<i>Bc-Ago2-F-outer</i>	CCGAAGACCCTACGGGTCTCGC ACCGGTGCTGGTCAACAGCAGCG
ORF cloning (point mutation)	<i>Bc-Ago2-F-inner1</i>	TCGAAGACTAGGGACCCAAAGAAAGATGA
ORF cloning (point mutation)	<i>Bc-Ago2-R-inner1</i>	TCGAAGACAGTCCCTGGCGGGATCAAAGC
ORF cloning (point mutation)	<i>Bc-Ago2-F-inner2</i>	TCGAAGACGACAGCATTCGAGTCAACCAG
ORF cloning (point mutation)	<i>Bc-Ago2-R-inner2</i>	TCGAAGACATGCTGATTGCCTTGCTTGA
ORF cloning (point mutation)	<i>Bc-Ago2-R-outer</i>	CCGAAGACGTCAGAGGTCTCACCTTA ATGTACCACATGCCATTACGAAGCT
ORF cloning (point mutation)	<i>Bc-Ago1-probe-F</i>	TGTGGTCGATCGTGGTGTAC
ORF cloning (point mutation)	<i>Bc-Ago1-probe-R</i>	AGGTTCTGGTGTAGTCTGGC
ORF cloning (point mutation)	<i>Bc-Ago2-probe-F</i>	GTCGCTTCTATCTCGTCCCTC

Functionally distinct *Botrytis cinerea* Argonaute proteins in plant-microbe interaction

ORF cloning (point mutation)	<i>Bc-Ago2-probe-R</i>	GTGAGAATAGCGACGGCGAG
ORF cloning (point mutation)	<i>Bc-Ago3-probe-F</i>	TGGGGGATGCTCTTACTGGTGC
ORF cloning (point mutation)	<i>Bc-Ago3-probe-R</i>	CCAAACCCTGAACGCCGACT
ORF cloning (point mutation)	<i>Bc-Ago4-probe-F</i>	CAAATGGTGGGTGTTGATGC
ORF cloning (point mutation)	<i>Bc-Ago4-probe-R</i>	GGTTCGGCTAGAGATTGTGATGG
GFP genotyping	<i>Bc-GFP-Ago1-5'F</i>	GCCCTCCAAGGTTATCTCCA
GFP genotyping	<i>Bc-GFP-Ago1-5'R</i>	TTGAAATCGATGCCCTTCAAC
GFP genotyping	<i>Bc-GFP-Ago1-3'F</i>	AGCAGGCGCTCTACATGA
GFP genotyping	<i>Bc-GFP-Ago1-3'R</i>	CTCTTGCAACTTCAGCCT
GFP genotyping	<i>Bc-GFP-Ago1-inner-F</i>	AGGCAATTGGACATCTGGCA
GFP genotyping	<i>Bc-GFP-Ago1-inner-R</i>	TAGAAGACTTCAGAGGTCTCAGATTTT AAAGCTTAGCAGCGTAATCTGG
GFP genotyping	<i>Bc-GFP-Ago2-5'F</i>	CAATCAATGCCATATATTGTG
GFP genotyping	<i>Bc-GFP-Ago2-5'R</i>	TTGAAATCGATGCCCTTCAAC
GFP genotyping	<i>Bc-GFP-Ago2-3'F</i>	AGCAGGCGCTCTACATGA
GFP genotyping	<i>Bc-GFP-Ago2-3'R</i>	GTCGGTGGAAATTTGAATAAGAG
GFP genotyping	<i>Bc-GFP-Ago2-inner-F</i>	AAGGCACCCTCTAGCCAAAC
GFP genotyping	<i>Bc-GFP-Ago2-inner-R</i>	TCAGAGGTCTCAGATTTT AAAGCTTAGCAGCGTAATCTGG
Complement genotyping	<i>Bc-cAgo2-5'F1</i>	CAATCAATGCCATATATTGTG
Complement genotyping	<i>Bc-cAgo2-5'R1</i>	TCCCTGGCGGGATCAAAGC
Complement genotyping	<i>Bc-cAgo2-5'F2</i>	CAATCAATGCCATATATTGTG
Complement genotyping	<i>Bc-cAgo2-5'R2</i>	TCAGAGGTCTCAGGTGCCAA GCTTAGCAGCGTAATCTGG
Complement genotyping	<i>Bc-cAgo2-3'F</i>	AGCAGGCGCTCTACATGA
Complement genotyping	<i>Bc-cAgo2-3'R</i>	GTCGGTGGAAATTTGAATAAGAG
Complement genotyping	<i>Bc-cAgo2-inner-F</i>	TTACGGGTCTCATCTGAAC AATGGCTGGATCTCGCATC
Complement genotyping	<i>Bc-cAgo2-inner-R</i>	TCCCTGGCGGGATCAAAGC
Stem-loop RT	<i>Bc-siR3.2-RT</i>	GTCGTATCCAGTGCAGGGTCCGAGGTA TTCGCACTGGATACGACACTCAC
sRNA amplification	<i>Bc-siR3.2-F</i>	GCGGCGGTACATTGTGGATCT
sRNA amplification	sRNA universal-R	GTATCCAGTGCAGGGTCCGAGGT
PCR	<i>Bc-tub-RT-F</i>	GAGGTTGAGGACCAAATGCG
PCR	<i>Bc-tub-RT-R</i>	GGACATCTTGAGACCACGGG

References

- Aamlid, K. (1952). A study of cauliflower, *Brassica oleracea* Linn., var. *Botrytis*, D.C.
- Agorio, A., & Vera, P. (2007). Argonaute4 is required for resistance to *Pseudomonas syringae* in *Arabidopsis*. *Plant Cell*, 19(11), 3778-3790. <https://doi.org/10.1105/tpc.107.054494>
- Alexander, W. G., Raju, N. B., Xiao, H., Hammond, T. M., Perdue, T. D., Metzberg, R. L., Pukkila, P. J., & Shiu, P. K. (2008). DCL-1 colocalizes with other components of the MSUD machinery and is required for silencing. *Fungal Genet Biol*, 45(5), 719-727. <https://doi.org/10.1016/j.fgb.2007.10.006>
- Allen, E., Xie, Z., Gustafson, A. M., & Carrington, J. C. (2005). microRNA-directed phasing during trans-acting siRNA biogenesis in plants. *Cell*, 121(2), 207-221. <https://doi.org/10.1016/j.cell.2005.04.004>
- Allen, G. C., Flores-Vergara, M. A., Krasynanski, S., Kumar, S., & Thompson, W. F. (2006). A modified protocol for rapid DNA isolation from plant tissues using cetyltrimethylammonium bromide. *Nat Protoc*, 1(5), 2320-2325. <https://doi.org/10.1038/nprot.2006.384>
- Altschul, S. F., Gish, W., Miller, W., Myers, E. W., & Lipman, D. J. (1990). Basic local alignment search tool. *J Mol Biol*, 215(3), 403-410. [https://doi.org/10.1016/S0022-2836\(05\)80360-2](https://doi.org/10.1016/S0022-2836(05)80360-2)
- Ando, S., Jaskiewicz, M., Mochizuki, S., Koseki, S., Miyashita, S., Takahashi, H., & Conrath, U. (2021). Priming for enhanced Argonaute2 activation accompanies induced resistance to cucumber mosaic virus in *Arabidopsis thaliana*. *Mol Plant Pathol*, 22(1), 19-30. <https://doi.org/10.1111/mpp.13005>
- Aramayo, R., & Metzberg, R. L. (1996). Meiotic transvection in fungi. *Cell*, 86(1), 103-113. [https://doi.org/10.1016/s0092-8674\(00\)80081-1](https://doi.org/10.1016/s0092-8674(00)80081-1)
- Arribas-Hernandez, L., Marchais, A., Poulsen, C., Haase, B., Hauptmann, J., Benes, V., Meister, G., & Brodersen, P. (2016). The slicer activity of Argonaute1 is required specifically for the phasing, not production, of trans-acting short interfering RNAs in *Arabidopsis*. *Plant Cell*, 28(7), 1563-1580. <https://doi.org/10.1105/tpc.16.00121>
- Asman, A. K., Fogelqvist, J., Vetukuri, R. R., & Dixelius, C. (2016). *Phytophthora infestans* Argonaute1 binds microRNA and small RNAs from effector genes and transposable elements. *New Phytol*, 211(3), 993-1007. <https://doi.org/10.1111/nph.13946>
- Astier-Manificier, S., & Cornuet, P. (1971). RNA-dependent RNA polymerase in Chinese cabbage. *Biochim Biophys Acta*, 232(3), 484-493. [https://doi.org/10.1016/0005-2787\(71\)90602-2](https://doi.org/10.1016/0005-2787(71)90602-2)
- Axtell, M. J., Jan, C., Rajagopalan, R., & Bartel, D. P. (2006). A two-hit trigger for siRNA biogenesis in plants. *Cell*, 127(3), 565-577. <https://doi.org/10.1016/j.cell.2006.09.032>
- Bagnoli, J. W., Ziegenhain, C., Janjic, A., Wange, L. E., Vieth, B., Parekh, S., Geuder, J., Hellmann, I., & Enard, W. (2018). Sensitive and powerful single-cell RNA sequencing using mcSCR-seq. *Nat Commun*, 9(1), 2937. <https://doi.org/10.1038/s41467-018-05347-6>
- Bajczyk, M., Bhat, S. S., Szewc, L., Szweykowska-Kulinska, Z., Jarmolowski, A., & Dolata, J. (2019). Novel nuclear functions of *Arabidopsis* Argonaute1: beyond RNA interference. *Plant Physiol*, 179(3), 1030-1039. <https://doi.org/10.1104/pp.18.01351>
- Barkai-Golan, R., Ben-Yehoshua, S., Aharoni, N., Eisenberg, E., & Kahan, R. S. (1971). The development of *Botrytis cinerea* in irradiated strawberries during storage. *Int J Appl Radiat Isot*, 22(3), 155-158. [https://doi.org/10.1016/0020-708x\(71\)90118-9](https://doi.org/10.1016/0020-708x(71)90118-9)
- Baumberger, N., & Baulcombe, D. C. (2005). *Arabidopsis* Argonaute1 is an RNA slicer that selectively recruits microRNAs and short interfering RNAs. *Proc Natl Acad Sci U S A*, 102(33), 11928-11933. <https://doi.org/10.1073/pnas.0505461102>

- Baumberger, N., Tsai, C. H., Lie, M., Havecker, E., & Baulcombe, D. C. (2007). The Polerovirus silencing suppressor P0 targets Argonaute proteins for degradation. *Curr Biol*, *17*(18), 1609-1614. <https://doi.org/10.1016/j.cub.2007.08.039>
- Bernstein, E., Caudy, A. A., Hammond, S. M., & Hannon, G. J. (2001). Role for a bidentate ribonuclease in the initiation step of RNA interference. *NATURE*, *409*(6818), 363-366. <https://doi.org/10.1038/35053110>
- Blankenberg, D., Von Kuster, G., Coraor, N., Ananda, G., Lazarus, R., Mangan, M., Nekrutenko, A., & Taylor, J. (2010). Galaxy: a web-based genome analysis tool for experimentalists. *Curr Protoc Mol Biol*, Chapter 19, Unit 19 10 11-21. <https://doi.org/10.1002/0471142727.mb1910s89>
- Blaszczyk, J., Tropea, J. E., Bubunencko, M., Routzahn, K. M., Waugh, D. S., Court, D. L., & Ji, X. (2001). Crystallographic and modeling studies of RNase III suggest a mechanism for double-stranded RNA cleavage. *Structure*, *9*(12), 1225-1236. [https://doi.org/10.1016/s0969-2126\(01\)00685-2](https://doi.org/10.1016/s0969-2126(01)00685-2)
- Bohmert, K., Camus, I., Bellini, C., Bouchez, D., Caboche, M., & Benning, C. (1998). AGO1 defines a novel locus of *Arabidopsis* controlling leaf development. *EMBO J*, *17*(1), 170-180. <https://doi.org/10.1093/emboj/17.1.170>
- Boland, A., Huntzinger, E., Schmidt, S., Izaurralde, E., & Weichenrieder, O. (2011). Crystal structure of the MID-PIWI lobe of a eukaryotic Argonaute protein. *Proc Natl Acad Sci U S A*, *108*(26), 10466-10471. <https://doi.org/10.1073/pnas.1103946108>
- Boland, A., Tritschler, F., Heimstadt, S., Izaurralde, E., & Weichenrieder, O. (2010). Crystal structure and ligand binding of the MID domain of a eukaryotic Argonaute protein. *EMBO Rep*, *11*(7), 522-527. <https://doi.org/10.1038/embor.2010.81>
- Boller, T., & He, S. Y. (2009). Innate immunity in plants: an arms race between pattern recognition receptors in plants and effectors in microbial pathogens. *Science*, *324*(5928), 742-744. <https://doi.org/10.1126/science.1171647>
- Bollmann, S. R., Fang, Y., Press, C. M., Tyler, B. M., & Grunwald, N. J. (2016). Diverse evolutionary trajectories for small RNA biogenesis genes in the oomycete genus *Phytophthora*. *Front Plant Sci*, *7*, 284. <https://doi.org/10.3389/fpls.2016.00284>
- Bologna, N. G., Iselin, R., Abriata, L. A., Sarazin, A., Pumplun, N., Jay, F., Grentzinger, T., Dal Peraro, M., & Voinnet, O. (2018). Nucleo-cytosolic shuttling of Argonaute1 prompts a revised model of the plant microRNA pathway. *Mol Cell*, *69*(4), 709-719 e705. <https://doi.org/10.1016/j.molcel.2018.01.007>
- Brodersen, P., Sakvarelidze-Achard, L., Bruun-Rasmussen, M., Dunoyer, P., Yamamoto, Y. Y., Sieburth, L., & Voinnet, O. (2008). Widespread translational inhibition by plant miRNAs and siRNAs. *Science*, *320*(5880), 1185-1190. <https://doi.org/10.1126/science.1159151>
- Brosseau, C., El Oirdi, M., Adurogbangba, A., Ma, X., & Moffett, P. (2016). Antiviral defense involves AGO4 in an *Arabidopsis*-potexvirus interaction. *Mol Plant Microbe Interact*, *29*(11), 878-888. <https://doi.org/10.1094/MPMI-09-16-0188-R>
- Brosseau, C., & Moffett, P. (2015). Functional and genetic analysis identify a role for *Arabidopsis* Argonaute5 in antiviral RNA silencing. *Plant Cell*, *27*(6), 1742-1754. <https://doi.org/10.1105/tpc.15.00264>
- Bucher, G., Scholten, J., & Klingler, M. (2002). Parental RNAi in *Tribolium* (Coleoptera). *Curr Biol*, *12*(3), R85-86. [https://doi.org/10.1016/s0960-9822\(02\)00666-8](https://doi.org/10.1016/s0960-9822(02)00666-8)
- Buckley, B. A., Burkhart, K. B., Gu, S. G., Spracklin, G., Kershner, A., Fritz, H., Kimble, J., Fire, A., & Kennedy, S. (2012). A nuclear Argonaute promotes multigenerational epigenetic inheritance and germline immortality. *NATURE*, *489*(7416), 447-451. <https://doi.org/10.1038/nature11352>
- Buddhika, U. V. A., Savocchia, S., & Steel, C. C. (2020). Copper induces transcription of *BcLCC2* laccase gene in phytopathogenic fungus, *Botrytis cinerea*. *Mycology*, *12*(1), 48-57. <https://doi.org/10.1080/21501203.2020.1725677>

Functionally distinct *Botrytis cinerea* Argonaute proteins in plant-microbe interaction

- Buker, S. M., Iida, T., Buhler, M., Villen, J., Gygi, S. P., Nakayama, J., & Moazed, D. (2007). Two different Argonaute complexes are required for siRNA generation and heterochromatin assembly in fission yeast. *Nat Struct Mol Biol*, 14(3), 200-207. <https://doi.org/10.1038/nsmb1211>
- Buttner, P., Koch, F., Voigt, K., Quidde, T., Risch, S., Blaich, R., Bruckner, B., & Tudzynski, P. (1994). Variations in ploidy among isolates of *Botrytis cinerea*: implications for genetic and molecular analyses. *Curr Genet*, 25(5), 445-450. <https://doi.org/10.1007/BF00351784>
- Cai, Q., Qiao, L., Wang, M., He, B., Lin, F. M., Palmquist, J., Huang, S. D., & Jin, H. (2018). Plants send small RNAs in extracellular vesicles to fungal pathogen to silence virulence genes. *Science*, 360(6393), 1126-1129. <https://doi.org/10.1126/science.aar4142>
- Campo, S., Gilbert, K. B., & Carrington, J. C. (2016). Small RNA-based antiviral defense in the phytopathogenic fungus *Colletotrichum higginsianum*. *PLoS Pathog*, 12(6), e1005640. <https://doi.org/10.1371/journal.ppat.1005640>
- Carbonell, A., Fahlgren, N., Garcia-Ruiz, H., Gilbert, K. B., Montgomery, T. A., Nguyen, T., Cuperus, J. T., & Carrington, J. C. (2012). Functional analysis of three *Arabidopsis* Argonautes using slicer-defective mutants. *Plant Cell*, 24(9), 3613-3629. <https://doi.org/10.1105/tpc.112.099945>
- Carroll, A. M., Sweigard, J. A., & Valent, B. (1994). Improved vectors for selecting resistance to hygromycin. *Fungal Genetics Reports*, 41(1). <https://doi.org/10.4148/1941-4765.1367>
- Catalanotto, C., Azzalin, G., Macino, G., & Cogoni, C. (2002). Involvement of small RNAs and role of the qde genes in the gene silencing pathway in *Neurospora*. *Genes Dev*, 16(7), 790-795. <https://doi.org/10.1101/gad.222402>
- Catalanotto, C., Pallotta, M., ReFalo, P., Sachs, M. S., Vayssie, L., Macino, G., & Cogoni, C. (2004). Redundancy of the two dicer genes in transgene-induced posttranscriptional gene silencing in *Neurospora crassa*. *Mol Cell Biol*, 24(6), 2536-2545. <https://doi.org/10.1128/mcb.24.6.2536-2545.2004>
- Cernilogar, F. M., Onorati, M. C., Kothe, G. O., Burroughs, A. M., Parsi, K. M., Breiling, A., Lo Sardo, F., Saxena, A., Miyoshi, K., Siomi, H., Siomi, M. C., Carninci, P., Gilmour, D. S., Corona, D. F., & Orlando, V. (2011). Chromatin-associated RNA interference components contribute to transcriptional regulation in *Drosophila*. *NATURE*, 480(7377), 391-395. <https://doi.org/10.1038/nature10492>
- Chang, S. S., Zhang, Z., & Liu, Y. (2012). RNA interference pathways in fungi: mechanisms and functions. *Annu Rev Microbiol*, 66, 305-323. <https://doi.org/10.1146/annurev-micro-092611-150138>
- Chekanova, J. A., Gregory, B. D., Reverdatto, S. V., Chen, H., Kumar, R., Hooker, T., Yazaki, J., Li, P., Skiba, N., Peng, Q., Alonso, J., Brukhin, V., Grossniklaus, U., Ecker, J. R., & Belostotsky, D. A. (2007). Genome-wide high-resolution mapping of exosome substrates reveals hidden features in the *Arabidopsis* transcriptome. *Cell*, 131(7), 1340-1353. <https://doi.org/10.1016/j.cell.2007.10.056>
- Chen, D. H., & Ronald, P. C. (1999). A rapid DNA miniprep method suitable for AFLP and other PCR applications. *Plant Mol Biol Reporter*, 17(1), 53-57. <https://doi.org/https://doi.org/10.1023/A:1007585532036>
- Chen, S., Zhou, Y., Chen, Y., & Gu, J. (2018). fastp: an ultra-fast all-in-one FASTQ preprocessor. *Bioinformatics*, 34(17), i884-i890. <https://doi.org/10.1093/bioinformatics/bty560>
- Chen, X. (2004). A microRNA as a translational repressor of APETALA2 in *Arabidopsis* flower development. *Science*, 303(5666), 2022-2025. <https://doi.org/10.1126/science.1088060>
- Chendrimada, T. P., Gregory, R. I., Kumaraswamy, E., Norman, J., Cooch, N., Nishikura, K., & Shiekhattar, R. (2005). TRBP recruits the Dicer complex to Ago2 for microRNA

- processing and gene silencing. *NATURE*, 436(7051), 740-744. <https://doi.org/10.1038/nature03868>
- Cho, J. H., Kim, S. A., Seo, Y. S., Park, S. G., Park, B. C., Kim, J. H., & Kim, S. (2017). The p90 ribosomal S6 kinase-UBR5 pathway controls Toll-like receptor signaling via miRNA-induced translational inhibition of tumor necrosis factor receptor-associated factor 3. *J Biol Chem*, 292(28), 11804-11814. <https://doi.org/10.1074/jbc.M117.785170>
- Choi, J., Kim, K. T., Jeon, J., Wu, J., Song, H., Asiegbu, F. O., & Lee, Y. H. (2014). funRNA: a fungi-centered genomics platform for genes encoding key components of RNAi. *BMC Genomics*, 15 Suppl 9, S14. <https://doi.org/10.1186/1471-2164-15-S9-S14>
- Chow, F. W., Koutsovoulos, G., Ovando-Vazquez, C., Neophytou, K., Bermudez-Barrientos, J. R., Laetsch, D. R., Robertson, E., Kumar, S., Claycomb, J. M., Blaxter, M., Abreu-Goodger, C., & Buck, A. H. (2019). Secretion of an Argonaute protein by a parasitic nematode and the evolution of its siRNA guides. *Nucleic Acids Res*, 47(7), 3594-3606. <https://doi.org/10.1093/nar/gkz142>
- Clutterbuck, A. J. (1969). A mutational analysis of conidial development in *Aspergillus nidulans*. *Genetics*, 63(2), 317-327. <https://www.ncbi.nlm.nih.gov/pubmed/5366214>
- Cogoni, C., Irelan, J. T., Schumacher, M., Schmidhauser, T. J., Selkerl, E. U., & Macino, G. (1996). Transgene silencing of the *al-1* gene in vegetative cells of *Neurospora* is mediated by a cytoplasmic effector and does not depend on DNA-DNA interactions or DNA methylation. *The EMBO Journal* 15(12), 3153-3163.
- Cogoni, C., & Macino, G. (1997). Isolation of quelling-defective (*qde*) mutants impaired in posttranscriptional transgene-induced gene silencing in *Neurospora crassa*. *Proc Natl Acad Sci U S A*, 94(19), 10233-10238. <https://doi.org/10.1073/pnas.94.19.10233>
- Cogoni, C., & Macino, G. (1999a). Gene silencing in *Neurospora crassa* requires a protein homologous to RNA-dependent RNA polymerase. *NATURE*, 399.
- Cogoni, C., & Macino, G. (1999b). Gene silencing in *Neurospora crassa* requires a protein homologous to RNA-dependent RNA polymerase. *NATURE*, 399(6732), 166-169. <https://doi.org/10.1038/20215>
- Cogoni, C., & Macino, G. (1999c). Posttranscriptional gene silencing in *Neurospora* by a RecQ DNA helicase. *Science*, 286(5448), 2342-2344. <https://doi.org/10.1126/science.286.5448.2342>
- Collins, R. E., & Cheng, X. (2005). Structural domains in RNAi. *FEBS Lett*, 579(26), 5841-5849. <https://doi.org/10.1016/j.febslet.2005.07.072>
- Cooley, J. S. (1931). Control of *Botrytis* rot of pears with chemically treated wrappers.
- Cora, E., Pandey, R. R., Xiol, J., Taylor, J., Sachidanandam, R., McCarthy, A. A., & Pillai, R. S. (2014). The MID-PIWI module of Piwi proteins specifies nucleotide- and strand-biases of piRNAs. *RNA*, 20(6), 773-781. <https://doi.org/10.1261/rna.044701.114>
- Cordin, O., Banroques, J., Tanner, N. K., & Linder, P. (2006). The DEAD-box protein family of RNA helicases. *Gene*, 367, 17-37. <https://doi.org/10.1016/j.gene.2005.10.019>
- Czech, B., Malone, C. D., Zhou, R., Stark, A., Schlingeheyde, C., Dus, M., Perrimon, N., Kellis, M., Wohlschlegel, J. A., Sachidanandam, R., Hannon, G. J., & Brennecke, J. (2008). An endogenous small interfering RNA pathway in *Drosophila*. *NATURE*, 453(7196), 798-802. <https://doi.org/10.1038/nature07007>
- Dalmay, T., Hamilton, A., Rudd, S., Angell, S., & Baulcombe, D. C. (2000). An RNA-dependent RNA polymerase gene in *Arabidopsis* is required for posttranscriptional gene silencing mediated by a transgene but not by a virus. *Cell*, 101(5), 543-553. [https://doi.org/10.1016/s0092-8674\(00\)80864-8](https://doi.org/10.1016/s0092-8674(00)80864-8)
- De Zotti, M., Sella, L., Bolzonello, A., Gabbatore, L., Peggion, C., Bortolotto, A., Elmaghraby, I., Tundo, S., & Favaron, F. (2020). Targeted amino acid substitutions in a *Trichoderma* peptaibol confer activity against fungal plant pathogens and protect host tissues from *Botrytis cinerea* infection. *Int J Mol Sci*, 21(20). <https://doi.org/10.3390/ijms21207521>

- Decker, L. M., Boone, E. C., Xiao, H., Shanker, B. S., Boone, S. F., Kingston, S. L., Lee, S. A., Hammond, T. M., & Shiu, P. K. (2015). Complex formation of RNA silencing proteins in the perinuclear region of *Neurospora crassa*. *Genetics*, *199*(4), 1017-1021. <https://doi.org/10.1534/genetics.115.174623>
- Deising, H., Nicholson, R. L., Haug, M., Howard, R. J., & Mendgen, K. (1992). Adhesion pad formation and the involvement of cutinase and esterases in the attachment of uredospores to the host cuticle. *Plant Cell*, *4*(9), 1101-1111. <https://doi.org/10.1105/tpc.4.9.1101>
- Derrien, B., Clavel, M., Baumberger, N., Iki, T., Sarazin, A., Hacquard, T., Ponce, M. R., Ziegler-Graff, V., Vaucheret, H., Micol, J. L., Voinnet, O., & Genschik, P. (2018). A Suppressor Screen for AGO1 Degradation by the Viral F-Box P0 Protein Uncovers a Role for AGO DUF1785 in sRNA Duplex Unwinding. *Plant Cell*, *30*(6), 1353-1374. <https://doi.org/10.1105/tpc.18.00111>
- Diederichs, S., & Haber, D. A. (2007). Dual role for Argonautes in microRNA processing and posttranscriptional regulation of microRNA expression. *Cell*, *131*(6), 1097-1108. <https://doi.org/10.1016/j.cell.2007.10.032>
- Ding, L., Spencer, A., Morita, K., & Han, M. (2005). The developmental timing regulator AIN-1 interacts with miRISCs and may target the Argonaute protein ALG-1 to cytoplasmic P bodies in *C. elegans*. *Mol Cell*, *19*(4), 437-447. <https://doi.org/10.1016/j.molcel.2005.07.013>
- Djuranovic, S., Nahvi, A., & Green, R. (2012). miRNA-mediated gene silencing by translational repression followed by mRNA deadenylation and decay. *Science*, *336*(6078), 237-240. <https://doi.org/10.1126/science.1215691>
- Dobin, A., Davis, C. A., Schlesinger, F., Drenkow, J., Zaleski, C., Jha, S., Batut, P., Chaisson, M., & Gingeras, T. R. (2013). STAR: ultrafast universal RNA-seq aligner. *Bioinformatics*, *29*(1), 15-21. <https://doi.org/10.1093/bioinformatics/bts635>
- Doehlemann, G., Berndt, P., & Hahn, M. (2006). Different signalling pathways involving a Galpha protein, cAMP and a MAP kinase control germination of *Botrytis cinerea* conidia. *Mol Microbiol*, *59*(3), 821-835. <https://doi.org/10.1111/j.1365-2958.2005.04991.x>
- Duan, C. G., Fang, Y. Y., Zhou, B. J., Zhao, J. H., Hou, W. N., Zhu, H., Ding, S. W., & Guo, H. S. (2012). Suppression of *Arabidopsis* ARGONAUTE1-mediated slicing, transgene-induced RNA silencing, and DNA methylation by distinct domains of the Cucumber mosaic virus 2b protein. *Plant Cell*, *24*(1), 259-274. <https://doi.org/10.1105/tpc.111.092718>
- Duan, C. G., Zhang, H., Tang, K., Zhu, X., Qian, W., Hou, Y. J., Wang, B., Lang, Z., Zhao, Y., Wang, X., Wang, P., Zhou, J., Liang, G., Liu, N., Wang, C., & Zhu, J. K. (2015). Specific but interdependent functions for *Arabidopsis* AGO4 and AGO6 in RNA-directed DNA methylation. *EMBO J*, *34*(5), 581-592. <https://doi.org/10.15252/embj.201489453>
- Dunker, F., Trutzenberg, A., Rothenpieler, J. S., Kuhn, S., Prols, R., Schreiber, T., Tissier, A., Kemen, A., Kemen, E., Huckelhoven, R., & Weiberg, A. (2020). Oomycete small RNAs bind to the plant RNA-induced silencing complex for virulence. *Elife*, *9*. <https://doi.org/10.7554/eLife.56096>
- Duran-Figueroa, N., & Vielle-Calzada, J. P. (2010). Argonaute9-dependent silencing of transposable elements in pericentromeric regions of *Arabidopsis*. *Plant Signal Behav*, *5*(11), 1476-1479. <https://doi.org/10.1038/nature08828>
- Elbashir, S. M., Harborth, J., Lendeckel, W., Yalcin, A., Weber, K., & Tuschl, T. (2001a). Duplexes of 21-nucleotide RNAs mediate RNA interference in cultured mammalian cells. *NATURE*, *411*(6836), 494-498. <https://doi.org/10.1038/35078107>
- Elbashir, S. M., Lendeckel, W., & Tuschl, T. (2001). RNA interference is mediated by 21- and 22-nucleotide RNAs. *Genes Dev*, *15*(2), 188-200. <https://doi.org/10.1101/gad.862301>

- Ellendorff, U., Fradin, E. F., de Jonge, R., & Thomma, B. P. (2009). RNA silencing is required for *Arabidopsis* defence against *Verticillium* wilt disease. *J Exp Bot*, *60*(2), 591-602. <https://doi.org/10.1093/jxb/ern306>
- Elmayan, T., Balzergue, S., Beon, F., Bourdon, V., Daubremet, J., Guenet, Y., Mourrain, P., Palauqui, J. C., Vernhettes, S., Vialle, T., Wostrikoff, K., & Vaucheret, H. (1998). *Arabidopsis* mutants impaired in cosuppression. *Plant Cell*, *10*(10), 1747-1758. <https://doi.org/10.1105/tpc.10.10.1747>
- Endo, Y., Iwakawa, H. O., & Tomari, Y. (2013). *Arabidopsis* Argonaute7 selects miR390 through multiple checkpoints during RISC assembly. *EMBO Rep*, *14*(7), 652-658. <https://doi.org/10.1038/embor.2013.73>
- Engels, B. M., & Hutvagner, G. (2006). Principles and effects of microRNA-mediated post-transcriptional gene regulation. *Oncogene*, *25*(46), 6163-6169. <https://doi.org/10.1038/sj.onc.1209909>
- Eulalio, A., Huntzinger, E., & Izaurralde, E. (2008). GW182 interaction with Argonaute is essential for miRNA-mediated translational repression and mRNA decay. *Nat Struct Mol Biol*, *15*(4), 346-353. <https://doi.org/10.1038/nsmb.1405>
- Fagard, M., Boutet, S., Morel, J. B., Bellini, C., & Vaucheret, H. (2000b). AGO1, QDE-2, and RDE-1 are related proteins required for post-transcriptional gene silencing in plants, quelling in fungi, and RNA interference in animals. *Proc Natl Acad Sci U S A*, *97*(21), 11650-11654. <https://doi.org/10.1073/pnas.200217597>
- Fei, Q., Xia, R., & Meyers, B. C. (2013). Phased, secondary, small interfering RNAs in posttranscriptional regulatory networks. *Plant Cell*, *25*(7), 2400-2415. <https://doi.org/10.1105/tpc.113.114652>
- Feinberg, E. H., & Hunter, C. P. (2003). Transport of dsRNA into cells by the transmembrane protein SID-1. *Science*, *301*(5639), 1545-1547. <https://doi.org/10.1126/science.1087117>
- Fire, A., Xu, S., Montgomery, M. K., Kostas, S. A., Driver, S. E., & Mello, C. C. (1998). Potent and specific genetic interference by double-stranded RNA in *Caenorhabditis elegans*. *NATURE*, *391*(6669), 806-811. <https://doi.org/10.1038/35888>
- Forrest, E. C., Cogoni, C., & Macino, G. (2004). The RNA-dependent RNA polymerase, QDE-1, is a rate-limiting factor in post-transcriptional gene silencing in *Neurospora crassa*. *Nucleic Acids Res*, *32*(7), 2123-2128. <https://doi.org/10.1093/nar/gkh530>
- Frank, F., Hauver, J., Sonenberg, N., & Nagar, B. (2012). *Arabidopsis* Argonaute MID domains use their nucleotide specificity loop to sort small RNAs. *EMBO J*, *31*(17), 3588-3595. <https://doi.org/10.1038/emboj.2012.204>
- Frank, F., Sonenberg, N., & Nagar, B. (2010). Structural basis for 5'-nucleotide base-specific recognition of guide RNA by human AGO2. *NATURE*, *465*(7299), 818-822. <https://doi.org/10.1038/nature09039>
- Galagan, J. E., & Selker, E. U. (2004). RIP: the evolutionary cost of genome defense. *Trends Genet*, *20*(9), 417-423. <https://doi.org/10.1016/j.tig.2004.07.007>
- Garcia-Ruiz, H., Carbonell, A., Hoyer, J. S., Fahlgren, N., Gilbert, K. B., Takeda, A., Giampetruzzi, A., Garcia Ruiz, M. T., McGinn, M. G., Lowery, N., Martinez Baladejo, M. T., & Carrington, J. C. (2015). Roles and programming of *Arabidopsis* Argonaute proteins during Turnip mosaic virus infection. *PLoS Pathog*, *11*(3), e1004755. <https://doi.org/10.1371/journal.ppat.1004755>
- Gascioli, V., Mallory, A. C., Bartel, D. P., & Vaucheret, H. (2005). Partially redundant functions of *Arabidopsis* DICER-like enzymes and a role for DCL4 in producing trans-acting siRNAs. *Curr Biol*, *15*(16), 1494-1500. <https://doi.org/10.1016/j.cub.2005.07.024>
- Geuder, J., Wange, L. E., Janjic, A., Radmer, J., Janssen, P., Bagnoli, J. W., Muller, S., Kaul, A., Ohnuki, M., & Enard, W. (2021). A non-invasive method to generate induced pluripotent stem cells from primate urine. *Sci Rep*, *11*(1), 3516. <https://doi.org/10.1038/s41598-021-82883-0>

- Gilkes, N. R., Henrissat, B., Kilburn, D. G., Miller, R. C., Jr., & Warren, R. A. (1991). Domains in microbial beta-1, 4-glycanases: sequence conservation, function, and enzyme families. *Microbiol Rev*, 55(2), 303-315. <https://doi.org/10.1128/mr.55.2.303-315.1991>
- Girardot, C., Scholtalbers, J., Sauer, S., Su, S. Y., & Furlong, E. E. (2016). Je, a versatile suite to handle multiplexed NGS libraries with unique molecular identifiers. *BMC Bioinformatics*, 17(1), 419. <https://doi.org/10.1186/s12859-016-1284-2>
- Glass, N. L., Vollmer, S. J., Staben, C., Grotelueschen, J., Metzenberg, R. L., & Yanofsky, C. (1988). DNAs of the two mating-type alleles of *Neurospora crassa* are highly dissimilar. *Science*, 241(4865), 570-573. <https://doi.org/10.1126/science.2840740>
- Grayburn, W. S., & Selker, E. U. (1989). A natural case of RIP: degeneration of the DNA sequence in an ancestral tandem duplication. *Mol Cell Biol*, 9(10), 4416-4421. <https://doi.org/10.1128/mcb.9.10.4416-4421.1989>
- Guinebretiere, M. H., Nguyen-The, C., Morrison, N., Reich, M., & Nicot, P. (2000). Isolation and characterization of antagonists for the biocontrol of the postharvest wound pathogen *Botrytis cinerea* on strawberry fruits. *J Food Prot*, 63(3), 386-394. <https://doi.org/10.4315/0362-028x-63.3.386>
- Guo, S., & Kemphues, K. J. (1995). par-1, a gene required for establishing polarity in *C. elegans* embryos, encodes a putative Ser/Thr kinase that is asymmetrically distributed. *Cell*, 81(4), 611-620. [https://doi.org/10.1016/0092-8674\(95\)90082-9](https://doi.org/10.1016/0092-8674(95)90082-9)
- Hale, C. R., Zhao, P., Olson, S., Duff, M. O., Graveley, B. R., Wells, L., Terns, R. M., & Terns, M. P. (2009). RNA-guided RNA cleavage by a CRISPR RNA-Cas protein complex. *Cell*, 139(5), 945-956. <https://doi.org/10.1016/j.cell.2009.07.040>
- Hamada, W., Reignault, P., Bompeix, G., & Boccara, M. (1994). Transformation of *Botrytis cinerea* with the hygromycin B resistance gene, hph. *Curr Genet*, 26(3), 251-255. <https://doi.org/10.1007/BF00309556>
- Hamilton, A. J., & Baulcombe, D. C. (1999). A species of small antisense RNA in posttranscriptional gene silencing in plants. *Science*, 286(5441), 950-952. <https://doi.org/10.1126/science.286.5441.950>
- Hammond, S. M., Bernstein, E., Beach, D., & Hannon, G. J. (2000). An RNA-directed nuclease mediates post-transcriptional gene silencing in *Drosophila* cells. *NATURE*, 404(6775), 293-296. <https://doi.org/10.1038/35005107>
- Hammond, S. M., Boettcher, S., Caudy, A. A., Kobayashi, R., & Hannon, G. J. (2001). Argonaute2, a link between genetic and biochemical analyses of RNAi. *Science*, 293(5532), 1146-1150. <https://doi.org/10.1126/science.1064023>
- Hammond, T. M., Xiao, H., Boone, E. C., Perdue, T. D., Pukkila, P. J., & Shiu, P. K. (2011). SAD-3, a Putative Helicase Required for Meiotic Silencing by Unpaired DNA, Interacts with Other Components of the Silencing Machinery. *G3 (Bethesda)*, 1(5), 369-376. <https://doi.org/10.1534/g3.111.000570>
- He, X. J., Hsu, Y. F., Zhu, S., Wierzbicki, A. T., Pontes, O., Pikaard, C. S., Liu, H. L., Wang, C. S., Jin, H., & Zhu, J. K. (2009). An effector of RNA-directed DNA methylation in *Arabidopsis* is an Argonaute4- and RNA-binding protein. *Cell*, 137(3), 498-508. <https://doi.org/10.1016/j.cell.2009.04.028>
- Hegge, J. W., Swarts, D. C., Chandradoss, S. D., Cui, T. J., Kneppers, J., Jinek, M., Joo, C., & van der Oost, J. (2019). DNA-guided DNA cleavage at moderate temperatures by *Clostridium butyricum* Argonaute. *Nucleic Acids Res*, 47(11), 5809-5821. <https://doi.org/10.1093/nar/gkz306>
- Henderson, I. R., Zhang, X., Lu, C., Johnson, L., Meyers, B. C., Green, P. J., & Jacobsen, S. E. (2006). Dissecting *Arabidopsis thaliana* DICER function in small RNA processing, gene silencing and DNA methylation patterning. *Nat Genet*, 38(6), 721-725. <https://doi.org/10.1038/ng1804>
- Hoffer, P., Ivashuta, S., Pontes, O., Vitins, A., Pikaard, C., Mroccka, A., Wagner, N., & Voelker, T. (2011). Posttranscriptional gene silencing in nuclei [Article]. *Proceedings of the*

- National Academy of Sciences of the United States of America*, 108(1), 409-414.
<https://doi.org/10.1073/pnas.1009805108>
- Hopkins, E. F. (1921). The *Botrytis* blight of tulips. <http://hdl.loc.gov/loc.gdc/scd0001.00028158762>
- Hou, C. Y., Lee, W. C., Chou, H. C., Chen, A. P., Chou, S. J., & Chen, H. M. (2016). Global analysis of truncated RNA ends reveals new insights into ribosome stalling in plants. *Plant Cell*, 28(10), 2398-2416. <https://doi.org/10.1105/tpc.16.00295>
- Hou, Y., Zhai, Y., Feng, L., Karimi, H. Z., Rutter, B. D., Zeng, L., Choi, D. S., Zhang, B., Gu, W., Chen, X., Ye, W., Innes, R. W., Zhai, J., & Ma, W. (2019). A *Phytophthora* effector suppresses trans-kingdom RNAi to promote disease susceptibility. *Cell Host Microbe*, 25(1), 153-165 e155. <https://doi.org/10.1016/j.chom.2018.11.007>
- Howell, M. D., Fahlgren, N., Chapman, E. J., Cumbie, J. S., Sullivan, C. M., Givan, S. A., Kasschau, K. D., & Carrington, J. C. (2007). Genome-wide analysis of the RNA-DEPENDENT RNA POLYMERASE6/DICER-LIKE4 pathway in *Arabidopsis* reveals dependency on miRNA- and tasiRNA-directed targeting. *Plant Cell*, 19(3), 926-942. <https://doi.org/10.1105/tpc.107.050062>
- Hu, B., Jin, J., Guo, A. Y., Zhang, H., Luo, J., & Gao, G. (2015). GSDD 2.0: an upgraded gene feature visualization server. *Bioinformatics*, 31(8), 1296-1297. <https://doi.org/10.1093/bioinformatics/btu817>
- Humphrey, J. E. (1891). The rotting of lettuce. *Rept. Mass. Exp. Sta.*, 9, 219-222.
- Hunter, C., Sun, H., & Poethig, R. S. (2003). The *Arabidopsis* heterochronic gene ZIPPY is an Argonaute family member. *Curr Biol*, 13(19), 1734-1739. <https://doi.org/10.1016/j.cub.2003.09.004>
- Huntzinger, E., Kuzuoglu-Ozturk, D., Braun, J. E., Eulalio, A., Wohlbold, L., & Izaurralde, E. (2013). The interactions of GW182 proteins with PABP and deadenylases are required for both translational repression and degradation of miRNA targets. *Nucleic Acids Res*, 41(2), 978-994. <https://doi.org/10.1093/nar/gks1078>
- Hutvagner, G., McLachlan, J., Pasquinelli, A. E., Balint, E., Tuschl, T., & Zamore, P. D. (2001). A cellular function for the RNA-interference enzyme Dicer in the maturation of the let-7 small temporal RNA. *Science*, 293(5531), 834-838. <https://doi.org/10.1126/science.1062961>
- Hutvagner, G., & Zamore, P. D. (2002). A microRNA in a multiple-turnover RNAi enzyme complex. *Science*, 297(5589), 2056-2060. <https://doi.org/10.1126/science.1073827>
- Ingelfinger, D., Arndt-Jovin, D. J., Luhrmann, R., & Achsel, T. (2002). The human LSm1-7 proteins colocalize with the mRNA-degrading enzymes Dcp1/2 and Xrn1 in distinct cytoplasmic foci. *RNA*, 8(12), 1489-1501. <https://www.ncbi.nlm.nih.gov/pubmed/12515382>
- Iwakawa, H. O., & Tomari, Y. (2013). Molecular insights into microRNA-mediated translational repression in plants. *Mol Cell*, 52(4), 591-601. <https://doi.org/10.1016/j.molcel.2013.10.033>
- Iwakawa, H. O., & Tomari, Y. (2015). The Functions of MicroRNAs: mRNA decay and translational repression. *Trends Cell Biol*, 25(11), 651-665. <https://doi.org/10.1016/j.tcb.2015.07.011>
- Jarvis, W. R. (1977). *Botryotinia and Botrytis* species : taxonomy, physiology, and pathogenicity Research Branch, Canada Dept. of Agriculture: obtainable from Information Division, Canada Dept. of Agriculture.
- Ji, L., Liu, X., Yan, J., Wang, W., Yumul, R. E., Kim, Y. J., Dinh, T. T., Liu, J., Cui, X., Zheng, B., Agarwal, M., Liu, C., Cao, X., Tang, G., & Chen, X. (2011). Argonaute10 and Argonaute 1 regulate the termination of floral stem cells through two microRNAs in *Arabidopsis*. *PLoS Genet*, 7(3), e1001358. <https://doi.org/10.1371/journal.pgen.1001358>

- Jose, A. M., Smith, J. J., & Hunter, C. P. (2009). Export of RNA silencing from *C. elegans* tissues does not require the RNA channel SID-1. *Proc Natl Acad Sci U S A*, *106*(7), 2283-2288. <https://doi.org/10.1073/pnas.0809760106>
- Jouannet, V., Moreno, A. B., Elmayan, T., Vaucheret, H., Crespi, M. D., & Maizel, A. (2012). Cytoplasmic *Arabidopsis* AGO7 accumulates in membrane-associated siRNA bodies and is required for ta-siRNA biogenesis. *EMBO J*, *31*(7), 1704-1713. <https://doi.org/10.1038/emboj.2012.20>
- Jover-Gil, S., Candela, H., Robles, P., Aguilera, V., Barrero, J. M., Micol, J. L., & Ponce, M. R. (2012). The microRNA pathway genes *AGO1*, *HEN1* and *HYL1* participate in leaf proximal-distal, venation and stomatal patterning in *Arabidopsis*. *Plant Cell Physiol*, *53*(7), 1322-1333. <https://doi.org/10.1093/pcp/pcs077>
- Kataoka, Y., Takeichi, M., & Uemura, T. (2001). Developmental roles and molecular characterization of a *Drosophila* homologue of *Arabidopsis* Argonaute1, the founder of a novel gene superfamily. *Genes Cells*, *6*(4), 313-325. <https://doi.org/10.1046/j.1365-2443.2001.00427.x>
- Kato, A., Akamatsu, Y., Sakuraba, Y., & Inoue, H. (2004). The *Neurospora crassa* *mus-19* gene is identical to the *qde-3* gene, which encodes a RecQ homologue and is involved in recombination repair and postreplication repair. *Curr Genet*, *45*(1), 37-44. <https://doi.org/10.1007/s00294-003-0459-3>
- Kiriakidou, M., Tan, G. S., Lamprinak, S., De Planell-Saguer, M., Nelson, P. T., & Mourelatos, Z. (2007). An mRNA m7G cap binding-like motif within human Ago2 represses translation. *Cell*, *129*(6), 1141-1151. <https://doi.org/10.1016/j.cell.2007.05.016>
- Klahre, U., Crete, P., Leuenberger, S. A., Iglesias, V. A., & Meins, F., Jr. (2002). High molecular weight RNAs and small interfering RNAs induce systemic posttranscriptional gene silencing in plants. *Proc Natl Acad Sci U S A*, *99*(18), 11981-11986. <https://doi.org/10.1073/pnas.182204199>
- Kuzmenko, A., Oguienko, A., Esyunina, D., Yudin, D., Petrova, M., Kudinova, A., Maslova, O., Ninova, M., Ryazansky, S., Leach, D., Aravin, A. A., & Kulbachinskiy, A. (2020). DNA targeting and interference by a bacterial Argonaute nuclease. *NATURE*, *587*(7835), 632-637. <https://doi.org/10.1038/s41586-020-2605-1>
- Kuzmenko, A., Yudin, D., Ryazansky, S., Kulbachinskiy, A., & Aravin, A. A. (2019). Programmable DNA cleavage by Ago nucleases from mesophilic bacteria *Clostridium butyricum* and *Limnothrix rosea*. *Nucleic Acids Res*, *47*(11), 5822-5836. <https://doi.org/10.1093/nar/gkz379>
- Lai, E. C. (2002). Micro RNAs are complementary to 3' UTR sequence motifs that mediate negative post-transcriptional regulation. *Nat Genet*, *30*(4), 363-364. <https://doi.org/10.1038/ng865>
- Lee, D. W., Pratt, R. J., McLaughlin, M., & Aramayo, R. (2003). An Argonaute-like protein is required for meiotic silencing. *Genetics*, *164*(2), 821-828. <https://www.ncbi.nlm.nih.gov/pubmed/12807800>
- Lee, H. C., Li, L., Gu, W., Xue, Z., Crosthwaite, S. K., Pertsemlidis, A., Lewis, Z. A., Freitag, M., Selker, E. U., Mello, C. C., & Liu, Y. (2010). Diverse pathways generate microRNA-like RNAs and Dicer-independent small interfering RNAs in fungi. *Mol Cell*, *38*(6), 803-814. <https://doi.org/10.1016/j.molcel.2010.04.005>
- Lee, K., Lee, J. G., Min, K., Choi, J. H., Lim, S., & Lee, E. J. (2021). Transcriptome analysis of the fruit of two strawberry cultivars "sunnyberry" and "kingsberry" that show different susceptibility to *Botrytis cinerea* after harvest. *Int J Mol Sci*, *22*(4). <https://doi.org/10.3390/ijms22041518>
- Lee, R. C., Feinbaum, R. L., & Ambros, V. (1993). The *C. elegans* heterochronic gene *lin-4* encodes small RNAs with antisense complementarity to *lin-14*. *Cell*, *75*(5), 843-854. [https://doi.org/10.1016/0092-8674\(93\)90529-y](https://doi.org/10.1016/0092-8674(93)90529-y)

- Leung, A. K., Calabrese, J. M., & Sharp, P. A. (2006). Quantitative analysis of Argonaute protein reveals microRNA-dependent localization to stress granules. *Proc Natl Acad Sci U S A*, *103*(48), 18125-18130. <https://doi.org/10.1073/pnas.0608845103>
- Lewis, B. P., Burge, C. B., & Bartel, D. P. (2005). Conserved seed pairing, often flanked by adenosines, indicates that thousands of human genes are microRNA targets. *Cell*, *120*(1), 15-20. <https://doi.org/10.1016/j.cell.2004.12.035>
- Lewis, B. P., Shih, I. H., Jones-Rhoades, M. W., Bartel, D. P., & Burge, C. B. (2003). Prediction of mammalian microRNA targets. *Cell*, *115*(7), 787-798. [https://doi.org/10.1016/s0092-8674\(03\)01018-3](https://doi.org/10.1016/s0092-8674(03)01018-3)
- Li, C. F., Henderson, I. R., Song, L., Fedoroff, N., Lagrange, T., & Jacobsen, S. E. (2008). Dynamic regulation of Argonaute4 within multiple nuclear bodies in *Arabidopsis thaliana*. *PLoS Genet*, *4*(2), e27. <https://doi.org/10.1371/journal.pgen.0040027>
- Li, C. F., Pontes, O., El-Shami, M., Henderson, I. R., Bernatavichute, Y. V., Chan, S. W., Lagrange, T., Pikaard, C. S., & Jacobsen, S. E. (2006). An Argonaute4-containing nuclear processing center colocalized with Cajal bodies in *Arabidopsis thaliana*. *Cell*, *126*(1), 93-106. <https://doi.org/10.1016/j.cell.2006.05.032>
- Li, J., Yang, Z., Yu, B., Liu, J., & Chen, X. (2005). Methylation protects miRNAs and siRNAs from a 3'-end uridylation activity in *Arabidopsis*. *Curr Biol*, *15*(16), 1501-1507. <https://doi.org/10.1016/j.cub.2005.07.029>
- Li, S., Liu, L., Zhuang, X., Yu, Y., Liu, X., Cui, X., Ji, L., Pan, Z., Cao, X., Mo, B., Zhang, F., Raikhel, N., Jiang, L., & Chen, X. (2013). MicroRNAs inhibit the translation of target mRNAs on the endoplasmic reticulum in *Arabidopsis*. *Cell*, *153*(3), 562-574. <https://doi.org/10.1016/j.cell.2013.04.005>
- Li, W., Cui, X., Meng, Z., Huang, X., Xie, Q., Wu, H., Jin, H., Zhang, D., & Liang, W. (2012). Transcriptional regulation of *Arabidopsis* MIR168a and Argonaute1 homeostasis in abscisic acid and abiotic stress responses. *Plant Physiol*, *158*(3), 1279-1292. <https://doi.org/10.1104/pp.111.188789>
- Li, X., Lei, M., Yan, Z., Wang, Q., Chen, A., Sun, J., Luo, D., & Wang, Y. (2014). The REL3-mediated TAS3 ta-siRNA pathway integrates auxin and ethylene signaling to regulate nodulation in *Lotus japonicus*. *New Phytol*, *201*(2), 531-544. <https://doi.org/10.1111/nph.12550>
- Limon, M. C., Chacon, M. R., Mejias, R., Delgado-Jarana, J., Rincon, A. M., Codon, A. C., & Benitez, T. (2004). Increased antifungal and chitinase specific activities of *Trichoderma harzianum* CECT 2413 by addition of a cellulose binding domain. *Appl Microbiol Biotechnol*, *64*(5), 675-685. <https://doi.org/10.1007/s00253-003-1538-6>
- Lingel, A., Simon, B., Izaurralde, E., & Sattler, M. (2003). Structure and nucleic-acid binding of the *Drosophila* Argonaute 2 PAZ domain. *NATURE*, *426*(6965), 465-469. <https://doi.org/10.1038/nature02123>
- Lingel, A., Simon, B., Izaurralde, E., & Sattler, M. (2004). Nucleic acid 3'-end recognition by the Argonaute2 PAZ domain. *Nat Struct Mol Biol*, *11*(6), 576-577. <https://doi.org/10.1038/nsmb777>
- Liu, C., Xin, Y., Xu, L., Cai, Z., Xue, Y., Liu, Y., Xie, D., Liu, Y., & Qi, Y. (2018). *Arabidopsis* Argonaute1 binds chromatin to promote gene transcription in response to hormones and stresses. *Dev Cell*, *44*(3), 348-361 e347. <https://doi.org/10.1016/j.devcel.2017.12.002>
- Liu, J., Carmell, M. A., Rivas, F. V., Marsden, C. G., Thomson, J. M., Song, J. J., Hammond, S. M., Joshua-Tor, L., & Hannon, G. J. (2004). Argonaute2 is the catalytic engine of mammalian RNAi. *Science*, *305*(5689), 1437-1441. <https://doi.org/10.1126/science.1102513>
- Liu, J., Valencia-Sanchez, M. A., Hannon, G. J., & Parker, R. (2005). MicroRNA-dependent localization of targeted mRNAs to mammalian P-bodies. *Nat Cell Biol*, *7*(7), 719-723. <https://doi.org/10.1038/ncb1274>

- Liu, Q., Yao, X., Pi, L., Wang, H., Cui, X., & Huang, H. (2009). The Argonaute10 gene modulates shoot apical meristem maintenance and establishment of leaf polarity by repressing miR165/166 in *Arabidopsis*. *Plant J*, 58(1), 27-40. <https://doi.org/10.1111/j.1365-313X.2008.03757.x>
- Livak, K. J., & Schmittgen, T. D. (2001). Analysis of relative gene expression data using real-time quantitative PCR and the 2(-Delta Delta C(T)) Method. *Methods*, 25(4), 402-408. <https://doi.org/10.1006/meth.2001.1262>
- Love, M. I., Huber, W., & Anders, S. (2014). Moderated estimation of fold change and dispersion for RNA-seq data with DESeq2. *Genome Biol*, 15(12), 550. <https://doi.org/10.1186/s13059-014-0550-8>
- Lynn, K., Fernandez, A., Aida, M., Sedbrook, J., Tasaka, M., Masson, P., & Barton, M. K. (1999). The PINHEAD/ZWILLE gene acts pleiotropically in *Arabidopsis* development and has overlapping functions with the Argonaute1 gene. *Development*, 126(3), 469-481. <https://www.ncbi.nlm.nih.gov/pubmed/9876176>
- Ma, J. B., Yuan, Y. R., Meister, G., Pei, Y., Tuschl, T., & Patel, D. J. (2005). Structural basis for 5'-end-specific recognition of guide RNA by the *A. fulgidus* Piwi protein. *NATURE*, 434(7033), 666-670. <https://doi.org/10.1038/nature03514>
- Ma, Z., & Zhang, X. (2018). Actions of plant Argonautes: predictable or unpredictable? *Curr Opin Plant Biol*, 45(Pt A), 59-67. <https://doi.org/10.1016/j.pbi.2018.05.007>
- Macrae, I. J., Li, F., Zhou, K., Cande, W. Z., & Doudna, J. A. (2006). Structure of Dicer and mechanistic implications for RNAi. *Cold Spring Harb Symp Quant Biol*, 71, 73-80. <https://doi.org/10.1101/sqb.2006.71.042>
- Maida, Y., Yasukawa, M., Furuuchi, M., Lassmann, T., Possemato, R., Okamoto, N., Kasim, V., Hayashizaki, Y., Hahn, W. C., & Masutomi, K. (2009). An RNA-dependent RNA polymerase formed by TERT and the RMRP RNA. *NATURE*, 461(7261), 230-235. <https://doi.org/10.1038/nature08283>
- Maiti, M., Lee, H. C., & Liu, Y. (2007). QIP, a putative exonuclease, interacts with the *Neurospora* Argonaute protein and facilitates conversion of duplex siRNA into single strands. *Genes Dev*, 21(5), 590-600. <https://doi.org/10.1101/gad.1497607>
- Makarova, K. S., Wolf, Y. I., van der Oost, J., & Koonin, E. V. (2009). Prokaryotic homologs of Argonaute proteins are predicted to function as key components of a novel system of defense against mobile genetic elements. *Biol Direct*, 4, 29. <https://doi.org/10.1186/1745-6150-4-29>
- Makeyev, E. V., & Bamford, D. H. (2002a). Cellular RNA-dependent RNA polymerase involved in posttranscriptional gene silencing has two distinct activity modes. *Mol Cell*, 10(6), 1417-1427. [https://doi.org/10.1016/s1097-2765\(02\)00780-3](https://doi.org/10.1016/s1097-2765(02)00780-3)
- Makeyev, E. V., & Bamford, D. H. (2002b). Cellular RNA dependent RNA polymerase involved in posttranscriptional gene silencing has two distinct activity modes. *Molecular Cell*, 10, 1417-1427.
- Mallory, A., & Vaucheret, H. (2010). Form, function, and regulation of Argonaute proteins. *Plant Cell*, 22(12), 3879-3889. <https://doi.org/10.1105/tpc.110.080671>
- Malonek, S., Rojas, M. C., Hedden, P., Gaskin, P., Hopkins, P., & Tudzynski, B. (2004). The NADPH-cytochrome P450 reductase gene from *Gibberella fujikuroi* is essential for gibberellin biosynthesis. *J Biol Chem*, 279(24), 25075-25084. <https://doi.org/10.1074/jbc.M308517200>
- Marraffini, L. A., & Sontheimer, E. J. (2010). CRISPR interference: RNA-directed adaptive immunity in bacteria and archaea. *Nat Rev Genet*, 11(3), 181-190. <https://doi.org/10.1038/nrg2749>
- Martinez, J., & Tuschl, T. (2004). RISC is a 5' phosphomonoester-producing RNA endonuclease. *Genes Dev*, 18(9), 975-980. <https://doi.org/10.1101/gad.1187904>

- Matranga, C., Tomari, Y., Shin, C., Bartel, D. P., & Zamore, P. D. (2005). Passenger-strand cleavage facilitates assembly of siRNA into Ago2-containing RNAi enzyme complexes. *Cell*, 123(4), 607-620. <https://doi.org/10.1016/j.cell.2005.08.044>
- Matsumoto, N., Nishimasu, H., Sakakibara, K., Nishida, K. M., Hirano, T., Ishitani, R., Siomi, H., Siomi, M. C., & Nureki, O. (2016). Crystal structure of silkworm PIWI-Clade Argonaute Siwi bound to piRNA. *Cell*, 167(2), 484-497 e489. <https://doi.org/10.1016/j.cell.2016.09.002>
- Mautino, M. R., & Rosa, A. L. (1998). Analysis of models involving enzymatic activities for the occurrence of C->T transition mutations during repeat-induced point mutation (RIP) in *Neurospora crassa*. *J Theor Biol*, 192(1), 61-71. <https://doi.org/10.1006/jtbi.1997.0608>
- McColloch, L. P., & Wright, W. R. (1966). *Botrytis rot of bell peppers*. Agricultural Research Service.
- Meister, G., & Tuschl, T. (2004). Mechanisms of gene silencing by double-stranded RNA. *NATURE*, 431(7006), 343-349. <https://doi.org/10.1038/nature02873>
- Mi, S., Cai, T., Hu, Y., Chen, Y., Hodges, E., Ni, F., Wu, L., Li, S., Zhou, H., Long, C., Chen, S., Hannon, G. J., & Qi, Y. (2008). Sorting of small RNAs into *Arabidopsis* Argonaute complexes is directed by the 5' terminal nucleotide. *Cell*, 133(1), 116-127. <https://doi.org/10.1016/j.cell.2008.02.034>
- Miler, M. A., Pfeiffer, W., & Schwartz, T. (2010). *Creating the CIPRES Science Gateway for inference of large phylogenetic trees" in Proceedings of the Gateway Computing Environments Workshop (GCE) New Orleans.*
- Miyashima, S., Hashimoto, T., & Nakajima, K. (2009). Argonaute1 acts in *Arabidopsis* root radial pattern formation independently of the SHR/SCR pathway. *Plant Cell Physiol*, 50(3), 626-634. <https://doi.org/10.1093/pcp/pcp020>
- Miyoshi, K., Tsukumo, H., Nagami, T., Siomi, H., & Siomi, M. C. (2005). Slicer function of *Drosophila* Argonautes and its involvement in RISC formation. *Genes Dev*, 19(23), 2837-2848. <https://doi.org/10.1101/gad.1370605>
- Miyoshi, T., Ito, K., Murakami, R., & Uchiumi, T. (2016). Structural basis for the recognition of guide RNA and target DNA heteroduplex by Argonaute. *Nat Commun*, 7, 11846. <https://doi.org/10.1038/ncomms11846>
- Montgomery, M. K., & Fire, A. (1998). Double-stranded RNA as a mediator in sequence-specific genetic silencing and co-suppression. *Trends Genet*, 14(7), 255-258. [https://doi.org/10.1016/s0168-9525\(98\)01510-8](https://doi.org/10.1016/s0168-9525(98)01510-8)
- Montgomery, T. A., Howell, M. D., Cuperus, J. T., Li, D., Hansen, J. E., Alexander, A. L., Chapman, E. J., Fahlgren, N., Allen, E., & Carrington, J. C. (2008). Specificity of Argonaute7-miR390 interaction and dual functionality in TAS3 trans-acting siRNA formation. *Cell*, 133(1), 128-141. <https://doi.org/10.1016/j.cell.2008.02.033>
- Montgomery, T. A., Yoo, S. J., Fahlgren, N., Gilbert, S. D., Howell, M. D., Sullivan, C. M., Alexander, A., Nguyen, G., Allen, E., Ahn, J. H., & Carrington, J. C. (2008). Ago1-miR173 complex initiates phased siRNA formation in plants. *Proc Natl Acad Sci U S A*, 105(51), 20055-20062. <https://doi.org/10.1073/pnas.0810241105>
- Morel, J. B., Godon, C., Mourrain, P., Beclin, C., Boutet, S., Feuerbach, F., Proux, F., & Vaucheret, H. (2002). Fertile hypomorphic Argonaute (ago1) mutants impaired in post-transcriptional gene silencing and virus resistance. *Plant Cell*, 14(3), 629-639. <https://doi.org/10.1105/tpc.010358>
- Mourrain, P., Beclin, C., Elmayan, T., Feuerbach, F., Godon, C., Morel, J. B., Jouette, D., Lacombe, A. M., Nikic, S., Picault, N., Remoue, K., Sanial, M., Vo, T. A., & Vaucheret, H. (2000). *Arabidopsis* SGS2 and SGS3 genes are required for posttranscriptional gene silencing and natural virus resistance. *Cell*, 101(5), 533-542. [https://doi.org/10.1016/s0092-8674\(00\)80863-6](https://doi.org/10.1016/s0092-8674(00)80863-6)
- Murray, M. G., & Thompson, W. F. (1980). Rapid isolation of high molecular weight plant DNA. *Nucleic Acid Research*.

- Nakanishi, K., Weinberg, D. E., Bartel, D. P., & Patel, D. J. (2012). Structure of yeast Argonaute with guide RNA. *NATURE*, *486*(7403), 368-374. <https://doi.org/10.1038/nature11211>
- Napoli, C., Lemieux, C., & Jorgensen, R. (1990). Introduction of a chimeric chalcone synthase gene into petunia results in reversible co-suppression of homologous genes in trans. *Plant Cell*, *2*(4), 279-289. <https://doi.org/10.1105/tpc.2.4.279>
- Neupane, A., Feng, C., Mochama, P. K., Saleem, H., & Lee Marzano, S. Y. (2019). Roles of Argonautes and Dicers on *Sclerotinia sclerotiorum* antiviral RNA silencing. *Front Plant Sci*, *10*, 976. <https://doi.org/10.3389/fpls.2019.00976>
- Ngo, H., Tschudi, C., Gull, K., & Ullu, E. (1998). Double-stranded RNA induces mRNA degradation in *Trypanosoma brucei*. *Proc Natl Acad Sci U S A*, *95*(25), 14687-14692. <https://doi.org/10.1073/pnas.95.25.14687>
- Nguyen, Q., Iritani, A., Ohkita, S., Vu, B. V., Yokoya, K., Matsubara, A., Ikeda, K. I., Suzuki, N., & Nakayashiki, H. (2018). A fungal Argonaute interferes with RNA interference. *Nucleic Acids Res*, *46*(5), 2495-2508. <https://doi.org/10.1093/nar/gkx1301>
- Nicholson, A. W. (1999). Function, mechanism and regulation of bacterial ribonucleases. *FEMS Microbiol Rev*, *23*(3), 371-390. <https://doi.org/10.1111/j.1574-6976.1999.tb00405.x>
- Nolan, T., Braccini, L., Azzalin, G., De Toni, A., Macino, G., & Cogoni, C. (2005). The post-transcriptional gene silencing machinery functions independently of DNA methylation to repress a LINE1-like retrotransposon in *Neurospora crassa*. *Nucleic Acids Res*, *33*(5), 1564-1573. <https://doi.org/10.1093/nar/gki300>
- Nolan, T., Cecere, G., Mancone, C., Alonzi, T., Tripodi, M., Catalanotto, C., & Cogoni, C. (2008). The RNA-dependent RNA polymerase essential for post-transcriptional gene silencing in *Neurospora crassa* interacts with replication protein A. *Nucleic Acids Res*, *36*(2), 532-538. <https://doi.org/10.1093/nar/gkm1071>
- Ogilvie, L., & Munro, M. (1947). Occurrence of *Botrytis fabae* Sardina in England. *NATURE*, *159*(4055), 96. <https://www.ncbi.nlm.nih.gov/pubmed/20256153>
- Okamura, K., Ishizuka, A., Siomi, H., & Siomi, M. C. (2004). Distinct roles for Argonaute proteins in small RNA-directed RNA cleavage pathways. *Genes Dev*, *18*(14), 1655-1666. <https://doi.org/10.1101/gad.1210204>
- Olmedo, G., Guo, H., Gregory, B. D., Nourizadeh, S. D., Aguilar-Henonin, L., Li, H., An, F., Guzman, P., & Ecker, J. R. (2006). ETHYLENE-INSENSITIVE5 encodes a 5'→3' exoribonuclease required for regulation of the EIN3-targeting F-box proteins EBF1/2. *Proc Natl Acad Sci U S A*, *103*(36), 13286-13293. <https://doi.org/10.1073/pnas.0605528103>
- Orban, T. I., & Izaurralde, E. (2005). Decay of mRNAs targeted by RISC requires XRN1, the Ski complex, and the exosome. *RNA*, *11*(4), 459-469. <https://doi.org/10.1261/rna.7231505>
- Padeken, J., Methot, S., Zeller, P., Delaney, C. E., Kalck, V., & Gasser, S. M. (2021). Argonaute NRDE-3 and MBT domain protein LIN-61 redundantly recruit an H3K9me3 HMT to prevent embryonic lethality and transposon expression. *Genes Dev*, *35*(1-2), 82-101. <https://doi.org/10.1101/gad.344234.120>
- Pak, J., & Fire, A. (2007). Distinct populations of primary and secondary effectors during RNAi in *C. elegans*. *Science*, *315*(5809), 241-244. <https://doi.org/10.1126/science.1132839>
- Pal-Bhadra, M., Bhadra, U., & Birchler, J. A. (2002). RNAi related mechanisms affect both transcriptional and posttranscriptional transgene silencing in *Drosophila*. *Mol Cell*, *9*(2), 315-327. [https://doi.org/10.1016/s1097-2765\(02\)00440-9](https://doi.org/10.1016/s1097-2765(02)00440-9)
- Palauqui, J. C., Elmayan, T., Pollien, J. M., & Vaucheret, H. (1997). Systemic acquired silencing: transgene-specific post-transcriptional silencing is transmitted by grafting from silenced stocks to non-silenced scions. *EMBO J*, *16*(15), 4738-4745. <https://doi.org/10.1093/emboj/16.15.4738>

- Pare, J. M., Tahbaz, N., Lopez-Orozco, J., LaPointe, P., Lasko, P., & Hobman, T. C. (2009). Hsp90 regulates the function of Argonaute 2 and its recruitment to stress granules and P-bodies. *Mol Biol Cell*, 20(14), 3273-3284. <https://doi.org/10.1091/mbc.E09-01-0082>
- Parekh, S., Ziegenhain, C., Vieth, B., Enard, W., & Hellmann, I. (2018). zUMIs - A fast and flexible pipeline to process RNA sequencing data with UMIs. *Gigascience*, 7(6). <https://doi.org/10.1093/gigascience/giy059>
- Park, J. H., & Shin, C. (2015). Slicer-independent mechanism drives small-RNA strand separation during human RISC assembly. *Nucleic Acids Res*, 43(19), 9418-9433. <https://doi.org/10.1093/nar/gkv937>
- Parker, J. S., Roe, S. M., & Barford, D. (2004). Crystal structure of a PIWI protein suggests mechanisms for siRNA recognition and slicer activity. *EMBO J*, 23(24), 4727-4737. <https://doi.org/10.1038/sj.emboj.7600488>
- Pawsey, R. G. (1969). *Grey mould in forest nurseries (Botrytis cinerea)* (Revised ed. . ed.). H.M.S.O.
- Peltier, G. L. (1912). A consideration of the physiology and life history of a parasitic *Botrytis* on pepper and lettuce. *Papers in Plant Pathology*.
- Peragine, A., Yoshikawa, M., Wu, G., Albrecht, H. L., & Poethig, R. S. (2004). SGS3 and SGS2/SDE1/RDR6 are required for juvenile development and the production of trans-acting siRNAs in *Arabidopsis*. *Genes Dev*, 18(19), 2368-2379. <https://doi.org/10.1101/gad.1231804>
- Pickford, A., Braccini, L., Macino, G., & Cogoni, C. (2003). The QDE-3 homologue RecQ-2 cooperates with QDE-3 in DNA repair in *Neurospora crassa*. *Curr Genet*, 42(4), 220-227. <https://doi.org/10.1007/s00294-002-0351-6>
- Qi, Y., Denli, A. M., & Hannon, G. J. (2005). Biochemical specialization within *Arabidopsis* RNA silencing pathways. *Mol Cell*, 19(3), 421-428. <https://doi.org/10.1016/j.molcel.2005.06.014>
- Qi, Y., He, X., Wang, X. J., Kohany, O., Jurka, J., & Hannon, G. J. (2006). Distinct catalytic and non-catalytic roles of Argonaute4 in RNA-directed DNA methylation. *NATURE*, 443(7114), 1008-1012. <https://doi.org/10.1038/nature05198>
- Qian, X., Hamid, F. M., El Sahili, A., Darwis, D. A., Wong, Y. H., Bhushan, S., Makeyev, E. V., & Lescar, J. (2016). Functional Evolution in Orthologous Cell-encoded RNA-dependent RNA Polymerases. *J Biol Chem*, 291(17), 9295-9309. <https://doi.org/10.1074/jbc.M115.685933>
- Qu, F., Ye, X., & Morris, T. J. (2008). *Arabidopsis* DRB4, AGO1, AGO7, and RDR6 participate in a DCL4-initiated antiviral RNA silencing pathway negatively regulated by DCL1. *Proc Natl Acad Sci U S A*, 105(38), 14732-14737. <https://doi.org/10.1073/pnas.0805760105>
- Quoc, N. B., & Nakayashiki, H. (2015). RNA silencing in filamentous fungi: from basics to applications. In *Genetic Transformation Systems in Fungi, Volume 2* (pp. 107-124). https://doi.org/10.1007/978-3-319-10503-1_8
- Rajagopalan, R., Vaucheret, H., Trejo, J., & Bartel, D. P. (2006). A diverse and evolutionarily fluid set of microRNAs in *Arabidopsis thaliana*. *Genes Dev*, 20(24), 3407-3425. <https://doi.org/10.1101/gad.1476406>
- Ramachandran, V., & Chen, X. (2008). Degradation of microRNAs by a family of exoribonucleases in *Arabidopsis*. *Science*, 321(5895), 1490-1492. <https://doi.org/10.1126/science.1163728>
- Rand, T. A., Petersen, S., Du, F., & Wang, X. (2005). Argonaute2 cleaves the anti-guide strand of siRNA during RISC activation. *Cell*, 123(4), 621-629. <https://doi.org/10.1016/j.cell.2005.10.020>
- Rashid, U. J., Paterok, D., Koglin, A., Gohlke, H., Piehler, J., & Chen, J. C. (2007). Structure of *Aquifex aeolicus* Argonaute highlights conformational flexibility of the PAZ domain as

- a potential regulator of RNA-induced silencing complex function. *J Biol Chem*, 282(18), 13824-13832. <https://doi.org/10.1074/jbc.M608619200>
- Ren, B., Wang, X., Duan, J., & Ma, J. (2019). Rhizobial tRNA-derived small RNAs are signal molecules regulating plant nodulation. *Science*, 365(6456), 919-922. <https://doi.org/10.1126/science.aav8907>
- Renaud, G., Stenzel, U., Maricic, T., Wiebe, V., & Kelso, J. (2015). deML: robust demultiplexing of Illumina sequences using a likelihood-based approach. *Bioinformatics*, 31(5), 770-772. <https://doi.org/10.1093/bioinformatics/btu719>
- Rivas, F. V., Tolia, N. H., Song, J. J., Aragon, J. P., Liu, J., Hannon, G. J., & Joshua-Tor, L. (2005). Purified Argonaute2 and an siRNA form recombinant human RISC. *Nat Struct Mol Biol*, 12(4), 340-349. <https://doi.org/10.1038/nsmb918>
- Rogers, K., & Chen, X. (2013). Biogenesis, turnover, and mode of action of plant microRNAs. *Plant Cell*, 25(7), 2383-2399. <https://doi.org/10.1105/tpc.113.113159>
- Roignant, J. Y., Carre, C., Mugat, B., Szymczak, D., Lepesant, J. A., & Antoniewski, C. (2003). Absence of transitive and systemic pathways allows cell-specific and isoform-specific RNAi in *Drosophila*. *RNA*, 9(3), 299-308. <https://doi.org/10.1261/rna.2154103>
- Romano, N., & Macino, G. (1992). Quelling: transient inactivation of gene expression in *Neurospora crassa* by transformation with homologous sequences. *Mol Microbiol*, 6(22), 3343-3353. <https://doi.org/10.1111/j.1365-2958.1992.tb02202.x>
- Sasaki, T., Kobayashi, A., Saze, H., & Kakutani, T. (2012). RNAi-independent de novo DNA methylation revealed in *Arabidopsis* mutants of chromatin remodeling gene DDM1. *Plant J*, 70(5), 750-758. <https://doi.org/10.1111/j.1365-313X.2012.04911.x>
- Schafer, W. (1993). The role of cutinase in fungal pathogenicity. *Trends Microbiol*, 1(2), 69-71. [https://doi.org/10.1016/0966-842x\(93\)90037-r](https://doi.org/10.1016/0966-842x(93)90037-r)
- Schiebel, W., Pelissier, T., Riedel, L., Thalmeir, S., Schiebel, R., Kempe, D., Lottspeich, F., Sanger, H. L., & Wassenegger, M. (1998). Isolation of an RNA-directed RNA polymerase-specific cDNA clone from tomato. *Plant Cell*, 10(12), 2087-2101. <https://doi.org/10.1105/tpc.10.12.2087>
- Schmitt, C. (1952). [Influence of light to the resistance of plantlets of *Lepidium sativum* L. to *Botrytis cinerea* Pers.]. *C R Hebd Seances Acad Sci*, 235(3), 258-260. <https://www.ncbi.nlm.nih.gov/pubmed/13009908> (Influence de la lumiere sur la resistance de plantules de *Lepidium sativum* L a *Botrytis cinerea* Pers.)
- Schott, G., Mari-Ordonez, A., Himber, C., Alioua, A., Voinnet, O., & Dunoyer, P. (2012). Differential effects of viral silencing suppressors on siRNA and miRNA loading support the existence of two distinct cellular pools of Argonaute1. *EMBO J*, 31(11), 2553-2565. <https://doi.org/10.1038/emboj.2012.92>
- Schumacher, J., Pradier, J. M., Simon, A., Traeger, S., Moraga, J., Collado, I. G., Viaud, M., & Tudzynski, B. (2012). Natural variation in the Velvet gene *bcvel1* affects virulence and light-dependent differentiation in *Botrytis cinerea*. *PLoS One*, 7(10), e47840. <https://doi.org/10.1371/journal.pone.0047840>
- Selker, E. U. (1990). Premeiotic instability of repeated sequences in *Neurospora crassa*. *Annu Rev Genet*, 24, 579-613. <https://doi.org/10.1146/annurev.ge.24.120190.003051>
- Selker, E. U. (2002). Repeat-induced gene silencing in fungi. *Adv Genet*, 46, 439-450. [https://doi.org/10.1016/s0065-2660\(02\)46016-6](https://doi.org/10.1016/s0065-2660(02)46016-6)
- Selker, E. U., Cambareri, E. B., Jensen, B. C., & Haack, K. R. (1987). Rearrangement of duplicated DNA in specialized cells of *Neurospora*. *Cell*, 51(5), 741-752. [https://doi.org/10.1016/0092-8674\(87\)90097-3](https://doi.org/10.1016/0092-8674(87)90097-3)
- Selker, E. U., & Stevens, J. N. (1985). DNA methylation at asymmetric sites is associated with numerous transition mutations. *Proc Natl Acad Sci U S A*, 82(23), 8114-8118. <https://doi.org/10.1073/pnas.82.23.8114>

- Sen, G. L., & Blau, H. M. (2005). Argonaute 2/RISC resides in sites of mammalian mRNA decay known as cytoplasmic bodies. *Nat Cell Biol*, 7(6), 633-636. <https://doi.org/10.1038/ncb1265>
- Sengoku, T., Nureki, O., Nakamura, A., Kobayashi, S., & Yokoyama, S. (2006). Structural basis for RNA unwinding by the DEAD-box protein *Drosophila* Vasa. *Cell*, 125(2), 287-300. <https://doi.org/10.1016/j.cell.2006.01.054>
- Sethi, B. K., Nanda, P. K., & Sahoo, S. (2016). Enhanced production of pectinase by *Aspergillus terreus* NCFT 4269.10 using banana peels as substrate. *3 Biotech*, 6(1), 36. <https://doi.org/10.1007/s13205-015-0353-y>
- Sheng, G., Zhao, H., Wang, J., Rao, Y., Tian, W., Swarts, D. C., van der Oost, J., Patel, D. J., & Wang, Y. (2014). Structure-based cleavage mechanism of *Thermus thermophilus* Argonaute DNA guide strand-mediated DNA target cleavage. *Proc Natl Acad Sci U S A*, 111(2), 652-657. <https://doi.org/10.1073/pnas.1321032111>
- Sheth, U., & Parker, R. (2003). Decapping and decay of messenger RNA occur in cytoplasmic processing bodies. *Science*, 300(5620), 805-808. <https://doi.org/10.1126/science.1082320>
- Shirane, N., Masuko, M., & Hayashi, Y. (1989). Light microscopic observation of nuclei and mitotic chromosomes of *Botrytis* species. *Phytopathology*, 79(7), 728-730. <https://doi.org/10.1094/Phyto-79-728>
- Shiu, P. K., Raju, N. B., Zickler, D., & Metzberg, R. L. (2001). Meiotic silencing by unpaired DNA. *Cell*, 107(7), 905-916. [https://doi.org/10.1016/s0092-8674\(01\)00609-2](https://doi.org/10.1016/s0092-8674(01)00609-2)
- Shiu, P. K., Zickler, D., Raju, N. B., Ruprich-Robert, G., & Metzberg, R. L. (2006). SAD-2 is required for meiotic silencing by unpaired DNA and perinuclear localization of SAD-1 RNA-directed RNA polymerase. *Proc Natl Acad Sci U S A*, 103(7), 2243-2248. <https://doi.org/10.1073/pnas.0508896103>
- Sigova, A., Rhind, N., & Zamore, P. D. (2004). A single Argonaute protein mediates both transcriptional and posttranscriptional silencing in *Schizosaccharomyces pombe*. *Genes Dev*, 18(19), 2359-2367. <https://doi.org/10.1101/gad.1218004>
- Sijen, T., Fleenor, J., Simmer, F., Thijssen, K. L., Parrish, S., Timmons, L., Plasterk, R. H., & Fire, A. (2001). On the role of RNA amplification in dsRNA-triggered gene silencing. *Cell*, 107(4), 465-476. [https://doi.org/10.1016/s0092-8674\(01\)00576-1](https://doi.org/10.1016/s0092-8674(01)00576-1)
- Sijen, T., Steiner, F. A., Thijssen, K. L., & Plasterk, R. H. (2007). Secondary siRNAs result from unprimed RNA synthesis and form a distinct class. *Science*, 315(5809), 244-247. <https://doi.org/10.1126/science.1136699>
- Simmer, F., Tijsterman, M., Parrish, S., Koushika, S. P., Nonet, M. L., Fire, A., Ahringer, J., & Plasterk, R. H. (2002). Loss of the putative RNA-directed RNA polymerase RRF-3 makes *C. elegans* hypersensitive to RNAi. *Curr Biol*, 12(15), 1317-1319. [https://doi.org/10.1016/s0960-9822\(02\)01041-2](https://doi.org/10.1016/s0960-9822(02)01041-2)
- Simon, B., Kirkpatrick, J. P., Eckhardt, S., Reuter, M., Rocha, E. A., Andrade-Navarro, M. A., Sehr, P., Pillai, R. S., & Carlomagno, T. (2011). Recognition of 2'-O-methylated 3'-end of piRNA by the PAZ domain of a Piwi protein. *Structure*, 19(2), 172-180. <https://doi.org/10.1016/j.str.2010.11.015>
- Singh, S., Katzer, K., Lambert, J., Cerri, M., & Parniske, M. (2014). CLOPS, A DNA Binding Transcriptional Activator, Orchestrates Symbiotic Root Nodule Development. *Cell Host & Microbe*.
- Smardon, A., Spoerke, J. M., Stacey, S. C., Klein, M. E., Mackin, N., & Maine, E. M. (2000). EGO-1 is related to RNA-directed RNA polymerase and functions in germ-line development and RNA interference in *C. elegans*. *Curr Biol*, 10(4), 169-178. [https://doi.org/10.1016/s0960-9822\(00\)00323-7](https://doi.org/10.1016/s0960-9822(00)00323-7)
- Song, J. J., Liu, J., Tolia, N. H., Schneiderman, J., Smith, S. K., Martienssen, R. A., Hannon, G. J., & Joshua-Tor, L. (2003). The crystal structure of the Argonaute2 PAZ domain

- reveals an RNA binding motif in RNAi effector complexes. *Nat Struct Biol*, 10(12), 1026-1032. <https://doi.org/10.1038/nsb1016>
- Song, J. J., Smith, S. K., Hannon, G. J., & Joshua-Tor, L. (2004). Crystal structure of Argonaute and its implications for RISC slicer activity. *Science*, 305(5689), 1434-1437. <https://doi.org/10.1126/science.1102514>
- Sorin, C., Bussell, J. D., Camus, I., Ljung, K., Kowalczyk, M., Geiss, G., McKhann, H., Garcion, C., Vaucheret, H., Sandberg, G., & Bellini, C. (2005). Auxin and light control of adventitious rooting in *Arabidopsis* require ARGONAUTE1. *Plant Cell*, 17(5), 1343-1359. <https://doi.org/10.1105/tpc.105.031625>
- Souret, F. F., Kastenmayer, J. P., & Green, P. J. (2004). AtXRN4 degrades mRNA in *Arabidopsis* and its substrates include selected miRNA targets. *Mol Cell*, 15(2), 173-183. <https://doi.org/10.1016/j.molcel.2004.06.006>
- Southern, E. M. (1975). Detection of specific sequences among DNA fragments separated by gel electrophoresis. *J Mol Biol*, 98(3), 503-517. [https://doi.org/10.1016/s0022-2836\(75\)80083-0](https://doi.org/10.1016/s0022-2836(75)80083-0)
- Stein, U. (1985). Standardization of inoculation and incubation in testing new grapevine varieties for *Botrytis* resistance. *Angewandte Botanik*, 59, 1-9.
- Stevens, N. E. (1916). *Pathological histology of strawberries affected by species of Botrytis and Rhizopus*.
- Sturani, E., Costantini, M. G., Zippel, R., & Alberghina, F. A. (1976). Regulation of RNA synthesis in *Neurospora crassa*. An analysis of a shift-up. *Exp Cell Res*, 99(2), 245-252. [https://doi.org/10.1016/0014-4827\(76\)90580-2](https://doi.org/10.1016/0014-4827(76)90580-2)
- Swarts, D. C., Hegge, J. W., Hinojo, I., Shiimori, M., Ellis, M. A., Dumrongkulraksa, J., Terns, R. M., Terns, M. P., & van der Oost, J. (2015). Argonaute of the archaeon *Pyrococcus furiosus* is a DNA-guided nuclease that targets cognate DNA. *Nucleic Acids Res*, 43(10), 5120-5129. <https://doi.org/10.1093/nar/gkv415>
- Swarts, D. C., Jore, M. M., Westra, E. R., Zhu, Y., Janssen, J. H., Snijders, A. P., Wang, Y., Patel, D. J., Berenguer, J., Brouns, S. J. J., & van der Oost, J. (2014). DNA-guided DNA interference by a prokaryotic Argonaute. *NATURE*, 507(7491), 258-261. <https://doi.org/10.1038/nature12971>
- Sweigard, J. A., Chumley, F. G., & Valent, B. (1992). Disruption of a Magnaporthe grisea cutinase gene. *Mol Gen Genet*, 232(2), 183-190. <https://www.ncbi.nlm.nih.gov/pubmed/1557024>
- Tabara, H., Sarkissian, M., Kelly, W. G., Fleenor, J., Grishok, A., Timmons, L., Fire, A., & Mello, C. C. (1999). The rde-1 gene, RNA interference, and transposon silencing in *C. elegans*. *Cell*, 99(2), 123-132. [https://doi.org/10.1016/s0092-8674\(00\)81644-x](https://doi.org/10.1016/s0092-8674(00)81644-x)
- Tamaru, H., & Selker, E. U. (2001). A histone H3 methyltransferase controls DNA methylation in *Neurospora crassa*. *NATURE*, 414(6861), 277-283. <https://doi.org/10.1038/35104508>
- Teixeira, D., Sheth, U., Valencia-Sanchez, M. A., Brengues, M., & Parker, R. (2005). Processing bodies require RNA for assembly and contain nontranslating mRNAs. *RNA*, 11(4), 371-382. <https://doi.org/10.1261/rna.7258505>
- Thieme, C. J., Schudoma, C., May, P., & Walther, D. (2012). Give It AGO: The Search for miRNA-Argonaute Sorting Signals in *Arabidopsis thaliana* Indicates a Relevance of Sequence Positions Other than the 5'-Position Alone. *Front Plant Sci*, 3, 272. <https://doi.org/10.3389/fpls.2012.00272>
- Tian, Y., Simanshu, D. K., Ma, J. B., & Patel, D. J. (2011). Structural basis for piRNA 2'-O-methylated 3'-end recognition by Piwi/PAZ (Piwi/Argonaute/Zwille) domains. *Proc Natl Acad Sci U S A*, 108(3), 903-910. <https://doi.org/10.1073/pnas.1017762108>
- Tomari, Y., Du, T., & Zamore, P. D. (2007). Sorting of *Drosophila* small silencing RNAs. *Cell*, 130(2), 299-308. <https://doi.org/10.1016/j.cell.2007.05.057>

- Tuschl, T., Zamore, P. D., Lehmann, R., Bartel, D. P., & Sharp, P. A. (1999). Targeted mRNA degradation by double-stranded RNA in vitro. *Genes Dev*, 13(24), 3191-3197. <https://doi.org/10.1101/gad.13.24.3191>
- van Dijk, E., Cougot, N., Meyer, S., Babajko, S., Wahle, E., & Seraphin, B. (2002). Human Dcp2: a catalytically active mRNA decapping enzyme located in specific cytoplasmic structures. *EMBO J*, 21(24), 6915-6924. <https://doi.org/10.1093/emboj/cdf678>
- van Kan, J., Eyres, G., Kohn, L., & Dyer, P. (2010). Mating type loci of *Botrytis cinerea*. In *Book of Abstracts 10th European Conference on Fungal Genetics, Noordwijkerhout, the Netherlands, 29 March – 1 April 2010* (pp. 113). <https://edepot.wur.nl/154220> (Book of Abstracts 10th European Conference on Fungal Genetics, Noordwijkerhout, the Netherlands, 29 March – 1 April 2010)
- van Kan, J. A. (2006). Licensed to kill: the lifestyle of a necrotrophic plant pathogen. *Trends Plant Sci*, 11(5), 247-253. <https://doi.org/10.1016/j.tplants.2006.03.005>
- van Kan, J. A., Stassen, J. H., Mosbach, A., Van Der Lee, T. A., Faino, L., Farmer, A. D., Papatotiriou, D. G., Zhou, S., Seidl, M. F., Cottam, E., Edel, D., Hahn, M., Schwartz, D. C., Dietrich, R. A., Widdison, S., & Scalliet, G. (2017). A gapless genome sequence of the fungus *Botrytis cinerea*. *Mol Plant Pathol*, 18(1), 75-89. <https://doi.org/10.1111/mpp.12384>
- van Kan, J. A., van't Klooster, J. W., Wagemakers, C. A., Dees, D. C., & van der Vlugt-Bergmans, C. J. (1997). Cutinase A of *Botrytis cinerea* is expressed, but not essential, during penetration of gerbera and tomato. *Mol Plant Microbe Interact*, 10(1), 30-38. <https://doi.org/10.1094/MPMI.1997.10.1.30>
- van Rij, R. P., Saleh, M. C., Berry, B., Foo, C., Houk, A., Antoniewski, C., & Andino, R. (2006). The RNA silencing endonuclease Argonaute 2 mediates specific antiviral immunity in *Drosophila melanogaster*. *Genes Dev*, 20(21), 2985-2995. <https://doi.org/10.1101/gad.1482006>
- Varkonyi-Gasic, E., Wu, R., Wood, M., Walton, E. F., & Hellens, R. P. (2007). Protocol: a highly sensitive RT-PCR method for detection and quantification of microRNAs. *Plant Methods*, 3, 12. <https://doi.org/10.1186/1746-4811-3-12>
- Vaucheret, H. (2008). Plant ARGONAUTES. *Trends Plant Sci*, 13(7), 350-358. <https://doi.org/10.1016/j.tplants.2008.04.007>
- Vazquez, F., Vaucheret, H., Rajagopalan, R., Lepers, C., Gascioli, V., Mallory, A. C., Hilbert, J. L., Bartel, D. P., & Crete, P. (2004). Endogenous trans-acting siRNAs regulate the accumulation of *Arabidopsis* mRNAs. *Mol Cell*, 16(1), 69-79. <https://doi.org/10.1016/j.molcel.2004.09.028>
- Verdel, A., Jia, S., Gerber, S., Sugiyama, T., Gygi, S., Grewal, S. I., & Moazed, D. (2004). RNAi-mediated targeting of heterochromatin by the RITS complex. *Science*, 303(5658), 672-676. <https://doi.org/10.1126/science.1093686>
- Vetukuri, R. R., Asman, A. K., Tellgren-Roth, C., Jahan, S. N., Reimegard, J., Fogelqvist, J., Savenkov, E., Soderbom, F., Avrova, A. O., Whisson, S. C., & Dixelius, C. (2012). Evidence for small RNAs homologous to effector-encoding genes and transposable elements in the oomycete *Phytophthora infestans*. *PLoS One*, 7(12), e51399. <https://doi.org/10.1371/journal.pone.0051399>
- Vetukuri, R. R., Avrova, A. O., Grenville-Briggs, L. J., Van West, P., Soderbom, F., Savenkov, E. I., Whisson, S. C., & Dixelius, C. (2011). Evidence for involvement of Dicer-like, Argonaute and histone deacetylase proteins in gene silencing in *Phytophthora infestans*. *Mol Plant Pathol*, 12(8), 772-785. <https://doi.org/10.1111/j.1364-3703.2011.00710.x>
- Voinnet, O., & Baulcombe, D. C. (1997). Systemic signalling in gene silencing. *NATURE*, 389(6651), 553. <https://doi.org/10.1038/39215>
- Voinnet, O., Vain, P., Angell, S., & Baulcombe, D. C. (1998). Systemic spread of sequence-specific transgene RNA degradation in plants is initiated by localized introduction of

- ectopic promoterless DNA. *Cell*, 95(2), 177-187. [https://doi.org/10.1016/s0092-8674\(00\)81749-3](https://doi.org/10.1016/s0092-8674(00)81749-3)
- Volpe, T. A., Kidner, C., Hall, I. M., Teng, G., Grewal, S. I., & Martienssen, R. A. (2002). Regulation of heterochromatic silencing and histone H3 lysine-9 methylation by RNAi. *Science*, 297(5588), 1833-1837. <https://doi.org/10.1126/science.1074973>
- Wagner, S. D., Yakovchuk, P., Gilman, B., Ponicsan, S. L., Drullinger, L. F., Kugel, J. F., & Goodrich, J. A. (2013). RNA polymerase II acts as an RNA-dependent RNA polymerase to extend and destabilize a non-coding RNA. *EMBO J*, 32(6), 781-790. <https://doi.org/10.1038/emboj.2013.18>
- Wang, H., Zhang, X., Liu, J., Kiba, T., Woo, J., Ojo, T., Hafner, M., Tuschl, T., Chua, N. H., & Wang, X. J. (2011). Deep sequencing of small RNAs specifically associated with *Arabidopsis* AGO1 and AGO4 uncovers new AGO functions. *Plant J*, 67(2), 292-304. <https://doi.org/10.1111/j.1365-313X.2011.04594.x>
- Wang, M., Weiberg, A., Dellota, E., Jr., Yamane, D., & Jin, H. (2017). *Botrytis* small RNA Bc-siR37 suppresses plant defense genes by cross-kingdom RNAi. *RNA Biol*, 14(4), 421-428. <https://doi.org/10.1080/15476286.2017.1291112>
- Wang, Y., Sheng, G., Juranek, S., Tuschl, T., & Patel, D. J. (2008). Structure of the guide-strand-containing Argonaute silencing complex. *NATURE*, 456(7219), 209-213. <https://doi.org/10.1038/nature07315>
- Waterhouse, P. M., Graham, M. W., & Wang, M. B. (1998). Virus resistance and gene silencing in plants can be induced by simultaneous expression of sense and antisense RNA. *Proc Natl Acad Sci U S A*, 95(23), 13959-13964. <https://doi.org/10.1073/pnas.95.23.13959>
- Weiberg, A., Wang, M., Lin, F. M., Zhao, H., Zhang, Z., Kaloshian, I., Huang, H. D., & Jin, H. (2013). Fungal small RNAs suppress plant immunity by hijacking host RNA interference pathways. *Science*, 342(6154), 118-123. <https://doi.org/10.1126/science.1239705>
- Wianny, F., & Zernicka-Goetz, M. (2000). Specific interference with gene function by double-stranded RNA in early mouse development. *Nat Cell Biol*, 2(2), 70-75. <https://doi.org/10.1038/35000016>
- Williams, R. W., & Rubin, G. M. (2002). ARGONAUTE1 is required for efficient RNA interference in *Drosophila* embryos. *Proceedings of the National Academy of Sciences of the United States of America*, 99(10), 6889-6894. <https://doi.org/10.1073/pnas.072190799>
- Williamson, B., Tudzynski, B., Tudzynski, P., & van Kan, J. A. (2007). *Botrytis cinerea*: the cause of grey mould disease. *Mol Plant Pathol*, 8(5), 561-580. <https://doi.org/10.1111/j.1364-3703.2007.00417.x>
- Winston, W. M., Molodowitch, C., & Hunter, C. P. (2002). Systemic RNAi in *C. elegans* requires the putative transmembrane protein SID-1. *Science*, 295(5564), 2456-2459. <https://doi.org/10.1126/science.1068836>
- Winter, J., & Diederichs, S. (2011). Argonaute proteins regulate microRNA stability: Increased microRNA abundance by Argonaute proteins is due to microRNA stabilization. *RNA Biol*, 8(6), 1149-1157. <https://doi.org/10.4161/rna.8.6.17665>
- Wu, J., Yang, R., Yang, Z., Yao, S., Zhao, S., Wang, Y., Li, P., Song, X., Jin, L., Zhou, T., Lan, Y., Xie, L., Zhou, X., Chu, C., Qi, Y., Cao, X., & Li, Y. (2017). ROS accumulation and antiviral defence control by microRNA528 in rice. *Nat Plants*, 3, 16203. <https://doi.org/10.1038/nplants.2016.203>
- Wu, Y., Xu, L., Yin, Z., Dai, Q., Gao, X., Feng, H., Voegelé, R. T., & Huang, L. (2018). Two members of the velvet family, *VmVeA* and *VmVeIB*, affect conidiation, virulence and pectinase expression in *Valsa mali*. *Mol Plant Pathol*, 19(7), 1639-1651. <https://doi.org/10.1111/mpp.12645>

- Xu, F., Feng, X., Chen, X., Weng, C., Yan, Q., Xu, T., Hong, M., & Guang, S. (2018). A Cytoplasmic Argonaute Protein Promotes the Inheritance of RNAi. *Cell Rep*, 23(8), 2482-2494. <https://doi.org/10.1016/j.celrep.2018.04.072>
- Xue, T., Dai, X., Wang, R., Wang, J., Liu, Z., & Xiang, F. (2017). ARGONAUTE10 Inhibits In Vitro Shoot Regeneration Via Repression of miR165/166 in *Arabidopsis thaliana*. *Plant Cell Physiol*, 58(10), 1789-1800. <https://doi.org/10.1093/pcpp/pcx117>
- Xue, Z., Yuan, H., Guo, J., & Liu, Y. (2012). Reconstitution of an Argonaute-dependent small RNA biogenesis pathway reveals a handover mechanism involving the RNA exosome and the exonuclease QIP. *Mol Cell*, 46(3), 299-310. <https://doi.org/10.1016/j.molcel.2012.03.019>
- Yamaguchi, S., Oe, A., Nishida, K. M., Yamashita, K., Kajiya, A., Hirano, S., Matsumoto, N., Dohmae, N., Ishitani, R., Saito, K., Siomi, H., Nishimasu, H., Siomi, M. C., & Nureki, O. (2020). Crystal structure of *Drosophila* Piwi. *Nat Commun*, 11(1), 858. <https://doi.org/10.1038/s41467-020-14687-1>
- Yang, L., Huang, W., Wang, H., Cai, R., Xu, Y., & Huang, H. (2006). Characterizations of a hypomorphic Argonaute1 mutant reveal novel AGO1 functions in *Arabidopsis* lateral organ development. *Plant Mol Biol*, 61(1-2), 63-78. <https://doi.org/10.1007/s11103-005-5992-7>
- Yang, X., Dong, W., Ren, W., Zhao, Q., Wu, F., & He, Y. (2021). Cytoplasmic HYL1 modulates miRNA-mediated translational repression. *Plant Cell*. <https://doi.org/10.1093/plcell/koab090>
- Yang, Z., Ebright, Y. W., Yu, B., & Chen, X. (2006). HEN1 recognizes 21-24 nt small RNA duplexes and deposits a methyl group onto the 2' OH of the 3' terminal nucleotide. *Nucleic Acids Res*, 34(2), 667-675. <https://doi.org/10.1093/nar/gkj474>
- Ye, R., Wang, W., Iki, T., Liu, C., Wu, Y., Ishikawa, M., Zhou, X., & Qi, Y. (2012). Cytoplasmic assembly and selective nuclear import of *Arabidopsis* Argonaute4/siRNA complexes. *Mol Cell*, 46(6), 859-870. <https://doi.org/10.1016/j.molcel.2012.04.013>
- Yigit, E., Batista, P. J., Bei, Y., Pang, K. M., Chen, C. C., Tolia, N. H., Joshua-Tor, L., Mitani, S., Simard, M. J., & Mello, C. C. (2006). Analysis of the *C. elegans* Argonaute family reveals that distinct Argonautes act sequentially during RNAi. *Cell*, 127(4), 747-757. <https://doi.org/10.1016/j.cell.2006.09.033>
- Yin, Y., Wu, S., Chui, C., Ma, T., Jiang, H., Hahn, M., & Ma, Z. (2018). The MAPK kinase *BcMkk1* suppresses oxalic acid biosynthesis via impeding phosphorylation of *BcRim15* by *BcSch9* in *Botrytis cinerea*. *PLoS Pathog*, 14(9), e1007285. <https://doi.org/10.1371/journal.ppat.1007285>
- Yoo, B. C., Kragler, F., Varkonyi-Gasic, E., Haywood, V., Archer-Evans, S., Lee, Y. M., Lough, T. J., & Lucas, W. J. (2004). A systemic small RNA signaling system in plants. *Plant Cell*, 16(8), 1979-2000. <https://doi.org/10.1105/tpc.104.023614>
- Yoshikawa, M., Peragine, A., Park, M. Y., & Poethig, R. S. (2005). A pathway for the biogenesis of trans-acting siRNAs in *Arabidopsis*. *Genes Dev*, 19(18), 2164-2175. <https://doi.org/10.1101/gad.1352605>
- Yu, B., Yang, Z., Li, J., Minakhina, S., Yang, M., Padgett, R. W., Steward, R., & Chen, X. (2005). Methylation as a crucial step in plant microRNA biogenesis. *Science*, 307(5711), 932-935. <https://doi.org/10.1126/science.1107130>
- Yu, G., Wang, L. G., Han, Y., & He, Q. Y. (2012). clusterProfiler: an R package for comparing biological themes among gene clusters. *OMICS*, 16(5), 284-287. <https://doi.org/10.1089/omi.2011.0118>
- Yu, Y., Ji, L., Le, B. H., Zhai, J., Chen, J., Luscher, E., Gao, L., Liu, C., Cao, X., Mo, B., Ma, J., Meyers, B. C., & Chen, X. (2017). Argonaute10 promotes the degradation of miR165/6 through the SDN1 and SDN2 exonucleases in *Arabidopsis*. *PLoS Biol*, 15(2), e2001272. <https://doi.org/10.1371/journal.pbio.2001272>

- Yuan, Y. R., Pei, Y., Ma, J. B., Kuryavyi, V., Zhadina, M., Meister, G., Chen, H. Y., Dauter, Z., Tuschl, T., & Patel, D. J. (2005). Crystal structure of *A. aeolicus* Argonaute, a site-specific DNA-guided endoribonuclease, provides insights into RISC-mediated mRNA cleavage. *Mol Cell*, *19*(3), 405-419. <https://doi.org/10.1016/j.molcel.2005.07.011>
- Zamore, P. D., Tuschl, T., Sharp, P. A., & Bartel, D. P. (2000). RNAi: double-stranded RNA directs the ATP-dependent cleavage of mRNA at 21 to 23 nucleotide intervals. *Cell*, *101*(1), 25-33. [https://doi.org/10.1016/S0092-8674\(00\)80620-0](https://doi.org/10.1016/S0092-8674(00)80620-0)
- Zeng, Y., Yi, R., & Cullen, B. R. (2003). MicroRNAs and small interfering RNAs can inhibit mRNA expression by similar mechanisms. *Proc Natl Acad Sci U S A*, *100*(17), 9779-9784. <https://doi.org/10.1073/pnas.1630797100>
- Zha, X., Xia, Q., & Yuan, Y. A. (2012). Structural insights into small RNA sorting and mRNA target binding by *Arabidopsis* Argonaute Mid domains. *FEBS Lett*, *586*(19), 3200-3207. <https://doi.org/10.1016/j.febslet.2012.06.038>
- Zhang, H., Kolb, F. A., Jaskiewicz, L., Westhof, E., & Filipowicz, W. (2004). Single processing center models for human Dicer and bacterial RNase III. *Cell*, *118*(1), 57-68. <https://doi.org/10.1016/j.cell.2004.06.017>
- Zhang, X., Niu, D., Carbonell, A., Wang, A., Lee, A., Tun, V., Wang, Z., Carrington, J. C., Chang, C. E., & Jin, H. (2014). Argonaute PIWI domain and microRNA duplex structure regulate small RNA sorting in *Arabidopsis*. *Nat Commun*, *5*, 5468. <https://doi.org/10.1038/ncomms6468>
- Zhang, X., Yuan, Y. R., Pei, Y., Lin, S. S., Tuschl, T., Patel, D. J., & Chua, N. H. (2006). Cucumber mosaic virus-encoded 2b suppressor inhibits *Arabidopsis* Argonaute1 cleavage activity to counter plant defense. *Genes Dev*, *20*(23), 3255-3268. <https://doi.org/10.1101/gad.1495506>
- Zhang, X., Zhao, H., Gao, S., Wang, W. C., Katiyar-Agarwal, S., Huang, H. D., Raikhel, N., & Jin, H. (2011). *Arabidopsis* Argonaute 2 regulates innate immunity via miRNA393(*)-mediated silencing of a Golgi-localized SNARE gene, MEMB12. *Mol Cell*, *42*(3), 356-366. <https://doi.org/10.1016/j.molcel.2011.04.010>
- Zhao, Y., Wei, T., Yin, K. Q., Chen, Z., Gu, H., Qu, L. J., & Qin, G. (2012). *Arabidopsis* RAP2.2 plays an important role in plant resistance to *Botrytis cinerea* and ethylene responses. *New Phytol*, *195*(2), 450-460. <https://doi.org/10.1111/j.1469-8137.2012.04160.x>
- Zhou, Y., Honda, M., Zhu, H., Zhang, Z., Guo, X., Li, T., Li, Z., Peng, X., Nakajima, K., Duan, L., & Zhang, X. (2015). Spatiotemporal sequestration of miR165/166 by *Arabidopsis* Argonaute10 promotes shoot apical meristem maintenance. *Cell Rep*, *10*(11), 1819-1827. <https://doi.org/10.1016/j.celrep.2015.02.047>
- Zhu, H., Hu, F., Wang, R., Zhou, X., Sze, S. H., Liou, L. W., Barefoot, A., Dickman, M., & Zhang, X. (2011). *Arabidopsis* Argonaute10 specifically sequesters miR166/165 to regulate shoot apical meristem development. *Cell*, *145*(2), 242-256. <https://doi.org/10.1016/j.cell.2011.03.024>
- Zilberman, D., Cao, X., & Jacobsen, S. E. (2003). Argonaute4 control of locus-specific siRNA accumulation and DNA and histone methylation. *Science*, *299*(5607), 716-719. <https://doi.org/10.1126/science.1079695>
- Zilberman, D., Cao, X., Johansen, L. K., Xie, Z., Carrington, J. C., & Jacobsen, S. E. (2004). Role of *Arabidopsis* Argonaute4 in RNA-directed DNA methylation triggered by inverted repeats. *Curr Biol*, *14*(13), 1214-1220. <https://doi.org/10.1016/j.cub.2004.06.055>
- Zisoulis, D. G., Kai, Z. S., Chang, R. K., & Pasquinelli, A. E. (2012). Autoregulation of microRNA biogenesis by let-7 and Argonaute. *NATURE*, *486*(7404), 541-544. <https://doi.org/10.1038/nature11134>

Acknowledgements

Time flies for the three and a half years since October 2017 when I officially worked in the laboratory of Genetics. Thinking back to the beginning in Genetics, I was excited for the fresh new world and anxious for the unknown environment. Thanks to the detailed and helpful laboratory introduction by the distinct responsible person, I adapted to the compact life in the laboratory in a short time. Here, I would like to express my most heartfelt gratitude and best wishes to all the teachers, colleagues, friends and family who have given me care, support and help.

I firstly would like to thank my supervisor, PD. Dr. Arne Weiberg. Thank his academic guidance when I encounter confusion in the experiments and my doctoral project. I am very appreciative of his direction on me to read the literature when I firstly entered the laboratory.

I would like to thank Prof. Dr. Martin Parniske for his management of Genetics. Prof. Dr. Martin Parniske listened carefully to the students' reports and pointed out questions in Tuesday Seminar and Journal Club. Although I am not focusing on symbiosis, I have learned a lot of supplementary knowledge from the two meetings. I am also impressed by his academic rigor. The posters made by his students are one of the most standard and beautiful posters I have ever seen.

I would like to thank my group members who once studied and worked together. Thank Dr. Antoine Porquier for teaching me to do fugal transformation and reminding me to pay attention to various experimental issues. Thank my group member Florian Dunker for every discussion in the group meeting and I am very thankful for his many bits of help in analyzing the sRNA-seq data. He was patient with my bothering every time.

I would like to thank Dr. Fan Du for patiently answering my numerous life questions and academic questions when I firstly entered the laboratory. Thank Dr. Debatosh Das, Philipp Bellon, Dr. Katarzyna Rybak and Dr. Samy Carbonnel for helpful discussions regarding my questions. I especially would like to thank Dr. RosaElena Andrade, who pointed out the issue of visualizing the figures that I have never realized and taught me to use drawing software and R studio.

I would like to thank Martin Bircheneder for taking care of the electrophoresis room while I was writing the thesis. I appreciated his warm-hearted help every time. Thank Bernerhd Ledrer for sharing his experience on WB with me.

I would like to thank my bachelor student Alexandru Stanciu. He was the only student I supervised during my doctoral study. Through the supervision and discussion with him, I recognized the things I lacked.

I would like to thank my friend Prof. Dr. Liangsheng Wang. Thank his guidance on my experiments and his solid professional knowledge is a role model for me; I would like to thank my friend Shangming Du. Without his help in analyzing mRNA-seq data, I could not manage to write the correct commands and conducted the downstream analysis. I would like to thank my friend Yen-Yu Lin, Juan Liang, Xiaoyun Gong and Rafael Espejel Venado. Because of them I did not feel alone.

I would like to thank our collaborator Lucas Wange and Ines Bliesener for preparing my mRNA-seq samples and conducting the upstream analysis of the mRNA- raw data.

I would like to thank the Graduate School of the University for providing many scientific workshops for international students. I have participated in many academic courses and they have been very helpful.

I would also like to thank the kitchen service by Adriana Hörmann and the greenhouse service by the Department of Botany, providing us a clean and well-organized environment to work in.

I would like to thank China Scholarship Council for supporting my four-year living expenses in Germany.

I would like to thank my Doctoral thesis Examination Committee, PD. Dr. Arne Weiberg, Prof. Dr. Wolfgang Frank, Prof. Christof Osman, Prof. Dr. Claude Becker, Prof. Dr. Heinrich Jung and PD. Dr. Tatjana Kleine. I appreciate very much for their reviewing and commenting on my dissertation and giving me suggestions in their busy schedule. I am very thankful for their attendance in my disputation.

I would like to thank my family for supporting me unconditionally and giving me unconditional love. I appreciate my mother, Luanying Xiong and my father, Renxi Huang for bringing our three children up well. You are always my strongest backing wherever I am going, especially my mother, Luanying Xiong. I appreciate her accompany for a challenging period in the final year of my doctoral study. I appreciate my brother Jingcheng Huang and my sister Xintong Huang. Although we are not as close as before because you have established your own family and I am far away from home, you are my forever love.

The curtain on my Ph.D. career has come to an end and my new life has just begun. In the days to come, I will redouble my efforts and move forward bravely.

Lihong Huang

Planegg, Munich

12th July, 2021